Genome-Wide CRISPR Screen Identifies Noncanonical NF-κB Signaling as a Regulator of Epithelial Homeostasis

By

Maria Fomicheva

Dissertation
Submitted to the Faculty of the
Graduate School of Vanderbilt University
in partial fulfilment of the requirements
for the degree of

DOCTOR OF PHILOSOPHY

in

Cell and Developmental Biology

January 31, 2021

Nashville, Tennessee

Approved:
Ian G. Macara, PhD, Advisor
Matthew Tyska, PhD, Committee Chair
Ken Lau, PhD
Marija Zanic, PhD
Andries Zijlstra, PhD

DEDICATION

To my loving family, my parents Tatiana and Grigory, my grandma Rufina Ivanovna, my sister Dasha and my little niece Eugenia. I am forever grateful for your love and support throughout my life.

To COVID-19 frontline responders who risk their lives and exhaust themselves to save patients and who give us strength by their example of dedication and humanism.

ACKNOWLEDGEMENTS

I would like to express my deep gratitude to my advisor Dr. Ian Macara for mentorship and guidance throughout my time here at Vanderbilt University. I would like to thank Ian for countless hours of discussion and troubleshooting, for criticism and inspiration, for teaching me how to see the big picture, as well as to pay attention to important details of designing and executing experiments. I am also thankful to Ian for creating an amazing team of scientists in his lab that were such a pleasure to work with.

I would also like to thank my committee members Dr. Matt Tyska, Dr. Marija Zanic, Dr. Ken Lau, and Dr. Andries Zijlstra for exciting discussions, valuable feedback and support over the years.

Thank you, my undergraduate mentor Dr. Elena Smirnova and my Vanderbilt University Summer Research Academy (VISRA) and research internship mentor Dr. Irina Kaverina, for all you taught me when I worked in your labs before my admission to Graduate School. The experience in your labs helped me enter graduate school and gave me foundation for laboratory work.

I am forever grateful for my undergraduate experience at Lomonosov Moscow State University that gave me unprecedented variety and depth of courses, exceptional mentorship and feeling of brotherhood and belonging. Memories about my *alma mater* are a life-long source of inspiration.

I would also like to thank the Department of Cell and Developmental Biology, VISRA, the Interdisciplinary Graduate Program in the Biomedical and Biological

Sciences, Program in Developmental Biology, The Office of Biomedical Research Education and Training, and other resources at Vanderbilt for helping me and my peers to develop our careers. The work presented in this dissertation was supported by NCI grant R35CA132898 to I.G.M.

It is my greatest pleasure to thank my lab members (current and past) for their help in navigating graduate school, limitless scientific advice, hands on help at the bench, priceless feedback on my presentations and writing, and also for being my family away from home. Throughout my life, I will carry the memories of how we shared our frustrations and excitement, argued and troubleshooted experiments, and had a tremendous amount of fun together.

I would also like to thank my friends Renee and Steve Marlowe, Amanda Erwin, Andrea Cuentas Condori, Aichurok Kamalova, Nilay Taneja, Oscar Ortega, Tanya Egorova-Arpag, Goker Arpag, and many others who I met here in Nashville. It was a great fortune to make friendships with such talented, motivated, fun, and kind people who enrich my life with great discussions, cultural exchange and much needed warmth and support. I also want to thank my childhood friend Nastya Lukyanova and university friend Masha Chelombitko who are my true soulmates regardless of life circumstances and geographical distances.

It takes a village to raise a child. Likewise, it takes a village to foster a graduate student and develop a dissertation project. For the long list of people who I did not mention, I would like to thank you for your insight, critiques, and support during my time in graduate school.

There are no words that can express in full my love and gratitude to my family. I thank my Mama and Papa, my Babushka Rufina Ivanovna, my sister Dasha, my brother-in-law Denis, and my little niece Eugenia. My family always believed in me like no one else did. They supported my interest in biology from my early years. They were patient when I asked countless questions and when I brought wildlife home. They provided me all necessary resources to pursue my dreams. They always supported and encouraged me to be a better person, a better professional, and, importantly, to be a true self.

TABLE OF CONTENTS

LIST OF FIGURES

I. INTRODUCTION

Figure

II. GENOME-WIDE CRISPR SCREEN IDENTIFIES NONCANONICAL NF-KB SIGNALING AS A REGULATOR OF DENSITY-DEPENDENT PROLIFERATION

LIST OF TABLES

LIST OF ABBREVIATIONS

CKI - cyclin-dependent kinase inhibitor

DPC - days post-confluency

FDR – false discovery rate

FUCCI – fluorescence ubiquitination cell cycle indicator

gDNA - genomic DNA

IPA - Ingenuity Pathway Analysis

KO - knockout

NT - non-targeted sgRNA control

P21 – CDKN1A

P27 – CDKN1B

P100 – NFKB2

qPCR – quantitative PCR

RRA - robust ranking aggregation

WT - wild type

I. INTRODUCTION

1.1. Epithelial tissues

Epithelial tissue consists of cells that are tightly connected with one another forming sheets that cover the surface of the body or line cavities of internal organs. Also, all glandular organs are comprised of epithelial cells. Epithelial cell functions include secretion, absorption, and barrier functions. The latter includes protection of the body and internal organs from mechanical damage, radiation, chemical, and infectious agents (Lowe, Anderson, & Anderson, 2018).

Epithelial cells are traditionally classified based on their shape and ability to form multiple layers. Flat, intermediate, and tall epithelial cells are called squamous, cuboidal, and columnar, respectively. Epithelial sheets are separated from underlying tissues by a layer of extracellular matrix called basement membrane, which anatomically separates epithelial cells from underlying tissues. Epithelial cells can form either a single layer (simple epithelium) or several layers in which only bottom layer is in contact with basement membrane (stratified epithelium) or all cells are in contact with it (pseudostratified epithelium). The shape and stratification of epithelial cells is directly dependent on the functions performed by epithelia. For instance, simple squamous epithelia can be found in lung alveoli where gas diffusion happens between air and blood. Columnar epithelia can be found in a gut where epithelial cells need a massive number of organelles for absorption and secretion of nutrients. On the other hand, stratified epithelium is observed in skin that protects the underlying organs from wounds, UV light,

and infections (Lowe et al., 2018). The mechanisms that determine cell shape, density, and stratification of epithelial cells are still not fully understood despite their importance for tissue function and pathologies.

Importantly, up to 90% of human cancers arise from epithelial cells (Frank, 2007). Transformed cells cannot organize normal tissue structure and lose proliferative control, in other words, they lose epithelial homeostasis.

1.2. Epithelial density homeostasis

Subchapters 1.2. and 1.3. are adapted with modifications from Fomicheva, Tross, and Macara, “Polarity proteins in oncogenesis” (Fomicheva, Tross, & Macara, 2019).

Epithelial cells either in culture or *in situ* can continue to proliferate even when attached to neighboring cells by intercellular junctions, but they arrest when they have achieved a characteristic density (Figure 1-1). Squamous epithelial cells usually arrest at a lower density than columnar epithelia, for example. In some cases, as in the intestine, proliferating stem cells generate transit amplifying cells that stop dividing when they differentiate, while in other tissues such as the kidney there is no clear hierarchy of stem to progenitor to mature cells, and during development the epithelial cells proliferate as needed to expand the surface area of the organ (Combes et al., 2019; Gehart & Clevers, 2019; Marcheque, Bussolati, Csete, & Perin, 2019).

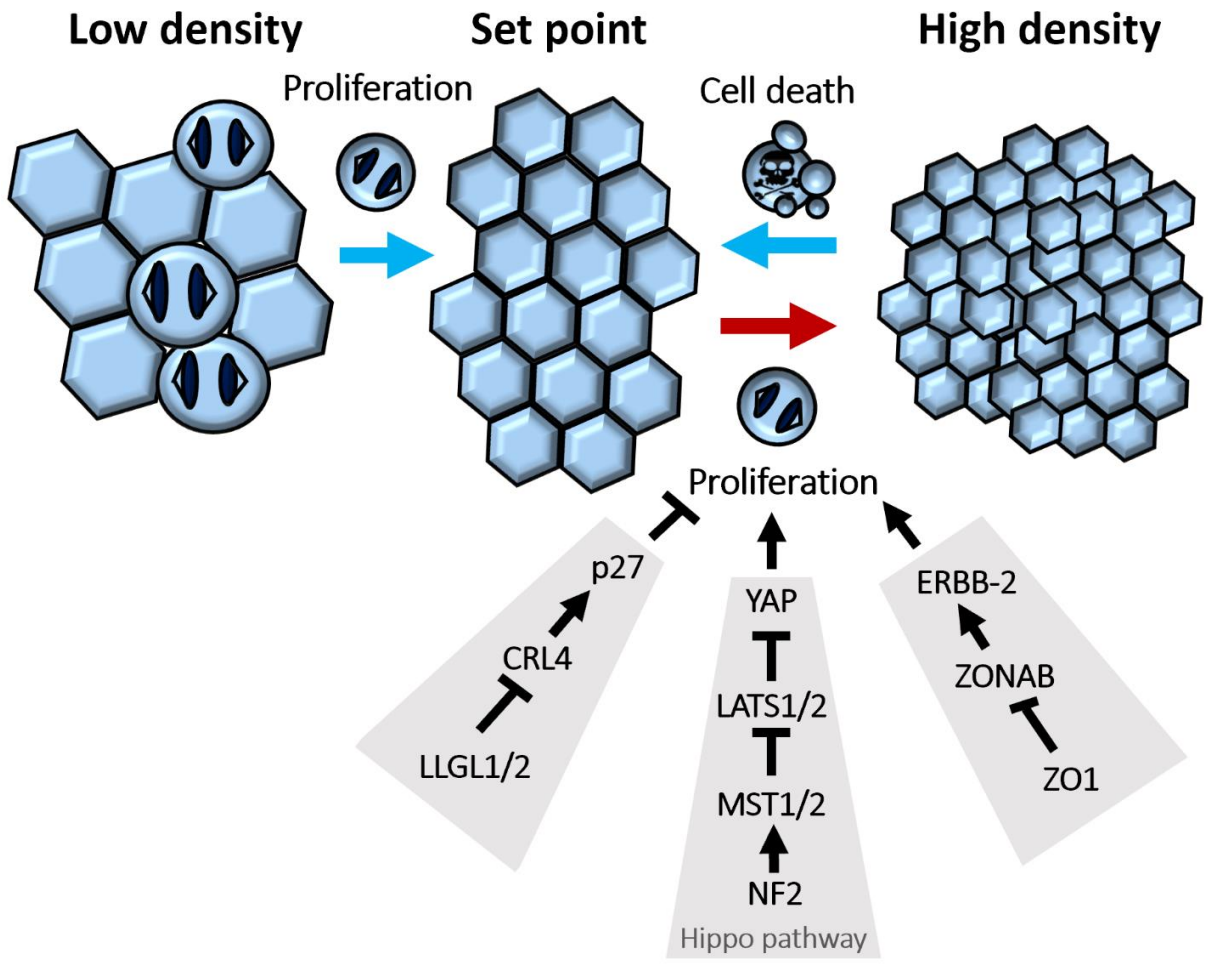

Figure 1-1. Established mechanisms of homeostatic cell density control.

If cell density is too low or too high, epithelial cells return to homeostatic density by proliferation or by cell extrusion and death, respectively (depicted by light blue arrows). If cells fail to respond to density signals, they continue to proliferate and cause hyperplasia (red arrow). Hippo signaling pathway, polarity proteins LLGL1/2 and tight junction protein ZO1 contribute to cell density control in epithelia.

Mechanical forces play a key role in determining epithelial cell density. So, for instance, stretching an epithelial sheet can trigger cells to enter mitosis (Aragona et al., 2013) while compression can induce cell extrusion and apoptosis (Eisenhoffer et al., 2012) (Figure 1-1). An early step in cancer initiation is a loss of homeostatic control, so that cells no longer respond to density signals and continue to proliferate. Hyperplasia within the epithelial sheet can inappropriately generate multi-layered structures through extrusion induced by over-crowding, or by cell migration, or misorientation of the division plane. One can conceive of apoptosis (or anoikis) of extruded cells as a fail-safe mechanism to eliminate epithelial cells that are not correctly positioned and have escaped the organizational constraints of the epithelial sheet. If apoptosis is inhibited, however, then cells that are extruded can survive to form disorganized tissue masses. In tubular organs such as the breast this can result in occlusion of the lumens, as occurs with ductal carcinoma *in situ* (Danes et al., 2008; Oudenaarden, van de Ven, & Derksen, 2018).

1.3. Mechanisms of epithelial homeostasis establishment

1.3.1. Hippo signaling

One key mechanism of density control is the Hippo signaling pathway that inhibits cell proliferation at high density. It is important for tissue growth and organ size control and has been implicated in multiple types of cancer. Hippo signaling was first discovered in *Drosophila* but is conserved in mammals, and involves a protein kinase cascade (Ma, Meng, Chen, & Guan, 2018).

The mammalian Hippo pathway includes the MST1/2 kinases that phosphorylate LATS1/2, which in turn phosphorylate the downstream effectors - YAP/TAZ transcriptional co-activators (Figure 1-1). When the Hippo kinase cascade is activated, YAP/TAZ are phosphorylated and degraded or sequestered to the cytoplasm and cell cortex. Inactivation of Hippo signaling permits nuclear accumulation of YAP/TAZ and binding to the TEAD transcription factors, which induces the expression of many genes that stimulate cell proliferation, such as CYCLIN D (Dupont et al., 2011; Ma et al., 2018).

Besides core kinases, the Hippo pathway includes multiple other components. One prominent positive regulator of Hippo signaling is the NF2 protein, the loss of which causes Neurofibromatosis Type 2 and other sporadic cancers. NF2 is believed to recruit the MST1/2 kinases to the cell cortex, but the precise mechanism by which it controls Hippo signaling remains unclear (Halder & Johnson, 2011).

In contrast to many other pathways regulated by receptor-ligand interactions, Hippo pathway is controlled in part by mechanical cues. Mechanical forces allow cells to sense cell density. Low cell density, stiff substrate or stretching result in high mechanical tension and increased actomyosin contractility, which inhibits Hippo pathway. As a result, YAP/TAZ gets dephosphorylated and translocates to the nucleus. On the other hand, high cell density or soft substrates activate Hippo cascade resulting in decreased proliferation (Aragona et al., 2013; Codelia, Sun, & Irvine, 2014). In a living organism increased cell density can be observed after wounding. Stretching of the tissue can be observed, for instance, during development.

Besides mechanical forces, other factors can contribute to Hippo signaling activation, including cell polarity, cell-cell adhesion proteins and diffusible factors, such as GPCR ligands (Fomicheva et al., 2019; Yu & Guan, 2013).

1.3.2. Hippo-independent cell density control

Despite the apparent ubiquity of Hippo signaling in epithelial growth control there are several mechanisms that appear to function independently of YAP/TAZ or their upstream regulators. For example, loss of the latero-basal polarity proteins LLGL1 and LLGL2 results in the over-proliferation of epithelial cells at high density, but not at low density. These two proteins appear to act redundantly in this homeostatic process, but not through Hippo. Instead, LLGL1/2 inhibit the multimeric CRL4 E3-ligase complex, by sequestering VprBP away from this complex. The CRL4 complex is necessary for degradation of the cell cycle kinase inhibitor p27, so loss of LLGL1/2 results in VprBP binding to and activating CRL4, which degrades p27 and allows the cell cycle to proceed even at high cell densities (Figure 1-1). Intriguingly, LLGL1/2 binding of VprBP increases with increasing cell density, suggesting a regulated mechanism. However, the molecular basis for this mechanism remains to be elucidated. Although phosphorylation of LLGL1/2 by atypical protein kinase C (aPKC) decreases LLGLl1/2 binding of VprBP and increases proliferation, this phosphorylation is independent of cell density (Yamashita et al., 2015).

Interestingly, $CRL4^{DCAF1}$ (DDB1- and CUL4-associated factor 1) has been reported to ubiquitylate and inhibit the Hippo-pathway LATS1/2 kinases in the nucleus, and NF2 binds to and suppresses CRL4 function (W. Li, Cooper, et al., 2014). The CULLIN that forms the platform for this multimeric E3 ligase is amplified in many types of solid tumors.

It seems possible, therefore, that this pathway is somehow linked to LLGL1/2 and Hippo signaling to control cell density-dependent proliferation.

Density-dependent proliferation can also be controlled by tight junction protein ZO-1 (Figure 1-1). When cell density increases, tight junctions mature and accumulate high levels of ZO-1 that sequester pro-proliferative transcription factor ZONAB at tight junctions. ZONAB regulates the expression of the proto-oncogene ERBB-2. Overexpression of ZO-1 leads to decreased homeostatic density in MDCK kidney epithelial cells. Overexpression of ZONAB results in the opposite phenotype – an increased cell density (Balda, Garrett, & Matter, 2003; Balda & Matter, 2000).

1.4. Cell cycle control

Cell density control mechanisms ultimately regulate cell cycle progression and cell proliferation. Regulation of these processes is critical for preventing over-proliferation and cancer. On the other hand, loss of proliferation would be detrimental as well since it would impair regeneration and wound healing. For these reasons, the cell cycle must be tightly controlled in epithelia.

The cell cycle consists of a DNA synthesis phase (S), mitosis (M), and two gap phases (G1 and G2) (Figure 1-5). Progression of the cell cycle from one phase to another is determined by elevation and decrease of CYCLIN-dependent kinases (CDKs) and CYCLINs. Different CDK/CYCLIN pairs are active at each stage of cell cycle. During G1, CDK4/6 in complex with CYCLIN D (D1, D2, D3) mono-phosphorylates RB (S807/811). When a cell passes the restriction point, or R-point (a time point of cell cycle,

after which removal of growth factors does not prevent cell cycle progression to S phase), CDK4/6 and CYCLIN D hyper-phosphorylate the RB protein (all 14 RB phosphorylation sites). As a result, RB dissociates from E2F allowing the latter to induce transcription of downstream genes - CYCLIN E and A. CYCLIN E binds CDK2 that gets activated in cells that passed the R-point, and they reinforce RB phosphorylation and cell cycle progression to S phase (Rubin, 2013). CDK2/CYCLIN E are also responsible for the pre-replication complex assembly that is prepared by licensing factors, such as CDT1 (Gopinathan, Ratnacaram, & Kaldis, 2011).

The amount of CYCLIN A/CDK2 complex increases resulting in initiation of DNA synthesis phase (S phase). DNA replication starts at origins of replication, and licensing factors, such as CDT1 are sent for proteasomal degradation or sequestered by GEMININ to prevent re-licensing of origins of replication. GEMININ levels remain high in S and G2 phase. From late S phase to late G2 phase, CYCLIN A forms complexes with CDK1. It is thought that CDK1/CYCLIN A are involved in activation of CYCLIN B/CDK1 complex that is necessary for progression into and out of mitosis (Gopinathan et al., 2011).

Unfortunately, the cell cycle is not as straightforward as textbook schemes suggest. For instance, the majority of cells proliferate normally in embryos deleted for all three CYCLIN Ds (D1, D2, D3) or CYCLIN Es (E1 and E2). These data suggest that CYCLIN Ds can compensate for CYCLIN Es and vice versa. Knock out of all CYCLIN Ds and CYCLIN Es together blocks proliferation in some of cells, but not in all of them. For example, embryonic stem cells were able to divide normally, likely by implementing CYCLIN A2 for CYCLIN Ds and CYCLIN Es functions (Pack, Daigh, & Meyer, 2019).

When cells exit cell cycle, they enter a so-called resting state, G0, that can differ by factors that induce cell cycle arrest and by reversibility of cell cycle arrest. There are reversible (quiescence) and irreversible (terminal differentiation and senescence) G0 states. Terminal differentiation occurs when cells differentiate to perform their specialized functions and lose their ability to divide. For instance, neurons and cardiomyocytes are highly specialized cells that perform vital functions in the body and can live for decades, but they permanently lost their ability to re-enter cell cycle. Senescence happens due to cell damage and stress, such as accumulated DNA damage, oncogene activation or telomere shortening. Senescence is important during development of kidney and inner ear, when some cells undergo senescence and get cleared. Cellular senescence is also associated with aging as damage accumulates in cells over cell lifetime. On the other hand, cells leave the cell cycle and enter quiescence when cells are devoid of growth factors, reach high density, or lose cell-substrate adhesion. In these cases, in contrast to senescence and terminal differentiation, quiescence can be reversed by addition of growth factors, reduction of cell density or plating cells on a suitable substrate (Pack et al., 2019; Terzi, Izmirli, & Gogebakan, 2016).

Mechanistically, cell cycle exit requires suppression of CDK and CYCLIN levels and/or increase in CDK inhibitor protein (Jarnicki, Putoczki, & Ernst) levels. Low levels of CDKs result in the absence of RB mono-phosphorylation at S807/811 that can be used as a G0 marker (Gookin et al., 2017). CKIs are divided into two families: the CDK interacting protein/kinase inhibitory protein family (CIP/KIP), which includes p21, p27, and p57, and the inhibitor of kinase 4 (INK4) family that consists of p15, p16, p18, and p19. CIP/KIP inhibits CDK4/6 and CDK2 complexes, and INK4 inhibits CDK4/6. CKIs get

activated under different conditions, e.g. p21 and p16 are often implicated in senescence. DNA damage induces p53 activity, which in turn increases p21 and p16 transcription. P57 is important for cell cycle regulation during development (Besson, Dowdy, & Roberts, 2008). Quiescent states induced by serum starvation or contact inhibition lead to p27 level increases (Besson et al., 2008). However, CKIs cannot serve as definitive markers to distinguish G0 states as CKI expression and functions vary depending on cell type and biological context (Terzi et al., 2016).

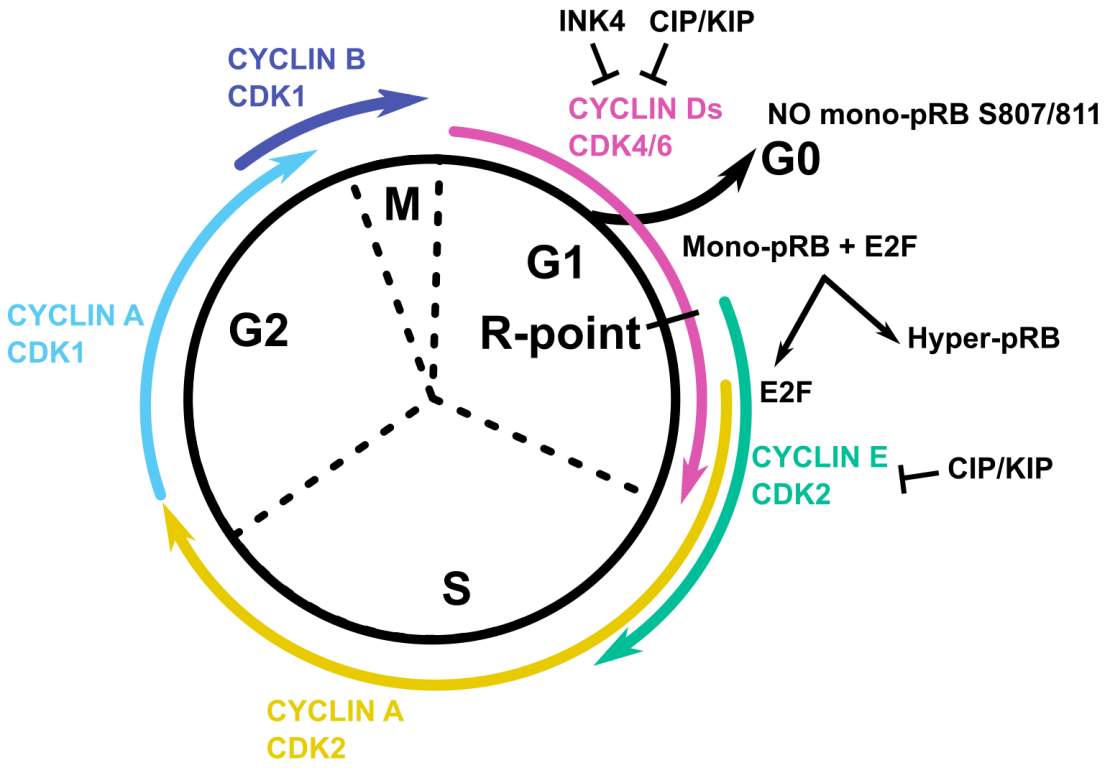

Figure 1-2. Cell cycle phases with key molecular events.

Details in text.

1.5. TRAF3

In addition to the mechanisms described above, there may be additional, unknown processes by which epithelial cells control their density, and the goal of my dissertation research was to screen for genes that are involved in such processes. I performed a whole-genome screen that identified a novel regulator called TRAF3 (TNF Receptor Associated Factor 3). TRAF3 had not previously been associated with cell density dependent proliferation control, perhaps because its functions have been studied predominantly in blood cells. TRAF3 is a negative regulator of multiple pathways critical for lymphocyte proliferation and immune responses (Zapata et al., 2009).

TRAF3 is a member of the TRAF family of proteins and, like other TRAF proteins, it has a C-terminal TRAF domain, which consists of an N-terminal coiled-coil region (TRAF-N) and a C-terminal β-sandwich (TRAF-C) (Figure 1-2). This domain is responsible for TRAF protein oligomerization into a trimeric structure, as well as protein-protein interaction with different signaling molecules. The N-terminal part of TRAF proteins contains a RING finger domain and zinc fingers. The RING finger domain is important for ubiquitin ligase catalytic activity in E3 ubiquitin ligases. Many TRAF proteins work as E3 ubiquitin ligases, but this function has been controversial for TRAF3. It serves primarily as a scaffold protein mediating interaction of receptors with various downstream effector proteins. TRAF3 works in conjunction with TRAF2 and cIAP1/2, and the latter act as E3 ligases (H. H. Park, 2018). However, there are emerging data that TRAF3 might also function an E3 ligase towards itself in response to TLR activation. It is proposed that activation of TRIF downstream TLRs induces TRAF3 K63-linked self-polyubiquitination,

which does not signal degradation, but instead, is required for recruitment of other proteins and downstream signaling activation (Lin, Hostager, & Bishop, 2015).

When a ligand binds a receptor in the TNFR superfamily (Claudio, Brown, Park, Wang, & Siebenlist, 2002; Coope et al., 2002; Dejardin et al., 2002; Hauer et al., 2005), Toll-like receptors (TLRs) (Hacker et al., 2006; Hoebe & Beutler, 2006; Oganesyan et al., 2006), NOD-like receptors (NLRs) (Guan et al., 2015), or RIG-I-like (RLRs) receptors (Michallet et al., 2008), the TRAF3 complex is recruited to the receptor, and consequently TRAF3 is targeted for degradation by cIAP1/2, which allows activation of downstream signaling. Pathways downstream of TRAF3 include the canonical and noncanonical NF-κB pathways (He et al., 2006; Ramakrishnan, Wang, & Wallach, 2004; Sun, 2017; Zarnegar, Yamazaki, He, & Cheng, 2008), STAT3 (Lin, Yi, et al., 2015; Yi, Lin, Stunz, & Bishop, 2014), and interferon pathway (Xie et al., 2011).

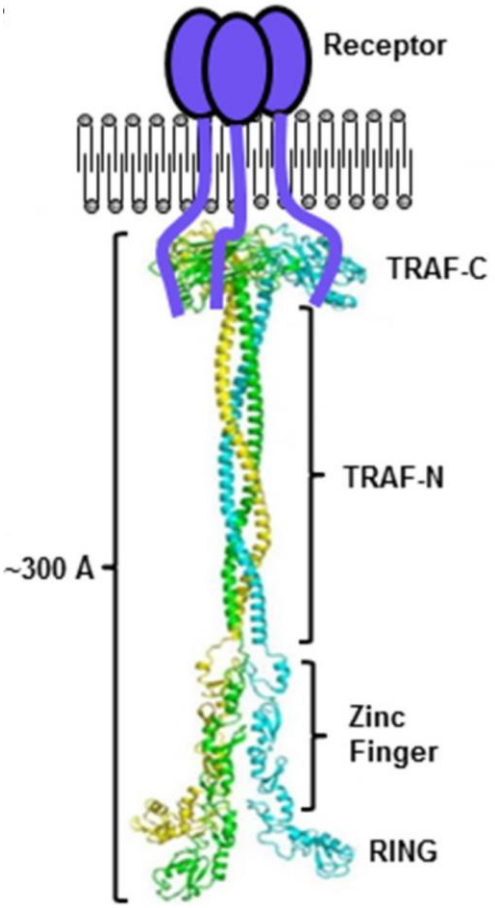

Figure 1-3. TRAF family protein structure.

The illustration is adapted from (H. H. Park, 2018).

1.6. NF-κB signaling pathway

As mentioned above, one of the prominent pathways downstream of TRAF3 is NF-κB signaling. This pathway is present in almost all multicellular organisms and even in some single cell protists and choanoflagellates. It plays an important role in development, and in innate and adaptive immune responses (Sullivan et al., 2009; Williams & Gilmore, 2020).

In mammals, the NF-κB protein family of transcription factors is comprised of five members: RELA (also known as p65), RELB, c-REL, NF-κB1 (p105) and NF-κB2 (p100). The latter two are partially degraded into their active forms p50 and p52, respectively. Activation of NF-κB proteins usually occurs via canonical and noncanonical branches of the NF-κB pathway (Figure 1-3). NF-κB proteins are known to act as dimers. In general, the canonical NF-κB pathway activates RELA:p50 or c-REL:p50 heterodimers, and the noncanonical pathway activates a RELB:p52 heterodimer. However, other variants of REL homo- and heterodimers can also form. Out of 15 possible dimers, 12 can form and bind DNA (all permutations except for RelB:RelB, RelB:RelA, and RelB:cRel) (Mitchell, Vargas, & Hoffmann, 2016). The dimers bind at κB sites upstream their target genes that are distinct for different pairs of REL proteins.

Canonical NF-κB signaling is activated by a number of receptors, including TNFR1, TLRs and IL1-R (Figure 1-3). Ligand binding of the above receptors induces activation of TAK1 (TGFβ-activated kinase 1), which in turn activates IKKα/β/γ (inhibitor of nuclear factor κB kinase subunits α, β, and γ. IKK γ is also known as NEMO). IKK complex phosphorylates IκB (inhibitor of nuclear factor κB) that sends it to proteasomal

degradation. Under unstimulated conditions, IκB inhibits RELA/p65 and p50 where p50 is coming from constitutive endoproteolysis of p105, which can also function as a pathway inhibitor in complex with IκBγ (Tao et al., 2014). However, pathway activation releases RelA:p50 complex that enters the nucleus and activates target genes (Mitchell et al., 2016)(Sun, 2017 #19). Although TRAF3 predominantly controls noncanonical NF-κB pathway, loss of TRAF3 can also induce canonical NF-κB signaling via a NIK – IKKα axis (Figure 1-2) (de Oliveira et al., 2016; Ramakrishnan et al., 2004; Zarnegar et al., 2008).

Knockout of canonical NF-κB signaling components results in embryonic lethality. Canonical NF-κB signaling is critical for lung, liver, muscle, skeletal, skin, and neural development, as well as dorso-ventral patterning (Espin-Palazon & Traver, 2016). Canonical NF-κB signaling is also involved in immune responses to pathogens, and its deregulation is observed in chronic inflammatory diseases such as rheumatoid arthritis, inflammatory bowel disease, asthma, and psoriasis (Tak & Firestein, 2001).

In the noncanonical pathway (Figure 1-2), the TRAF3 complex constitutively promotes proteasomal degradation of NIK, a kinase that activates the downstream noncanonical NF-κB signaling cascade. Ligand recruitment to upstream TNF receptor (TNFR) family (LTβR, BAFFR, RANK, TNFR2, FN14, OX40, CD40, etc.) or non-TNFR receptors (e.g. macrophage colony-stimulating factor receptor (MCSFR) and TLRs), recruits TRAF3 to the receptor and results in TRAF3 polyubiquitylation by cIAP1/2 and consequent degradation. The loss of TRAF3 leads to increased NIK levels, and as a result, NIK phosphorylates its downstream target IKKα, which in turn phosphorylates p100. Phosphorylated p100 is polyubiquitylated and partially degraded to p52, which enters the nucleus in association with RELB and regulates the transcription of target

genes (Mitchell et al., 2016); Sun, 2017 #19). Besides generating p52, p100 proteasomal processing is important for pathway activation since it depletes p100 which, in complex with IκBδ, serves as an inhibitor for both the canonical and noncanonical NF-κB pathways (Tao et al., 2014).

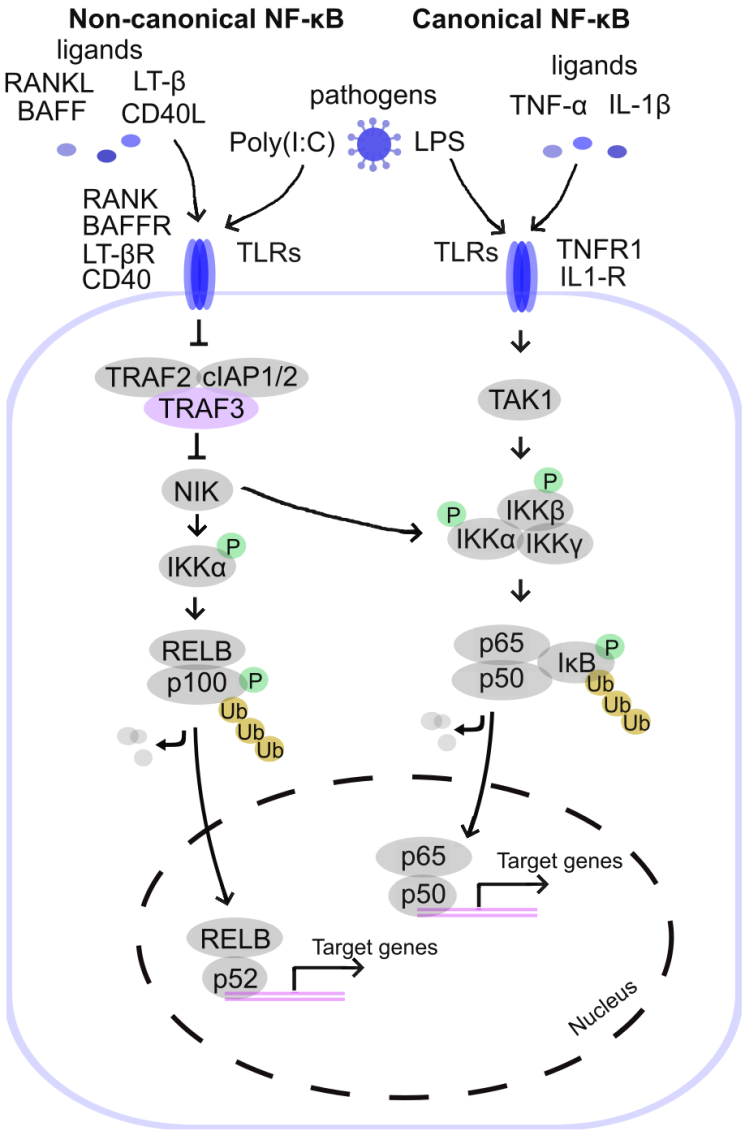

Figure 1-4. Canonical and noncanonical NF-κB pathways.

Details in text.

The noncanonical NF-κB pathway is implicated in lymphoid organ development, osteoclastogenesis, B cell maturation, innate and adaptive immunity (Espin-Palazon & Traver, 2016; Sun, 2017). The noncanonical NF-κB pathway is also involved in several autoimmune and inflammatory diseases, for instance, rheumatoid arthritis, systemic lupus erythematosus, and IgA nephropathy. It also has been implicated in pathogenesis of metabolic syndrome and diabetes (Sun, 2017).

Besides being activated by ligands, the noncanonical NF-κB pathway can also be directly activated by some viruses, for instance, HIV (Manches, Fernandez, Plumas, Chaperot, & Bhardwaj, 2012), influenza A virus (Ruckle et al., 2012), and many others (Struzik & Szulc-Dabrowska, 2019). It can also be activated by bacteria, such as *Helicobacter pylori*, a bacterium associated with gastritis and cancer (Ohmae et al., 2005), *Legionella pneumophila*, a bacterium infecting lung macrophages (Ge et al., 2009), and *Haemophilus influenzae*, a bacterium infecting ear mucosa (Cho, Pak, Webster, Kurabi, & Ryan, 2016). These data demonstrate that pathogens activate the noncanonical NF-κB pathway both in immune and non-immune cells.

1.7. NF-κB signaling target genes

As mentioned above, NF-κB proteins form different dimers that activate or suppress expression of unique gene sets. Since different dimers can bind DNA and regulate gene transcription, it immensely complicates the identification of unique roles for NF-κB protein in knockout animals or cell lines. Another level of complexity for studying NF-κB target genes is added by variations of target gene signatures depending on cell

type and stimuli. The literature has accumulated a lot of contradictory data on common and unique target genes for different NF-κB proteins.

There is agreement in the literature that NF-κB proteins have a preferential DNA consensus binding sequence in the enhancer regions of genes, which is 5'-GGRNNYYCC-3', where R, Y and N are purine, pyrimidine and any nucleotide base, respectively. Different NF-κB protein pairs have different preferences for central base pairs. Also, there are some κB DNA sites that significantly deviate from the consensus sequence (Mulero, Wang, Huxford, & Ghosh, 2019).

Under unstimulated conditions, most of the target genes remain inactive. However, a small fraction of NF-κB proteins can still reach the nucleus and stimulate some expression of target genes to support cell homeostasis (Mulero et al., 2019). When cells get stimulated, NF-κB protein in nuclei dramatically increases, which results in increased stimulation of target genes.

κB target genes that have been proven experimentally or predicted based on κB target sequences are summarized in online sources (http://www.bu.edu/nf-kb/gene-resources/target-genes/, https://maayanlab.cloud/Harmonizome/).

The noncanonical NF-κB pathway can stimulate various classes of genes, including chemokines (e.g., CCL9, CCL22, CXCL13, CCL21, and CCL19), interferon pathway genes, pro-proliferation genes (e.g. CYCLIN D1, D2, D3, c-MYC) anti-apoptotic genes (BCL-XL, CIAP1, CIAP2, cFLIP), NF-κB pathway genes (NFKB2, NFKBIA, NFKBIB, BCL3, etc.), and others (Annunziata et al., 2007; Bonizzi et al., 2004; de Oliveira

et al., 2016; Demicco et al., 2005; Dolcet, Llobet, Pallares, & Matias-Guiu, 2005; Hoesel & Schmid, 2013; Sasaki et al., 2008; Struzik & Szulc-Dabrowska, 2019).

Both canonical and noncanonical NF-κB pathway are involved in activation of the Major histocompatibility complex MHC-I and II genes encoding glycoproteins. These are synthesized either in most cells in a body (MHC-I) or specifically in immune cells (MHC-II) and serve to present peptides on cell surface to immune cells (Struzik & Szulc-Dabrowska, 2019).

1.8. Other TRAF3 dependent pathways

As mentioned before, TRAF3 participates in other molecular pathways besides NF-κB signaling cascade (Figure 1-4). It participates in pathways downstream of pattern recognition receptors (PRRs) that include TLRs, RLRs, and NLRs. PRRs are responsible for innate immune response to infectious agents and cellular injury. They are activated by molecules called pathogen-associated molecular patterns (PAMPs) that are derived from infectious agents, or by molecules of endogenous origin named damage-associated molecular patterns (DAMPs).

In TLR pathway, pathogen-associated molecular patterns (PAMPs), such as viral DNA or lipopolysaccharides (LPS), or damage-associated molecular patterns (DAMPs), such as HMGB1, cellular DNA, RNA, or ECM fragments, bind TLRs. It leads to TLR dimerization and recruitment of MyD88 (all TLRs except for TLR3) or TRIF (TLR3 and TLR4) (Hacker, Tseng, & Karin, 2011; J. Q. Wang, Jeelall, Ferguson, & Horikawa, 2014).

MyD88 recruits IRAK1, 2, 4, TRAF6, and TRAF3. TRAF3 undergoes polyubiquitination by cIAPs, which are activated by TRAF6. As a result of TRAF3 degradation, TBK1 and IKKε get activated and phosphorylate the transcription factor interferon-regulatory factor 7 (IRF7) that induces interferon α (IFNα) gene transcription. In case of TRIF dependent interferon activation, TRIF recruits TRAF3, which results in non-degradative self-ubiquitination and subsequent activation of TBK1 and IKKε that promote activation of transcription factor IRF3 inducing IFNβ. (Hacker et al., 2011; J. Q. Wang et al., 2014).

Interferons are cytokines that play an important role in innate immune response against infectious agents by activating antigen presentation genes, by stimulating immune cells and inducing cell death. IFNα and IFNβ are secreted from the cell and bind interferon receptors that results in STAT1/2 phosphorylation. STAT1/2 in complex with IRF9 translocate to the nucleus and activate interferon stimulated genes (ISGs) that contribute to cell defense against pathogens. MyD88 complex activation and TRAF3 degradation can also activate MAP kinases (p38 and JNK), as well as TAK1 kinase that activated NF-κB pathway (Apelbaum, Yarden, Warszawski, Harari, & Schreiber, 2013; Stanifer, Pervolaraki, & Boulant, 2019).

TRAF3 also participates in RLR signaling. Upon viral RNA recruitment, intracellular RLRs dimerize and bind mitochondrial antiviral signaling protein (MAVS). MAVS recruits TRAF3 and other proteins including other TRAFs, cIAP1/2, TBK1, and IKKε. It results in IRF3/7, NF-κB, and AP-1 transcription factor activation that together contribute to antiviral response. Similar cellular effects are induced by NLR receptor activation. NLRs are intracellular receptors that sample PAMPs like bacterial peptidoglycans and toxins or

DAMPs like ATP. Upon PAMP or DAMP binding, NLRs oligomerize and recruit RIP2 kinase, TRAF2, TRAF3, TRAF5, TRAF6, cIAP1/2, and other proteins. It results in activation of IRF7, the canonical NF-κB pathway, and IL1β, IL18 and/or MAPK pathways (Dhillon, Aleithan, Abdul-Sater, & Abdul-Sater, 2019; Xie, 2013).

In addition, it was shown that TRAF3 KO B cells have an increased IL-6 response. IL-6 binds IL6-R and induces JAK dependent phosphorylation of STAT3, which in turn translocates to the nucleus and induces target genes. However, TRAF3 limits IL-6 dependent STAT3 phosphorylation by recruiting the protein tyrosine phosphatase, non-receptor type 22 (PTPN22). This recruitment results in reduced STAT3 activity that ultimately restrains B cell maturation (Lin, Yi, et al., 2015).

TRAF3 has also been reported to localize in the nucleus in conjunction with TRAF2. Nuclear TRAF3/TRAF2 induce polyubiquitination and degradation of cyclic AMP response element binding protein (CREB), a pro-survival transcription factor. One of the CREB target genes is an anti-apoptotic member of the Bcl-2 family Mcl-1 (Mambetsariev et al., 2016).

The pathways described above are activated not only in immune cells, but in non-hematopoietic cells as well. For decades, epithelial cells were perceived just as a physical barrier to limit pathogen invasion, but recently they were recognized as important players in primary responses to pathogens. Epithelial cells are fully equipped for an innate immune response. They express TNFRs and PRRs that can activate NF-κB pathway, antigen presentation, and interferon response pathway to counteract various types of damage and infections (Ross & Herzberg, 2016).

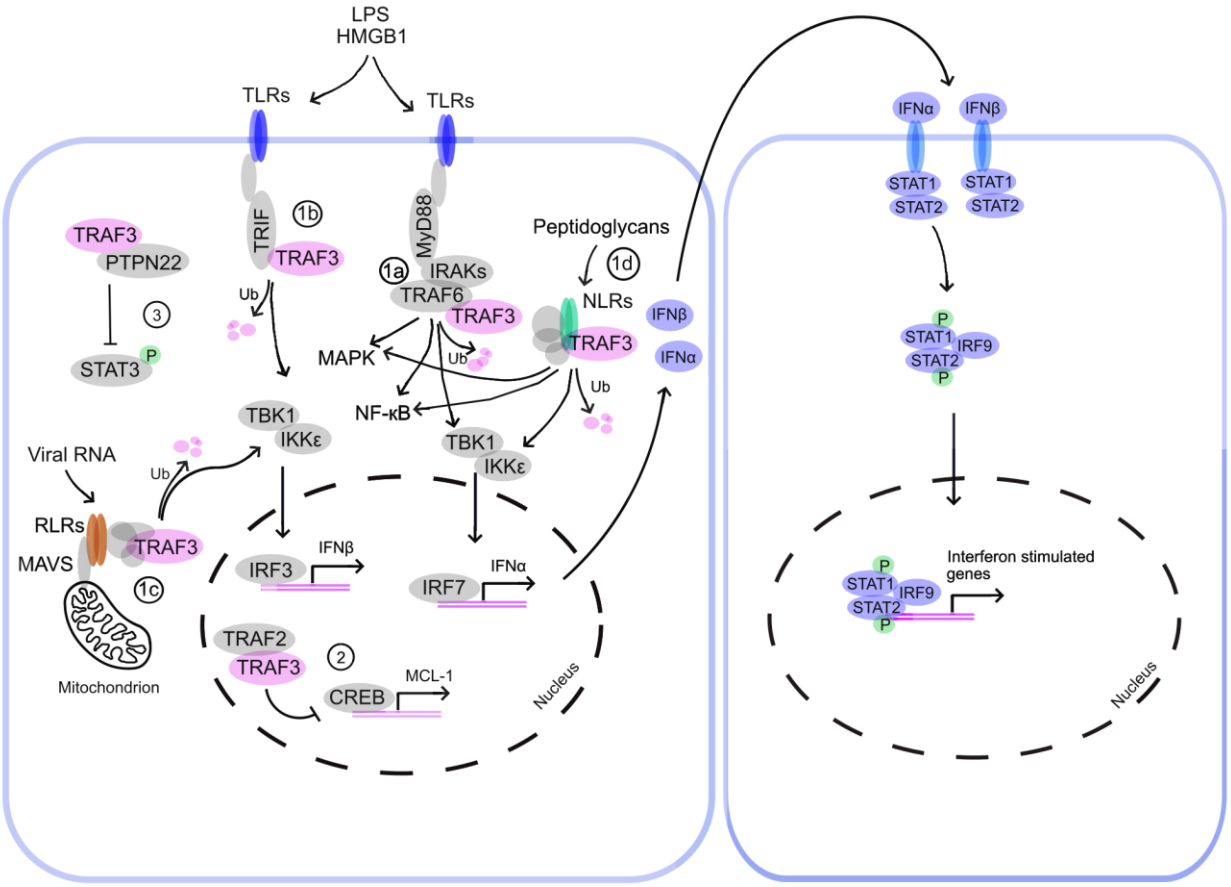

Figure 1-5. TRAF3 involvement in other pathways besides NF-κB pathway.

The role of TRAF3 in interferon pathway via TLRs (1a, 1b), RLRs (1c), NLRs(1d), inhibition of CREB dependent transcription (2), inhibition of STAT3 pathway by recruitment of PTPN22 phosphatase (3). Details in text.

1.9. TRAF3 and TRAF3 dependent pathways in cancer

Loss of TRAF3 and/or abnormal activation of noncanonical NF-κB pathway is widely observed in hematologic malignancies. *Traf3* mutations are most common in multiple myeloma, a malignancy of B lymphocytes, where *Traf3* mutations are observed in up to 20% of patients (Bishop, Stunz, & Hostager, 2018). Mutations are also observed in solid tumors too although at a much smaller frequency. *Traf3* is mutated at a rate of 3-5% in different cancers of epithelial origin and low expression is associated with worse outcomes (Nagy, Lanczky, Menyhart, & Gyorffy, 2018; Zhu et al., 2018).

NF-κB signaling is also associated with different cancers. Mutations and alterations in NF-κB component activity were shown in B-cell and T-cell lymphomas and multiple myelomas (Dolcet et al., 2005). It is also observed in solid cancers, including breast cancer (Rojo et al., 2016; Sovak et al., 1997), lung cancer (Dimitrakopoulos et al., 2019), pancreatic cancer (Wharry, Haines, Carroll, & May, 2009), and others.

Aberrant reduction of TRAF3 levels and activation of downstream pathways can occur without genetic changes of TRAF3 or downstream pathway components. PAMPs and DAMPs generated during chronic infection or tissue damage induce TLR activation which in turn activates NF-κB signaling, STAT3, MAPK pathway, and other pathways that contribute to cancer development (Pandey et al., 2015).

NF-κB signaling pathway can promote cancer using multiple mechanisms, for instance, by promoting survival by expression of anti-apoptotic genes and proliferation by inducing the expression of CYCLINs and c-MYC. It can promote metastasis by controlling the expression of matrix metalloproteinase and cell adhesion genes. It can induce

glycolytic enzyme expression while repressing mitochondrial genes thus promoting a switch to glycolysis in malignant cells. It can also promote angiogenesis by VEGF synthesis. NF-κB signaling pathway also has a prominent role in the inflammatory response, and it is known that inflammation plays an important role in cancer development (Perkins, 2012).

Aberrant STAT3 activation also contributes to cancer progression by upregulating pro-survival Bcl-2 proteins, stimulating cell cycle proteins, inhibiting CKIs, and promoting angiogenesis (Jarnicki et al., 2010). On the other hand, interferons and their downstream targets STAT1/2 are classically associated with antitumor activity by promoting tumor cell death, inhibiting cell cycle progression, and modulating antitumor immune response (Parker, Rautela, & Hertzog, 2016). However, recent data show that interferon and STAT1/2 can increase tumor cell resistance to genotoxic stress and stimulate tumor growth (Khodarev, Roizman, & Weichselbaum, 2012).

1.10. Overview of the work presented in this dissertation

Epithelial cells maintain homeostatic cell density, at which they rarely proliferate. This regulation is critical for normal tissue structure maintenance. However, mechanisms of proliferation control at homeostatic cell density are not fully understood. It has been recently appreciated that homeostatic cell density control is complex and involves multiple molecular players. One of the major density control pathways, Hippo signaling pathway, has a lot of components discovered over the past few years. In addition, Hippo-independent mechanisms have also been recently discovered, such as the LLGL/p27 and ZO-1/ZONAB pathway. It is therefore highly possible that other Hippo pathway members

and/or currently unknown Hippo-independent mechanisms exist. However, there has been no systemic approach to screen for regulators of cell density dependent proliferation.

In our study, we aimed to establish a strategy to discover genes controlling cell density dependent proliferation. We designed and performed a whole genome CRISPR/Cas9 KO screen that separated KO cells over-proliferating at high density.

My whole genome screen revealed a known regulator of cell density - *Nf2* - that activates Hippo signaling. Excitingly, we also enriched for *Traf3* and *Ube2m* genes, which were not previously known to be involved in density-dependent cell proliferation. We focused on studying the mechanisms underlying over-proliferation at high density upon loss of the TRAF3 protein. We found that the noncanonical NF-κB pathway is constitutively activated upon TRAF3 loss, and it is necessary and sufficient for over-proliferation at high density.

However, we did not know what allows TRAF3 KO cells over-proliferate at high density. After a series of negative results, in which we demonstrated that TRAF3 KO cells proliferate independently of YAP/TAZ, secretory molecules, and presence of CKIs, we found that loss of TRAF3 at high density prevents cells from leaving the cell cycle to enter G0.

II. GENOME-WIDE CRISPR SCREEN IDENTIFIES NONCANONICAL NF-ΚB SIGNALING AS A REGULATOR OF DENSITY-DEPENDENT PROLIFERATION

Adapted from Fomicheva and Macara, “Genome-wide CRISPR screen identifies noncanonical NF-κB signaling as a regulator of density-dependent proliferation” (Fomicheva & Macara, 2020).

2.1. Abstract

Epithelial cells possess intrinsic mechanisms to maintain an appropriate cell density for normal tissue morphogenesis and homeostasis. Defects in such mechanisms likely contribute to hyperplasia and cancer initiation. To identify genes that regulate the density-dependent proliferation of murine mammary epithelial cells, we developed a fluorescence-activated cell sorting assay based on fluorescence ubiquitination cell cycle indicator, which marks different stages of the cell cycle with distinct fluorophores. Using this powerful assay, we performed a genome-wide CRISPR/Cas9 knockout screen, selecting for cells that proliferate normally at low density but continue to divide at high density. Unexpectedly, one top hit was *Traf3*, a negative regulator of NF-κB signaling that has never previously been linked to density-dependent proliferation. We demonstrate that loss of *Traf3* specifically activates noncanonical NF-κB signaling. This in turn triggers an innate immune response and drives cell division independently of known density-dependent proliferation mechanisms, including YAP/TAZ signaling and cyclin-dependent kinase inhibitors, by blocking entry into quiescence.

2.2. Introduction

An important characteristic of epithelial cells is that, unlike fibroblasts, they do not undergo contact inhibition but continue to proliferate at confluence. This behavior enables the expansion of epithelial tissues during organismal growth without compromising the barrier function created by intercellular junctions. Importantly, however, proliferation is not indefinite but terminates at a preset cell density (Fomicheva et al., 2019). Stretching or wounding an epithelial sheet, which reduces the cell density, can re-initiate cell division (Aragona et al., 2013). Conversely, compression, which increases density, can result in extrusion and apoptosis of cells so as to bring the epithelial layer back to its homeostatic state (Eisenhoffer et al., 2012). This control mechanism that prevents tissue overgrowth is essential for normal development, and it is lost in hyperplasia and in cancer. However, the mechanisms that underlie homeostatic cell density maintenance remain incompletely understood.

One system through which epithelial cells can respond to changes in density is the Hippo pathway and its effectors YAP and TAZ. These transcriptional co-activators are nuclear at low cell density or under conditions of high mechanical strain, but become phosphorylated and are cytoplasmic (or junction-associated) and nonfunctional at high density and/or low strain (Dupont et al., 2011). Independently of YAP/TAZ, however, the polarity proteins LLGL1/2 can also control density-dependent proliferation, by inhibiting proteasomal degradation of the cyclin-dependent kinase inhibitor CDKN1B (p27). Loss of LLGL1/2 reduces the expression of p27, which is often upregulated at high cell density to arrest proliferation (Yamashita et al., 2015). Numerous studies on Hippo/YAP have

demonstrated the complexity of this pathway, and several novel Hippo pathway components have been revealed over the past few years. In addition, as mentioned previously, Hippo-independent mechanisms have also been recently reported, such as the LLGL/p27 pathway. It is therefore likely that other Hippo pathway components and/or currently unknown Hippo-independent signaling mechanisms exist, however no strategy has been designed to identify such mechanisms.

With the goal of discovering novel factors that regulate epithelial homeostasis, we developed a powerful new assay based on a fluorescence activated cell sorting (FACS) approach that we integrated with a genome-wide CRISPR-Cas9 sgRNA knockout (KO) screen to select for genes that are essential for cell cycle arrest at high density, but which do not impact proliferation of cells below the threshold for arrest. The screen employs a fluorescence ubiquitination cell cycle indicator (FUCCI) system to mark proliferating cells in S/G2/M phases of cell cycle with a green fluorescent protein, and cells in G1/G0 with a red fluorescent protein (Sladitschek & Neveu, 2015). We found that mammary EpH4 epithelial cells robustly arrest in G1 or G0 by 4 days post-confluency (DPC). When these cells were transduced with a pooled whole-genome CRISPR KO library, and then sorted 4 DPC for cycling cells, we identified several candidate genes that may regulate cell density-dependent proliferation activity. The top hit was *Nf2* (also called *Merlin*), a known tumor suppressor that negatively regulates YAP/TAZ, which validated our approach (Petrilli & Fernandez-Valle, 2016). A second, unexpected hit was *Traf3*, a negative regulator of NF-κB signaling, which has never previously been reported to regulate cell density-dependent proliferation. We demonstrate that loss of *Traf3* robustly and specifically activates the noncanonical NF-κB pathway. This in turn triggers an innate

immune response and cell autonomously drives cell division independently of both YAP/TAZ signaling and cyclin-dependent kinase inhibitors, overriding these classical mechanisms of density-dependent proliferation control and preventing cells at high density from entering quiescence.

2.3. Results

2.3.1. A FUCCI-based screen for density-dependent cell cycle arrest

Our goal was to design a screen for the rapid and efficient selection of epithelial cells that continue to proliferate inappropriately at high cell density. For the screen, we needed to identify a cell line that retained epithelial features, including homeostatic density control. We chose the murine EpH4 mammary epithelial cell line for this screen, because EpH4 cells are highly polarized, form confluent epithelial sheets, and, most importantly, we confirmed that they efficiently arrest at high density. We also needed a tool to specifically identify and select cells that maintain proliferative activity at high density. To distinguish cycling from non-cycling cells, we established a stable EpH4 line that expresses ES-FUCCI, which labels cells in G1/G0 with mCherry and cells in S/G2/M with mCitrine (Figure 2-1A) (Sladitschek & Neveu, 2015). As expected, the EpH4-FUCCI cells remain proliferative at 1 DPC but very few cells cycle at high density, with only about 1% of cells expressing mCitrine at 4 DPC (Figure 2-1B, Figure 2-1 - Figure supplement 1A).

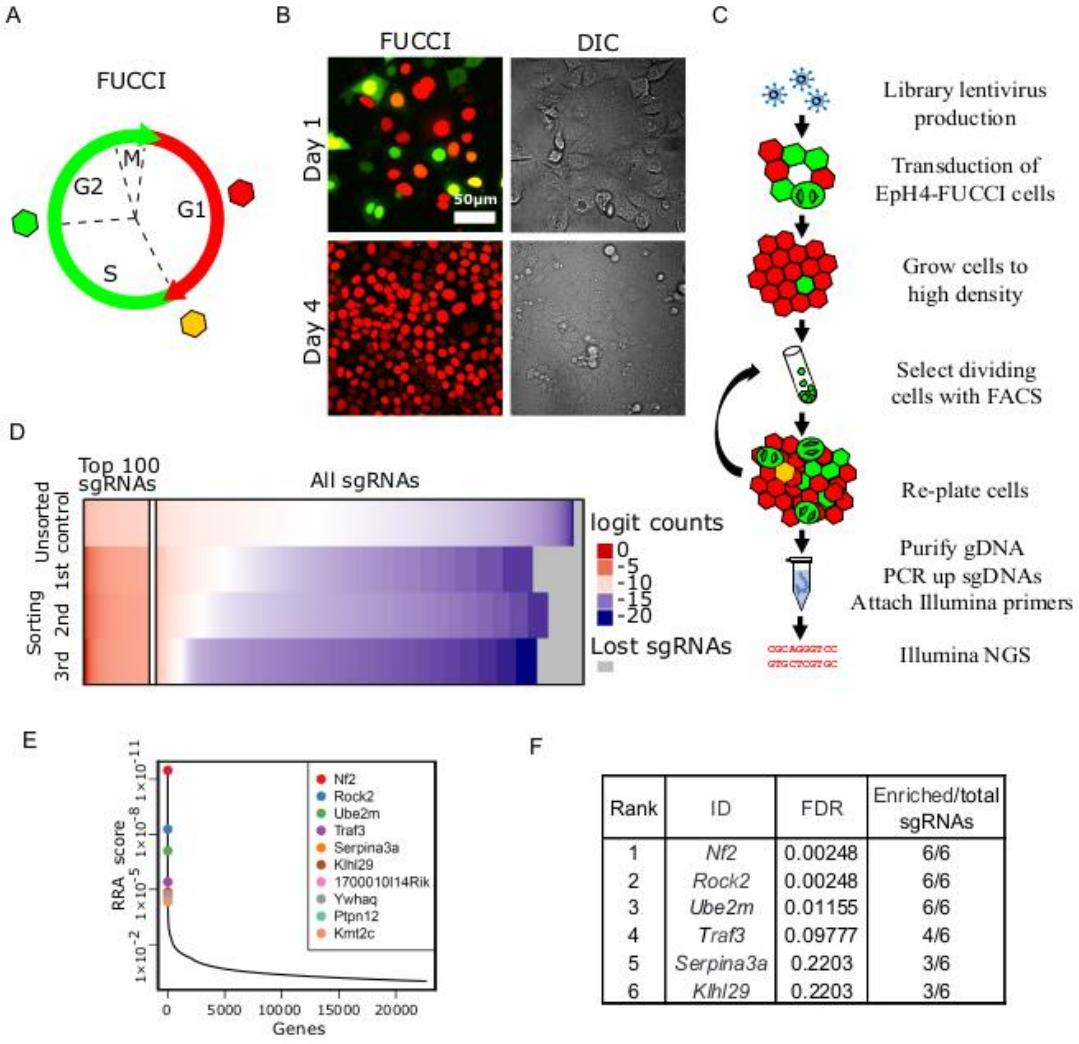

Rank	ID	FDR	Enriched/total sgRNAs
1	*Nf2*	0.00248	6/6
2	*Rock2*	0.00248	6/6
3	*Ube2m*	0.01155	6/6
4	*Traf3*	0.09777	4/6
5	*Serpina3a*	0.2203	3/6
6	*Klhl29*	0.2203	3/6

Figure 2-1. Whole-genome screening for genes that inhibit proliferation at homeostatic cell density.

(A) A Schematic of FUCCI color transitions through cell cycle. (B) EpH4-FUCCI stable cell line grown at 1 and 4 DPC. (C) Whole-genome CRISPR KO screening strategy. (D) Read count distribution for samples before sorting and after different rounds of sorting. Data are logit transformed ($f(p) = \log_2(p/1 - p)$ where p is the proportion of a given sgRNA in the total number of sgRNAs in a sample). Color coding shows depleted sgRNAs in blue, enriched sgRNAs in red and sgRNA with no enrichment in white. Gray shows lost

sgRNAs. (E) Genes plotted based on their RRA enrichment score (3rd sorting). (F) List of genes with FDR below 0.25 and >= 3 sgRNAs enriched compared to control after 3rd sort.

We reasoned that the expression of any shRNA or sgRNA that disrupts expression of a gene involved in density-dependent arrest could be identified by employing FACS to enrich for green cells from an EpH4-FUCCI population grown to high density. To test this concept, we used a shRNA lentiviral construct to deplete the cyclin-dependent kinase inhibitor *p27*, which is known to be associated with cell cycle arrest post-confluency (Yamashita et al., 2015). Quantitative PCR for the *p27* transcript showed that ~60% of *p27* mRNA was lost in cells expressing the *p27* shRNA (Figure 2-1 - Figure supplement 1B) compared to EpH4-FUCCI cells expressing scrambled shRNA. The p27-depleted cells display increased cell proliferation after 4 DPC, in contrast to cells expressing scrambled shRNA (Figure 2-1 - Figure supplement 1A). As a proof-of-principle experiment, we next mixed wild type (WT) EpH4-FUCCI cells and sh-*p27* EpH4-FUCCI cells at a 10:1 ratio (Figure 2-1 - Figure supplement 1C). The mixed cells were then plated at a cell density of 100,000 cells/cm^2, such that they reached confluency 24 hrs after seeding. We grew the mixture of cells for 4 DPC and sorted mCitrine-positive (mCitrine+) cells by FACS. After sorting, we isolated genomic DNA (gDNA) and performed qPCR using primers against the puromycin gene, located in the lentiviral plasmid insert, to assess the fraction of p27-depleted cells in the cell mixture. We observed an average of 1.4x and 3.5x enrichment of the puromycin gene after the 1st and 2nd rounds of sorting, respectively (Figure 2-1 - Figure supplement 1D). These data support the validity of our screen design.

Based on these encouraging results, we proceeded to developing an EpH4-FUCCI cell line, in which every cell has lost a single gene. We transduced EpH4-FUCCI cells with the pooled GeCKO CRISPR v2 KO lentivirus library (Sanjana, Shalem, & Zhang,

2014; Shalem et al., 2014). (Figure 2-1D). The library contains 6 sgRNAs against each of 20,611 genes, plus 1000 non-targeting controls, for a total of 130,209 sgRNAs. To ensure that our EpH4-FUCCI cells would receive only 1 sgRNA on average, we transduced cells with viruses at a multiplicity of infection (MOI) of 0.3. It is critical to maintain a large enough cell population to ensure that all sgRNAs in the library are retained. Therefore, we aimed to have 150-300 cells per sgRNA in each step of the screen. Based on these values, $6.7x10^7$ EpH4-FUCCI cells were transduced to obtain about $2x10^7$ cells that had acquired viruses (~150 cells per sgRNA). Cells that were not infected with virus were eliminated by puromycin selection. We plated the cells at 100,000 cells/cm^2 and grew them for 4 DPC. To maintain library representation, we sorted $4x10^7$ cells (300 cells per sgRNA) by FACS to select mCitrine+ cells. We re-grew cells for the next round of selection and for gDNA isolation. In total, we performed three FAC sorts. We observed a steady increase in the number of mCitrine+ cells after each round of FACS (Figure 2-1 - Figure supplement 1E, F). Genomic DNA was purified, and integrated sgRNA cassettes were amplified from the DNA by PCR, as described previously (Sanjana et al., 2014; Shalem et al., 2014) (Figure 2-1 - Figure supplement 2A, B). A second PCR reaction attached Illumina index primers (Figure 2-1 - Figure supplement 2A, C), and the pooled product was then sequenced.

We used the MAGeCK program (W. Li, Xu, et al., 2014) to map sequencing reads to the library (Figure 2-1E, Figure 2-1 - Figure supplement 2D, D'). Read count distribution was relatively uniform in the control (unsorted) sample, with depletion of those sgRNAs that target essential genes. After each round of selection, more sgRNAs were depleted, but a small portion of sgRNAs was highly enriched. We utilized the MAGeCK algorithm

to find genes that were enriched after sorts compared to control. MAGeCK takes into account changes in the abundance of all sgRNAs targeting a single gene, measured by the robust ranking aggregation (RRA) score. The most enriched genes have the smallest RRA scores (Figure 2-1F, Figure 2-1 - Figure supplement 2E, E'). We selected genes with FDR below 0.25 and with 3 or more sgRNAs/gene selected (Figure 2-1G, Figure 2-1 - Figure supplement 2F, F').

2.3.2. The CRISPR screen identifies a component of the Hippo pathway, a lymphocyte proliferation control factor and NEDD8-conjugating E2 enzyme

Interestingly, the top enriched target was *Nf2/Merlin*, which is a known tumor suppressor gene and a regulator of Hippo signaling necessary for cell density control (Petrilli & Fernandez-Valle, 2016). This hit, the sgRNAs for which were enriched by >1000x above the control abundance, strongly validated our screening strategy. Two unexpected hits were for the *Traf3* and *Ube2m (Ubc12)* genes (Figure 2-1G), which have not previously been implicated in density-dependent cell cycle arrest.

TRAF3 (TNF Receptor Associated Factor 3) is critical for lymphocyte proliferation control and immune responses (Zapata et al., 2009). It negatively regulates signaling through multiple pathways, including the canonical and noncanonical NF-κB pathways (He et al., 2006; Ramakrishnan et al., 2004; Sun, 2017; Zarnegar et al., 2008).

Deletions and mutations of *TRAF3* are among the most common genetic alterations in human B cell malignancies (Zhu et al., 2018). B cell-specific KO of the *Traf3* gene in mice leads to increased B cell numbers and spontaneous lymphomas (Moore et

al., 2012). Myeloid-specific *Traf3* KO causes histiocytic sarcomas of macrophage origin (Lalani et al., 2015). Therefore, TRAF3 is critical for the prevention of malignant growth in blood cells; however, TRAF3 roles in epithelia have not yet been widely investigated, despite its ubiquitous expression in mouse and human tissues (Yue et al., 2014).

A third hit from our screen was *Ube2m* (Ubiquitin Conjugating Enzyme E2 M, also known as *Ubc12*). UBE2M is a NEDD8 conjugation E2 enzyme, which neddylates CULLIN-RING ligases to stimulate their activity (Lydeard, Schulman, & Harper, 2013). Interestingly, stress induces UBE2M expression and promotes its ubiquitylation of UBE2F, the degradation of which can suppress cell proliferation (Zhou et al., 2018).

To confirm that loss of our top candidates indeed results in over-proliferation at high density, we developed two new sgRNA CRISPR v2 plasmids per gene. The sgRNA sequences were different from those in the GeCKO library. We transduced EpH4 cells with these sgRNA lentiviruses and confirmed efficient KO of each gene by immunoblotting for NF2, TRAF3 and UBE2M (Figure 2-2A-C'). To test if loss of the target genes leads to a failure in cell cycle arrest at high density, we analyzed BrdU incorporation at 1 and 4 DPC. BrdU was added to cells for 1 hr, then cells were fixed and stained. When cells had just reached a confluent state, we found that BrdU incorporation was similar for the non-targeted sgRNA control (NT) and each of the KO cell lines, but that at high density the KO cells incorporated more BrdU than did the NT control cells (Figure 2-2D). These differences were statistically significant at high density, as determined by cytometric analysis of BrdU+ cells (Figure 2-2E, F, Figure 2-2 - Figure supplement 1A). We also observed that all three KO cell lines formed multiple layers at high density, while control cells remained as a single, uniform layer (Figure 2-2G, H, Figure 2-2 - Figure supplement

1B). Together, these data demonstrate that our screen successfully identified genes that are essential for the restriction of proliferation at high cell density. Importantly, loss of these genes has no effect on the cell cycle at lower densities.

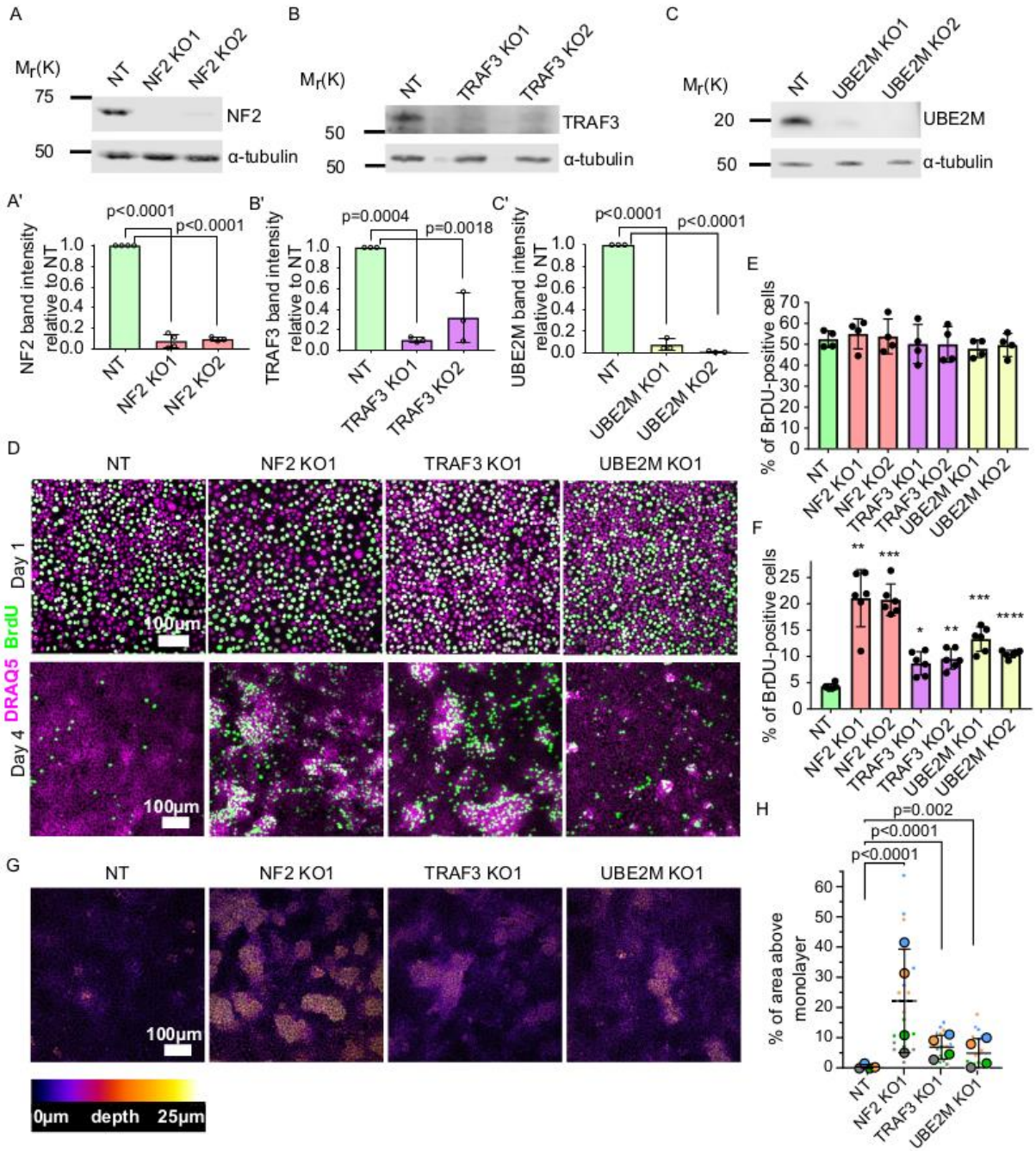

Figure 2-2. Validation of candidate genes identified from the screen.

(A) - (C) Immunoblots of NT control and NF2 (A), TRAF3 (B) and UBE2M (C) KO EpH4 cells for NF2, TRAF3 and UBE2M, respectively. α-tubulin or GAPDH was used as a

loading control. (A') - (C') Quantification of NF2 (A'), TRAF3 (B') and UBE2M (C') levels based on immunoblotting in (A) - (C). (A') - (C') Histograms show mean ± 1 s.d. (n=3). P values were calculated by one-way ANOVA followed by Dunnett's multiple comparisons test. (D) NT control, NF2, TRAF3 and UBE2M KO cells grown for 1 or 4 DPC. BrdU was added for 1 hr, then cells were fixed and stained for BrdU, with DAPI as a nuclear marker. (E), (F) Cytometric analysis of NT control, NF2, TRAF3 and UBE2M KO cells stained for BrdU to assess proliferation at 1 or 4 DPC, respectively. N=4 (E) and n=6 (F) Histograms show mean ± 1 s.d. P values were calculated by one-way ANOVA followed by Dunnett's multiple comparisons test. (G) Control and KO cells stained with Hoechst dye. Confocal images are depth color coded. The color code scale is shown below. (H) 5 fields of view in 4 biological repeats were used to quantify the level of multilayering. Data shown as a SuperPlot (Lord, Velle, Mullins, & Fritz-Laylin, 2020). P values were calculated by mixed model two-way ANOVA.

2.3.3. TRAF3 suppresses proliferation of mammary organoids, human mammary epithelial cells and fibroblasts

Little is known about the function of TRAF3 in epithelial cells, and its role in density-dependent cell cycle arrest has not been previously investigated. Interestingly, however, genetic alterations in *Traf3* occur in a variety of human epithelial cancers, though at a level < 6% (Zhu et al., 2018). Low *Traf3* mRNA expression is also associated with significantly worse survival for lung and gastric cancer patients (Figure 2-2 - Figure supplement 1C) (Nagy et al., 2018). Therefore, we focused on this gene for further analysis.

To determine the generality of the phenotype induced by deletion of *Traf3*, we first asked if the effects are confined to the EpH4 mammary epithelial line or are also important in primary mammary tissue. To address this question, we used murine mammary organoids, which recapitulate many aspects of normal morphogenesis of the mammary gland (Ewald, Brenot, Duong, Chan, & Werb, 2008; Pasic et al., 2011). Mammary gland ductal fragments were isolated from WT C3H mice, transduced with lentivirus, and then grown as organoids in Matrigel culture, as described previously (Pasic et al., 2011) (Figure 2-3A). As shown in Figure 2-3B, WT organoids form buds with hollow lumens, but organoids lacking TRAF3 formed multilayered buds with small or no detectable lumens. Additionally, staining for phospho-HISTONE H3 revealed a substantially higher mitotic index in organoids deleted for *Traf3*, compared to organoids transduced with a control sgRNA (Figure 2-3B, C), demonstrating that TRAF3 normally suppresses WT tissue overgrowth.

To extend our analysis across species, we transduced the normal human mammary gland cell line MCF10A with sgRNAs designed to target human *Traf3*. Loss of the gene product was confirmed by immunoblotting (Figure 2-3 - Figure supplement 1A, A'). We assessed cell proliferation by immunofluorescence and cytometric analysis of BrdU incorporation as described above, and found that, similar to EpH4 cells, MCF10a TRAF3 KO cells, but not WT MCF10a cells, over-proliferate at high density (Figure 2-3 - Figure supplement 1B, B').

Finally, we determined if this role for TRAF3 is confined to epithelial cells, by knocking out the gene in NIH 3T3 fibroblasts. Normally, these cells contact-inhibit at high density. CRISPR KO of *Traf3* (confirmed by Western blotting (Figure 2-3 - Figure supplement 1D-D')) promoted cell proliferation at high density as measured by cytometric analysis of BrdU staining (Figure 2-3 - Figure supplement 1D-D'). These data suggest that loss of TRAF3 broadly interferes with cell cycle arrest including cells of epithelial and mesenchymal lineages.

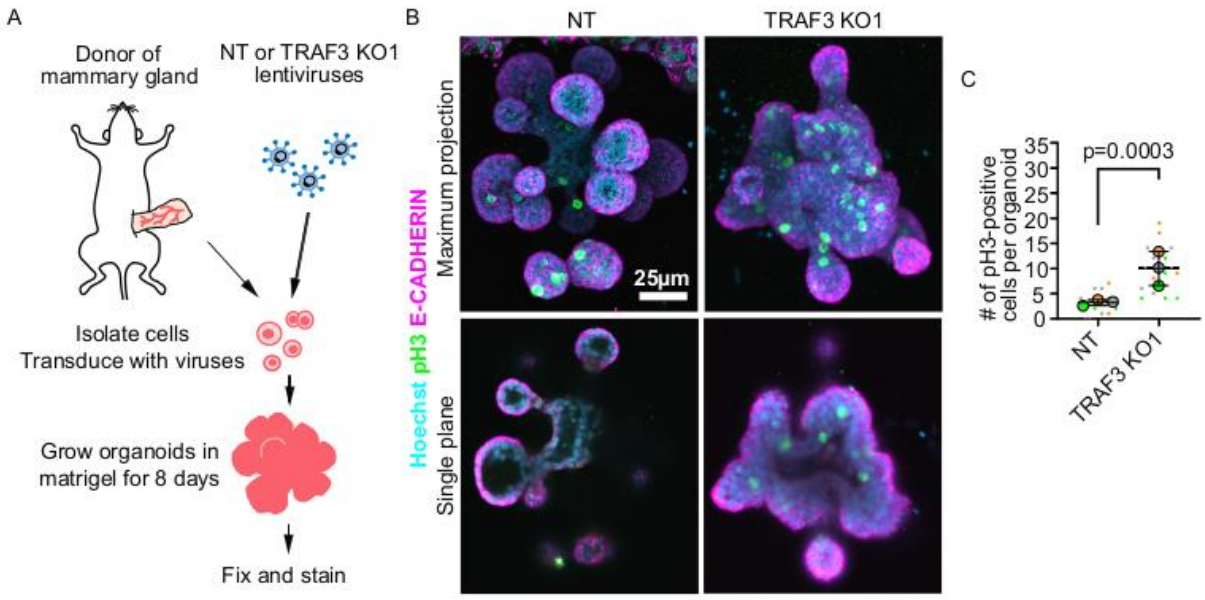

Figure 2-3. Loss of TRAF3 causes over-proliferation in primary mammary organoids.

(A) Primary mammary organoid experiment workflow. (B) Maximum intensity projection of NT and TRAF3 KO1 mammary organoids stained for phospho-HISTONE H3 (pH3), E-CADHERIN and DNA (Hoechst). Bottom panel – single confocal plane of NT and TRAF3 KO1 organoids. (C) Quantifications of the number of pH3-positive cells per organoid; 5-10 organoids of comparable size were quantified per condition per repeat. Data shown as a SuperPlot (n=3). P values were calculated by mixed model two-way ANOVA.

2.3.4. Loss of TRAF3 activates noncanonical NF-κB signaling to promote over-proliferation

How does TRAF3 regulate proliferation? We hypothesized that TRAF3 might be involved in the same pathways as in blood cells, where it negatively regulates both the canonical and noncanonical NF-κB pathways (He et al., 2006; Ramakrishnan et al., 2004; Sun, 2017; Zarnegar et al., 2008). In the noncanonical pathway, TRAF3 constitutively promotes proteasomal degradation of MAP3K14 (NIK), a kinase that is essential for activation of the downstream signaling cascade. Ligand recruitment to an upstream receptor triggers TRAF3 poly-ubiquitinylation and degradation. As a result, NIK levels increase, and it phosphorylates its downstream target IKKα, which in turn phosphorylates NFKB2 (p100). Phosphorylated p100 is partially degraded to p52, which enters the nucleus in association with RELB and regulates the transcription of target genes (Sun, 2017).

To test if loss of TRAF3 activates noncanonical NF-κB signaling, we examined the location of RELB in control and TRAF3 KO EpH4 cells and primary mammary gland organoids (Figure 2-4A-C). As expected, RELB was predominantly cytoplasmic in control cells and organoids. However, loss of TRAF3 caused a substantial nuclear accumulation, indicative of noncanonical NF-κB activation. We also performed immunoblotting for noncanonical NF-κB signaling components in control and TRAF3 KO cells at 1 and 4 DPC (Figure 2-4D, E). TRAF3 KO cells at both 1 and 4 DPC had substantially increased NIK levels and enhanced processing of p100 to p52 compared to NT control cells. However, cell density differences had no impact on NIK, RELB, TRAF3 and p100/p52 protein levels.

Therefore, TRAF3 KO leads to activation of noncanonical NF-κB signaling, but regulation of these pathway components is independent of cell density.

Based on previous literature, we predicted that loss of TRAF3 could also stimulate canonical NF-κB signaling (Figure 2-4F). IκB normally blocks RELA/p65 and p50 from entering the nucleus, but activation of upstream kinases IKKα/β by phosphorylation induces IκB phosphorylation and degradation (Ramakrishnan et al., 2004; Zarnegar et al., 2008). Surprisingly, however, RELA/p65 did not accumulate in the nuclei of TRAF3 KO cells (Figure 2-4G). Immunoblotting for the canonical NF-κB pathway components showed activation of IKKα/β phosphorylation at high density both in control and TRAF3 KO cells; but no IκB degradation was observed in control and TRAF3 KO cells either at low or at high density (Figure 2-4H). Together, these data demonstrate that in mammary epithelial cells, the loss of TRAF3 specifically activates noncanonical but not canonical NF-κB signaling.

If TRAF3 affects cell proliferation via the noncanonical NF-κB pathway, then deletion of p100 in TRAF3 KO cells should reduce proliferation to control levels (Figure 2-5A). To test this prediction, we generated a lentivector encoding a p100 sgRNA, plus GFP as a selection marker.

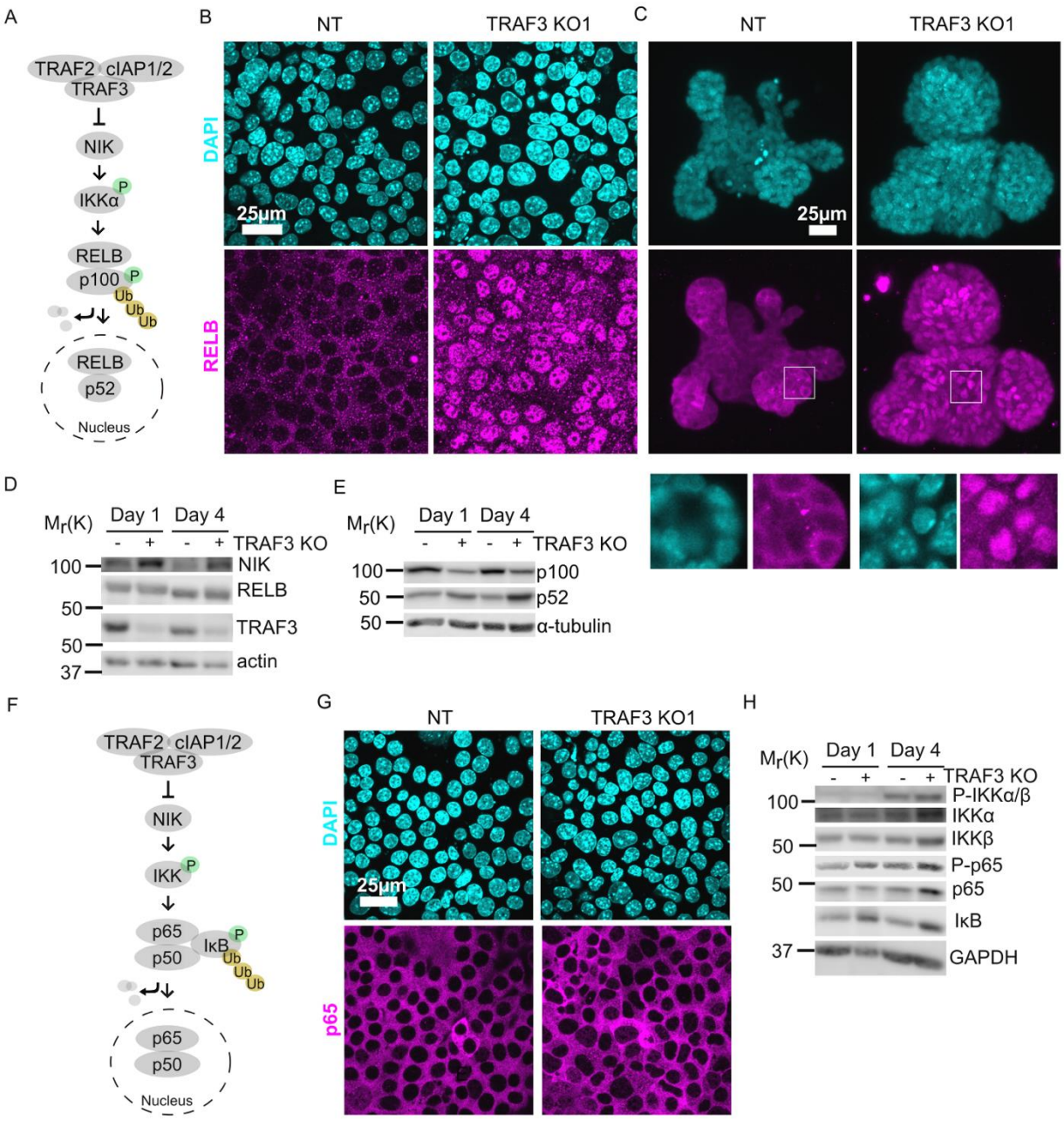

Figure 2-4. Loss of TRAF3 specifically activates noncanonical but not canonical NF-κB pathway.

(A) Simplified schematic of noncanonical NF-κB pathway. TRAF3 sends NIK for degradation. In the absence of TRAF3, NIK levels increase, and it activates the

downstream cascade, resulting in increased p100 processing to p52. RELB/p52 enters the nucleus where it regulates transcription of target genes. In experiments (B) – (C) RELB localization was tested in NT and TRAF3 KO1 cells. (B) – (C) Fluorescence staining of NT and TRAF3 KO1 EpH4 cells (B) and organoids (C) with anti-RELB antibodies and DAPI. (B) – single confocal planes. (C) – maximum intensity projection. White boxed ROIs are shown in enlarged images as single confocal planes. (D) Immunoblots of NT and TRAF3 KO1 lysates grown to 1 or 4 DPC probed for NIK, RELB, TRAF3 and actin as loading control. (E) Immunoblots of NT and TRAF3 KO1 lysates grown to 1 or 4 DPC probed for p100/p52 and α-tubulin as loading control. (F) A schematic of TRAF3-dependent activation of canonical NF-κB pathway. (G) Fluorescence staining of NT and TRAF3 KO1 cells with antibodies against p65 and with DAPI. (H) Western blotting of NT and TRAF3 KO1 cells at 1 DPC and 4 DPC probed for components of canonical NF-κB pathway and GAPDH as loading control.

We transduced EpH4 cells with virus and isolated GFP+ cells by FACS. Immunoblotting confirmed efficient knockout of p100 in NT control and TRAF3 KO cells (Figure 2-5B, B'). Blotting also showed increased cleavage of p100 to p52 in TRAF3 KO cells as compared to control cells (Figure 2-5B), and both bands were lost in cells expressing the *p100* sgRNA, confirming that the detected 52 kDa band is indeed the product of p100. We next grew cells to high density and analyzed pulsed BrdU incorporation by flow cytometry. There was no significant difference between control and NT/p100 KO cells, indicating that TRAF3 does not regulate cell cycling at low cell density. The proliferation of TRAF3/p100 double KO cells was, however, substantially reduced compared to TRAF3 KO cells (Figure 2-5 C, D) demonstrating that noncanonical NF-κB signaling is required for the phenotype induced by loss of TRAF3.

As a further test, we knocked out the effector kinase NIK. Immunoblotting (Figure 2-5E, E') revealed that, as expected, NIK is undetectable in NT control cells, but accumulates in TRAF3 KO cells. However, expression was lost in TRAF3/NIK double KO cells. Similar to p100 KO, deletion of NIK caused reduced proliferation in TRAF3 KO cells (Figure 2-5F, G).

To further confirm that noncanonical NF-κB pathway is necessary for the high density over-proliferation phenotype, we treated cells with BV6, a selective inhibitor of IAP proteins. cIAP1/2 is a part of the TRAF3 complex that degrades NIK. Therefore, we predicted that treatment with BV6 would induce over-proliferation. We treated cells with BV6 at low and high density (Figure 2-5H and I, respectively) and observed that BV6 treatment induces over-proliferation of NT cells at high density but not at low density, as shown by cytometric analysis of BrdU staining (Figure 2-5H, I).

We next asked if the noncanonical NF-κB pathway is sufficient to induce over-proliferation. We cloned and over-expressed a mutant NIK protein lacking the TRAF3-binding motif (NIK-ΔT3) (Liao, Zhang, Harhaj, & Sun, 2004), to prevent NIK degradation (Figure 2-5J). Flow cytometry and immunofluorescent staining showed strong over-proliferation of NT NIK-ΔT3 cells at 4 DPC compared to NT control cells (Figure 2-5K, L) demonstrating that activation of noncanonical NF-κB pathway is sufficient for increased proliferation at high density.

We conclude that TRAF3 normally suppresses proliferation at high cell density via inhibition of the noncanonical NF-κB pathway but does not impact proliferation at lower cell density. This pathway does not contribute to proliferation in WT EpH4 cells but is constitutively activated by loss of TRAF3. Activation of noncanonical NF-κB pathway downstream of TRAF3 is both necessary and sufficient for over-proliferation phenotype at high density.

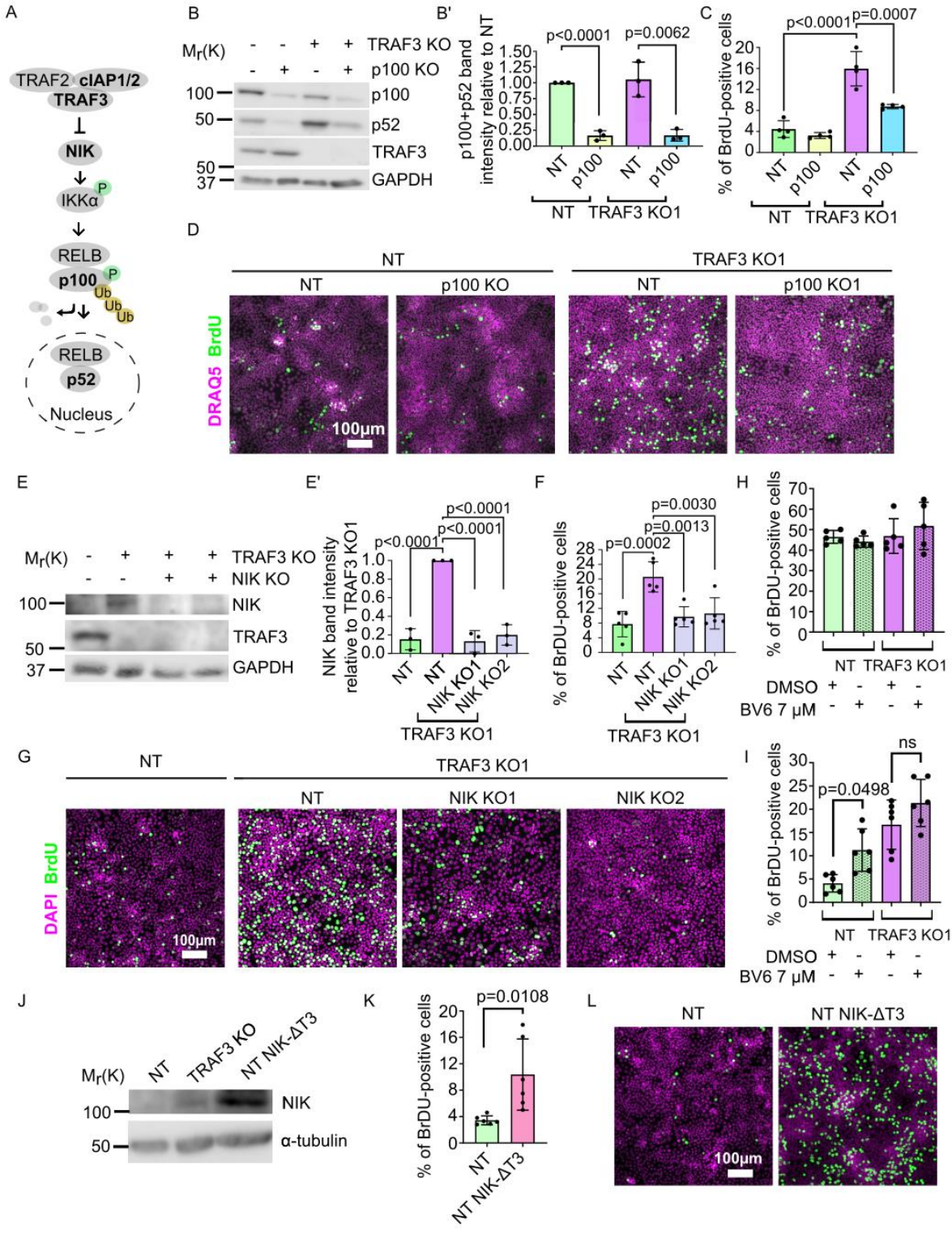

Figure 2-5. Noncanonical NF-κB signaling is necessary and sufficient for over-proliferation in TRAF3 KO cells.

(A) Noncanonical NF-κB pathway schematic. Proteins shown in bold were manipulated in this study. (B) Immunoblotting of NT and TRAF3 KO1 cells transduced with pLVTHM GFP NT or *p100* sgRNAs. Blot was stained for p100/p52, TRAF3 and GAPDH (loading control). (B') Quantifications of Western blot (B), histogram shows mean ± 1 s.d. (n=3). P values were calculated by Student's t-test. (C) Cytometric analysis of NT and TRAF3 KO cells transduced with pLVTHM GFP NT or *p100* sgRNAs. Graph shows mean ± s.d. (n=4). P values were calculated by one-way ANOVA followed by Tukey's multiple comparisons test. (D) NT and TRAF3 KO1 cells transduced with pLVTHM GFP NT or *p100* sgRNAs were treated with BrdU at 4 DPC and immunostained for BrdU and DAPI. (E) Immunoblot of NT and TRAF3 KO1 cells transduced with NT, NIK KO1 or KO2. Blot was stained for NIK, TRAF3 and GAPDH (loading control). (E') Quantifications of Western blot (E) Histogram shows mean ± 1 s.d (n=3). P values were calculated by one-way ANOVA followed by Tukey's multiple comparisons test. (F) Cytometric analysis of NT cells and TRAF3 KO1 cells transduced with control NT, NIK KO1 and KO2. Histogram shows mean ± 1 s.d. (n=5). P values were calculated by one-way ANOVA followed by Tukey's multiple comparisons test. (G) NT and TRAF3 KO1 cells transduced with control NT, NIK KO1 and KO2 were treated with BrdU at 4 DPC and immunostained for BrdU and DAPI. (H), (I) Cytometric analysis of NT and TRAF3 KO cells treated with 7 μM BV6 at low (H) and high (I) density. Histogram shows mean ± 1 s.d. (n=5 (H), n=6 (I)). P values were calculated by one-way ANOVA followed by Dunnett's (H) or Tukey's (I) multiple comparisons test (J) Immunoblot of NT, TRAF3 KO1 (positive control) and NT cells expressing pWPI mScarlet NIK ΔT3. Blot was stained for NIK and GAPDH (loading control). (K) Cytometric analysis of NT cells and NT pWPI mScarlet NIK ΔT3 cells.

Histogram shows mean ± 1 s.d. (n=6). P values were calculated by Student t-test. (L) NT and NT pWPI mScarlet NIK ΔT3 cells were treated with BrdU at 4 DPC and immunostained for BrdU and DAPI.

2.3.5. Noncanonical NF-κB signaling activates an innate immune response

Our data show that the loss of TRAF3 results in increased levels of the transcription factor p52, which is necessary for over-proliferation. However, gene expression changes downstream of noncanonical NF-κB signaling have not been investigated in epithelia; nor is it known which genes are targets of p52 in epithelial cells. Therefore, to identify downstream effectors of TRAF3 and noncanonical NF-κB signaling, we performed genome-wide transcriptomics analysis on NT control cells, TRAF3 KO, and TRAF3/p100 double KO cells. For these studies, we used our EpH4-FUCCI mammary epithelial cell line, which was transduced with NT, *Traf3*, or *Traf3* plus *p100* sgRNA lentiviruses, and sorted for G1/G0 phase (mCherry+) cells (Figure 2-6A). This strategy eliminates indirect gene expression differences reflective of the larger fraction of cycling (mCitrine+) cells caused by loss of TRAF3 but will not remove constitutive changes in gene expression.

Two biological replicates of each cell line were processed, and fastq files were analyzed using CLC Genomics Workbench and Ingenuity Pathway Analysis (IPA). Differential gene expression was filtered for > 2-fold differences, FDR < 0.05. Surprisingly, IPA did not detect any stimulation by TRAF3 KO of those signaling pathways classically involved in proliferation, including PI3K/AKT, JNK, TGF-β, WNT and Hippo (Figure 2-6B). There was, however, a dramatic induction of innate immune response genes. Antigen presentation, interferon response genes and genes responsible for foreign DNA and RNA recognition were strongly upregulated by deletion of TRAF3 (Figure 2-6B-E). Additionally, TRAF3 KO cells over-express adhesion molecules *Icam1* and *Vcam1* that facilitate adhesion of recruited leukocytes (Figure 2-6F). Superoxide-

producing NADPH-oxidase complex genes, which eliminate bacteria and fungi, were also induced (Figure 2-6G), as were several chemokines and growth factors (Figure 2-6H), but some genes that normally respond to pathogens, such as defensins, IL-8, and IL-17, were not affected.

The comparison of TRAF3 KO and TRAF3/p100 double KO samples revealed that not all pathways activated by TRAF3 KO could be reversed by blocking noncanonical NF-κB signaling. We found that p100 KO partially reduces antigen presentation gene expression, the interferon response pathway, and foreign DNA and RNA recognition genes (Figure 2-6B-E), but differential gene expression of other pathways was not significantly changed. These data argue that antigen presentation, interferon pathways and foreign DNA and RNA recognition genes are downstream targets of noncanonical NF-κB signaling in mammary epithelial cells. However, none of these pathways are likely to promote cell proliferation. Rather, the data suggest that noncanonical NF-κB signaling instead suppresses signals that normally would cause cell cycle exit.

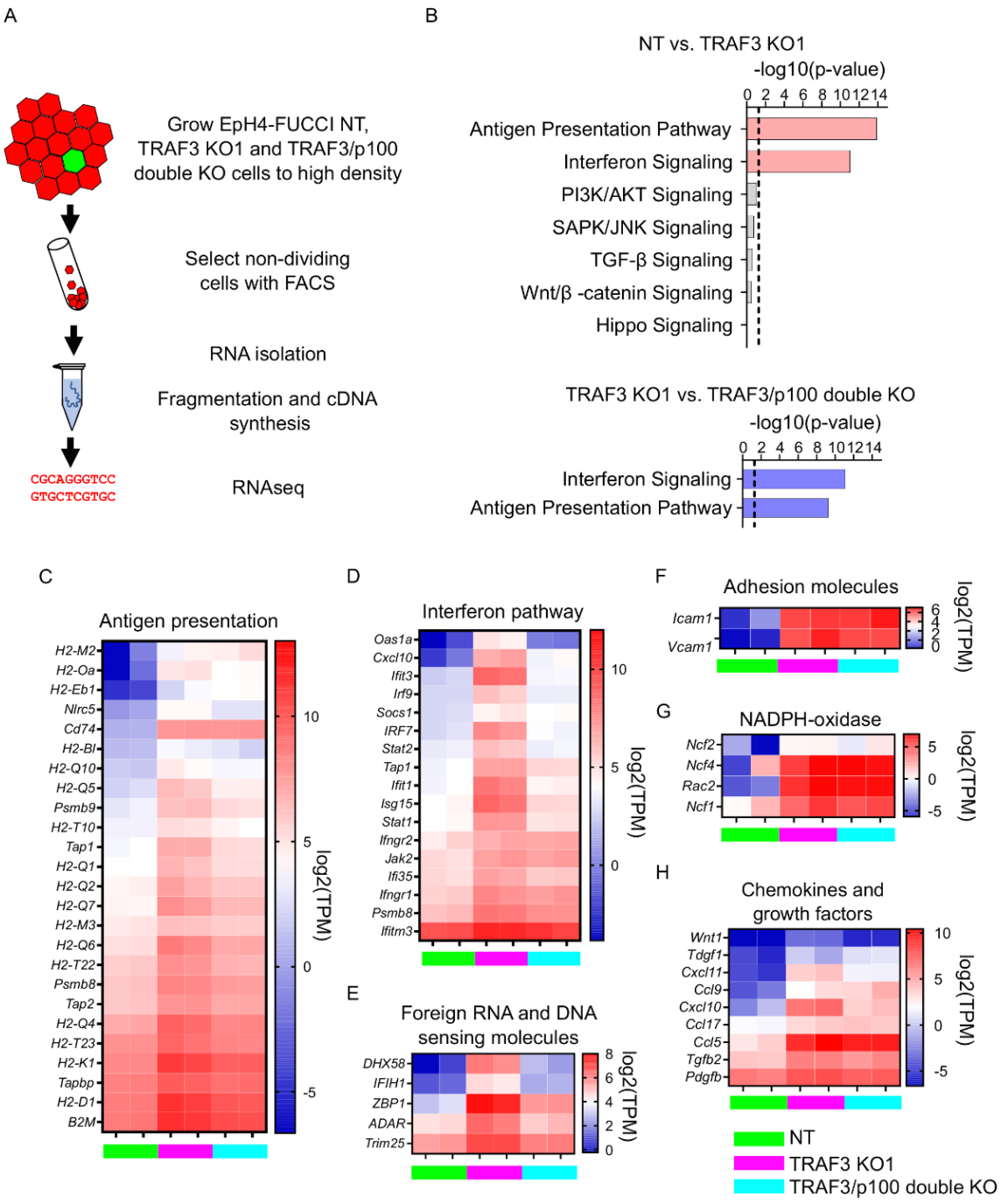

Figure 2-6. Loss of TRAF3 in EpH4 cells induces immune response pathways.

(A) RNAseq experiment workflow. (B) Ingenuity Pathway Analysis (IPA) of RNAseq data showing significant upregulation of pathways related to infection response in TRAF3 KO

cells compared to NT control (top, pink bars), and significant reduction of these pathways in TRAF3/p100 double KO cells compared to TRAF3 KO cells (bottom, blue bars). Notably, Hippo signaling and other pathways that regulate proliferation were unchanged. Threshold line is $p<0.05$. (C)-(H). Heatmaps comparing mRNA levels of antigen presentation (C), interferon (D), foreign RNA and DNA recognition (E) pathway components, adhesion molecules (F), NADPH-oxidase components (G), chemokines and growth factors (H) between NT, TRAF3 KO1 and TRAF3/p100 double KO in two experimental repeats. NT, TRAF3 KO1 and TRAF3/p100 double KO are color-coded with green, purple and light blue, respectively. Data are presented as log2 of transcripts per million (TPM).

2.3.6. Loss of TRAF3 does not affect YAP signaling

Hippo/YAP signaling is a key mechanism that prevents abnormal proliferation at high density. Therefore, we tested whether the response to deletion of TRAF3 is independent of this pathway. The transcriptional co-activator YAP, a downstream effector of Hippo, is nuclear at low cell density and promotes cell cycling, but becomes phosphorylated and is cytoplasmic at high density (Ma, Meng, Chen, & Guan, 2019). Therefore, we asked if loss of TRAF3 induces YAP translocation to the nucleus. We immunostained control, NF2 KO cells (positive control) and TRAF3 KO cells with anti-YAP antibodies. In dense cultures, YAP was predominantly cytoplasmic in the NT control cells, but nuclear in NF2 KO cells, as expected. However, deletion of TRAF3 did not induce significant nuclear accumulation of YAP, as compared to the NT control (Figure 2-7A, B). Moreover, comparison of expression profiles for conserved YAP target genes (Cordenonsi et al., 2011) from our RNAseq data showed an absence of any significant induction for more than 90% of conserved YAP target genes in TRAF3 KO cells compared to the NT control (Figure 2-7C). We conclude, therefore, that TRAF3 loss promotes over-proliferation independently of YAP, a major regulator of cell density-dependent proliferation.

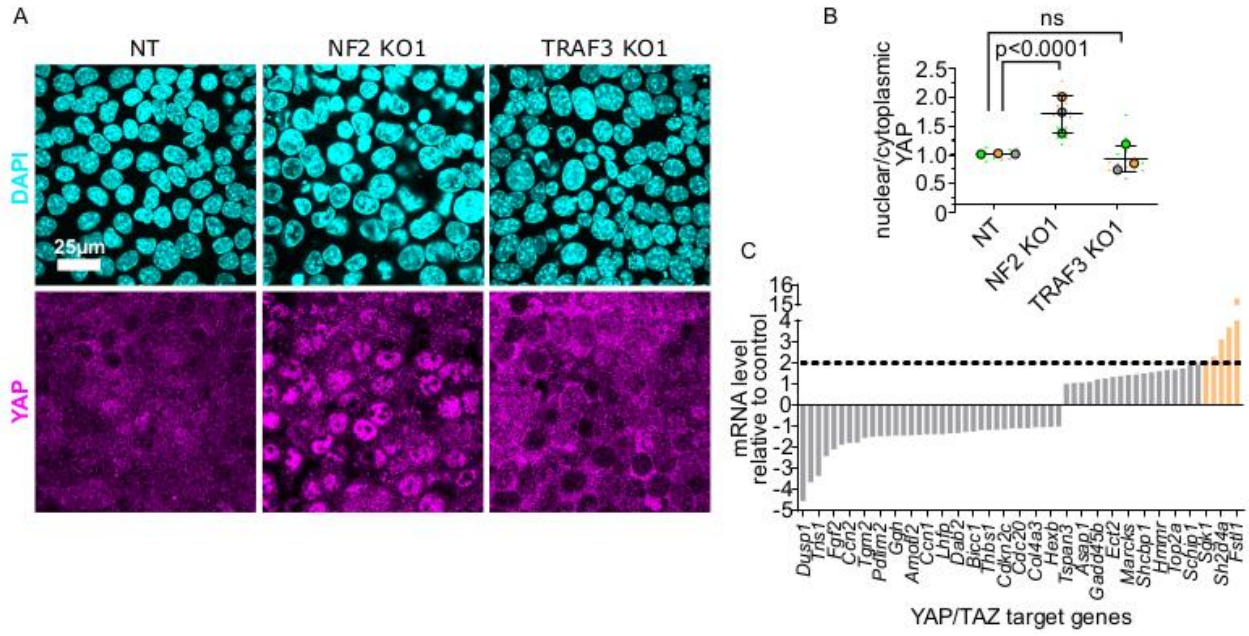

Figure 2-7. YAP/TAZ signaling is not activated by loss of TRAF3.

(A) NT, NF2 KO1 and TRAF3 KO1 cells stained for YAP and DAPI. (B) Quantifications of nuclear to cytoplasmic YAP ratio in NT, NF2 KO1 and TRAF3 KO1 cells. Measurements were of at least 12 fields of view per condition per experimental replicate, and the average ratio was calculated. Data are presented as a SuperPlot (n=3). P values were calculated by mixed model two-way ANOVA. (C) Conserved YAP/TAZ gene signature expression in TRAF3 KO1 cells shown as fold differences between NT control and TRAF3 KO1. Dashed threshold line is based on 2x increase in gene expression.

2.3.7. The TRAF3 KO cell over-proliferation phenotype is cell autonomous

Our RNAseq data showed that several secreted factors including chemokines and growth factors (Figure 2-6H) are induced by loss of TRAF3, and we hypothesized that

these factors might be secreted and trigger over-proliferation at high density in neighboring cells. To test this possibility, we labeled NT control cells with GFP and, separately, control or TRAF3 KO cells with mScarlet, then mixed red and green cells (NT + TRAF3 KO, or NT + NT) at a 1:1 ratio, and after 4 DPC stained them for the proliferation marker KI-67 and DAPI (Figure 2-7 - Figure supplement 1A). Cytokines released from the TRAF3 KO cells could then, in principle, stimulate proliferation of surrounding NT (GFP+) control cells. However, there was no significant difference in the fraction of KI-67+ cells between NT GFP cells mixed with NT mScarlet and NT GFP cells mixed with TRAF3 KO mScarlet cells (Figure 2-7 - Figure supplement 1B). These data strongly argue that the over-proliferation phenotype is cell autonomous and is not a consequence of secreted cytokines or other factors.

2.3.8. Loss of TRAF3 does not affect the levels of cyclin-dependent kinase inhibitors (CKIs)

The p27 CKI has been reported to inhibit density-dependent proliferation in response to changes in LLGL1/2 expression (Yamashita et al., 2015). Moreover, we demonstrated that shRNA knockdown of *p27* can promote cell proliferation in EpH4 cells (Figure 2-1B, C, Figure 2-1 - Figure supplement 1A, B). Therefore, we asked if the noncanonical NF-κB pathway suppresses CKI induction at high cell density. We immunoblotted for p27 and other CKIs including CDKN1A (p21), CDKN2C (p18) and CDKN2D (p19), in subconfluent and dense (4 DPC) cultures of NT, NT/p100 KO, TRAF3 KO1, and TRAF3/p100 double KO cells (Figure 2-7 - Figure supplement 2A-C). p21 levels were low in cells at low density, but were high in all dense cultures, irrespective of

TRAF3 or p100 expression. No significant changes in any of the other CKIs we tested were detected at low versus high cell density, or in the absence of TRAF3 or p100 (Figure 2-7 - Figure supplement 2A'-C'). These data argue that noncanonical NF-κB signaling overrides the ability of these CKIs to induce cell cycle arrest in EpH4 cells.

2.3.9. Loss of TRAF3 blocks cells from entering G0

It was previously shown that TRAF3 induces over-proliferation by triggering CYCLIN D1 expression (Demicco et al., 2005; S. G. Park, Chung, Kang, Kim, & Jung, 2006); (Rocha, Martin, Meek, & Perkins, 2003; Zhang, Warren, Shoemaker, & Ip, 2007); (Cao et al., 2001). We analyzed CYCLIN D1 in dense TRAF3 KO cells compared to NT cells by immunofluorescence. Indeed, we observed a small increase of CYCLIN D1 levels in TRAF3 KO cells compared to control (Figure 2-8A, B).

We hypothesized that loss of TRAF3 prevents cells from entering the G0 quiescent state. Through this mechanism loss of TRAF3 should give a proliferative advantage to cells not only at high density, but also under other challenging conditions, such as starvation, that also promote entry into G0. To test this idea, we grew NT and TRAF3 KO cells in normal medium or medium devoid of FBS (Figure 2-8C). We observed no difference in proliferation between NT and TRAF3 KO cells in normal medium after 1 DPC. However, starvation decreased proliferation in control cells but not in TRAF3 KO cells. These data suggest that loss of TRAF3 prevents cells from entering G0.

To further explore this possibility, we labeled control and TRAF3 KO cells with markers to differentiate quiescent and cycling cells. Cells exiting the cell cycle and

entering G0 are known to have very low CDK2 activity. To determine if loss of TRAF3 prevents entry into G0, we used a previously validated biosensor, DHB-mVenus, which can quantitatively reveal CDK2 activity in live cells based on its distribution between the nucleus (G0/G1) and cytoplasm (G2/M) (Figure 2-8D) (Gookin et al., 2017; Spencer et al., 2013). As shown in Figure 2-8E and F, at high density control cells enter quiescence, with almost exclusive nuclear localization of the biosensor. In contrast, cells lacking TRAF3 show an increased percent of cytoplasmic DHB-mVenus localization at high density, consistent with them continuing in cycle instead of entering quiescence.

Finally, we stained the cells for phospho-Rb (Ser807/811). The retinoblastoma protein is a central regulator of the cell cycle, and becomes dephosphorylated in G0, but is progressively phosphorylated and inactivated as cells leave G0 and move through G1 into S phase (Figure 2-8D) (Gookin et al., 2017; Spencer et al., 2013). Rb phosphorylation was very low in NT control at high density but loss of TRAF3 induced a dramatic increase in phospho-Rb positive cells (Figure 2-8E, G). Together, these data strongly argue that the key effect of loss of TRAF3 is a failure to enter G0 under conditions that normally promote quiescence.

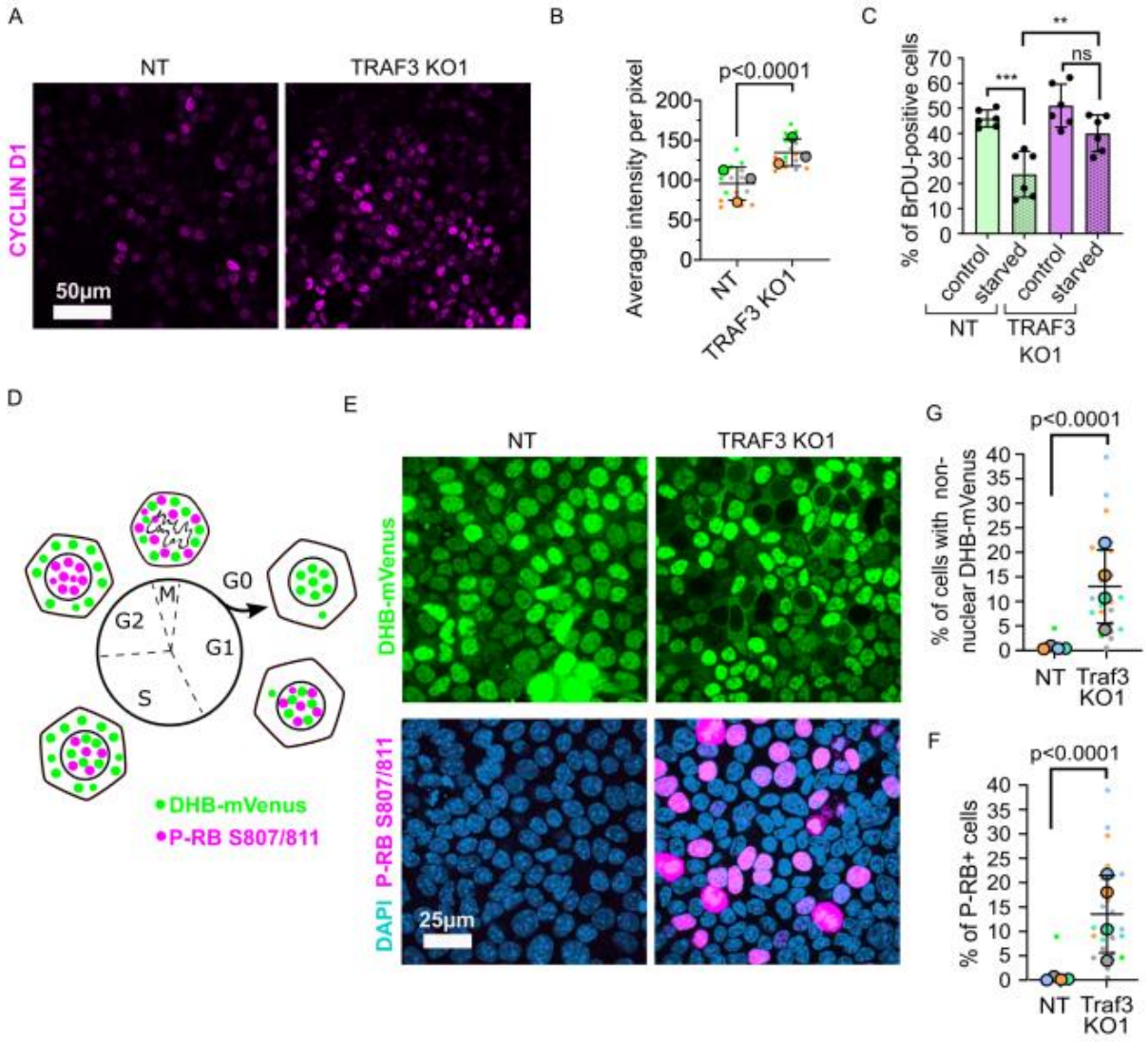

Figure 2-8. Loss of TRAF3 prevents cells from entering G0.

(A) NT and TRAF3 KO1 cells stained for CYCLIN D1 and DAPI. (B) Quantifications of CYCLIN D1 positive cells in NT and TRAF3 KO cells. Data are presented as a SuperPlot (n=3). P value was calculated by mixed model two-way ANOVA. (C) NT and TRAF3 KO1 cells grown for 24 hrs in regular media or media without FBS (starved) were treated with BrdU and analyzed by flow cytometry. (D) A schematic of DHB-mVenus and phospho-RB

S807/811 localization at different phases of cell cycle. (E) NT and TRAF3 KO1 cells stably expressing DHB-mVenus were grown to 4 DPC and stained for phospho-RB S807/811 and DAPI. (F) Quantifications of cells with non-nuclear DHB-mVenus localization. Data are presented as a SuperPlot (n=4). P value was calculated by mixed model two-way ANOVA. (G) Quantification of phospho-RB positive cells. Data are presented as a SuperPlot (n=4). P value was calculated by mixed model two-way ANOVA.

2.4. Discussion

Epithelial cells possess intrinsic mechanisms to achieve and maintain an appropriate cell density, which is essential for normal tissue morphogenesis and maintenance (Fomicheva et al., 2019). Mechanisms of homeostatic cell density establishment are not fully understood. One of the most recognized pathways controlling cell density-dependent proliferation is the Hippo/YAP signaling pathway (Dupont et al., 2011). However, there are other mechanisms that control cell density independently from Hippo/YAP; for instance, LLGL1/2 controls p27 levels in a density-dependent manner (Yamashita et al., 2015). With the goal of identifying novel components that control homeostatic cell density, we used an unbiased genome-wide CRISPR KO screen, in which we selected for cells that over-proliferate at high density. We uncovered a known (NF2) and two novel (TRAF3 and UBE2M) regulators of epithelial cell density. Loss of any of these genes results in increased cell proliferation at high density and multilayering of cells; however, proliferation at low cell density remains unaltered.

TRAF3 was of particular interest because this protein is essential for blood cell expansion and regulation of the immune response, but its functions in other tissues still remain unclear, although it is ubiquitously expressed (Yue et al., 2014). We discovered that loss of TRAF3 results in cell overgrowth in both mouse and human mammary gland cell lines, and mesenchymal cells (NIH 3T3 fibroblasts) as well as in primary mouse mammary gland organoids. We interrogated the mechanism of TRAF3-dependent proliferation control in mammary gland epithelial cells (Figure 2-9) and found that loss of TRAF3 specifically activates the noncanonical branch of NF-κB signaling, while having

no effect on canonical NF-κB signaling. We further discovered that the noncanonical pathway is necessary for over-proliferation at high density in cells lacking TRAF3.

Our RNAseq data revealed that loss of TRAF3 does not induce the transcription of classical proliferation pathway components, including YAP/TAZ, PI3K/AKT, MAPK, TGF-β and WNT signaling. We also demonstrated that over-proliferation caused by loss of TRAF3 is cell autonomous, as control cells did not over-proliferate when co-cultured with TRAF3 KO cells. Together, these data suggest that noncanonical NF-κB signaling does not positively drive proliferation but instead suppresses the ability of cells to exit the cell cycle. One key exit mechanism operates through induction of cyclin-dependent kinase inhibitors. For instance, in some epithelial cells p27 levels increase with density and high levels of p27 inhibit cell proliferation (Yamashita et al., 2015). However, we found no differences in levels of p27 or other CKIs (p21, p19 and p18) in cells lacking TRAF3 versus control EpH4 cells, although p21 levels do increase with increased cell density. Therefore, either EpH4 cells do not respond to CKIs or constitutive activation of the noncanonical NF-κB pathway overrides CKI-mediated cell cycle exit. Nonetheless, our data demonstrate that loss of TRAF3 prevents cells from entering quiescent state G0 as shown by increased CDK2 activity and RB phosphorylation.

RNAseq analysis revealed that loss of TRAF3 leads to the activation of immune response pathways, at least in part through noncanonical NF-κB signaling. Activated genes include antigen presentation, interferon response pathways, and genes responsible for foreign DNA and RNA recognition. Expression of these genes was reduced when p100 was deleted in theTRAF3 KO cells. However, certain genes induced in the TRAF3 KO cells, including adhesion molecules, superoxide-producing enzymes

and chemokines, were not reduced by deletion of p100. These data reveal that a mechanism-independent of noncanonical NF-κB signaling can drive gene expression responses activated by loss of TRAF3.

The literature suggests that the loss or reduction of *Traf3* expression or activation of noncanonical NF-κB signaling might be important for hyperplasia in response to infection or contribute to cancer development. It is known that epithelial cells can respond to infection by mounting an innate immune response. The noncanonical NF-κB pathway can be activated by contact with pathogens, and bronchial, intestinal, and mammary gland epithelia can each express a variety of innate immune factors that protect the organisms against infectious agents and attract immune cells (Philpott, Girardin, & Sansonetti, 2001; Strandberg et al., 2005). *H. pylori*, a bacterium associated with the development of gastritis and gastric cancer, activates noncanonical NF-κB signaling in a stomach epithelial cell line, and in *H. pylori*-associated gastritis (Feige, Vieth, Sokolova, Tager, & Naumann, 2018). Moreover, activation of the noncanonical NF-κB pathway in response to infection correlates with hyperplasia of the ear mucosa following otitis infection, although the mechanism was not investigated (Cho et al., 2016).

As discussed above, *Traf3* is mutated, though at low frequency, in different cancers of epithelial origin (Zhu et al., 2018), and low expression is associated with worse outcomes. Noncanonical NF-κB signaling is also associated with different epithelial cancers, including breast cancer (Rojo et al., 2016; Sovak et al., 1997) and lung cancer (Dimitrakopoulos et al., 2019). Further work will be required to determine the impact of this pathway in cancer development.

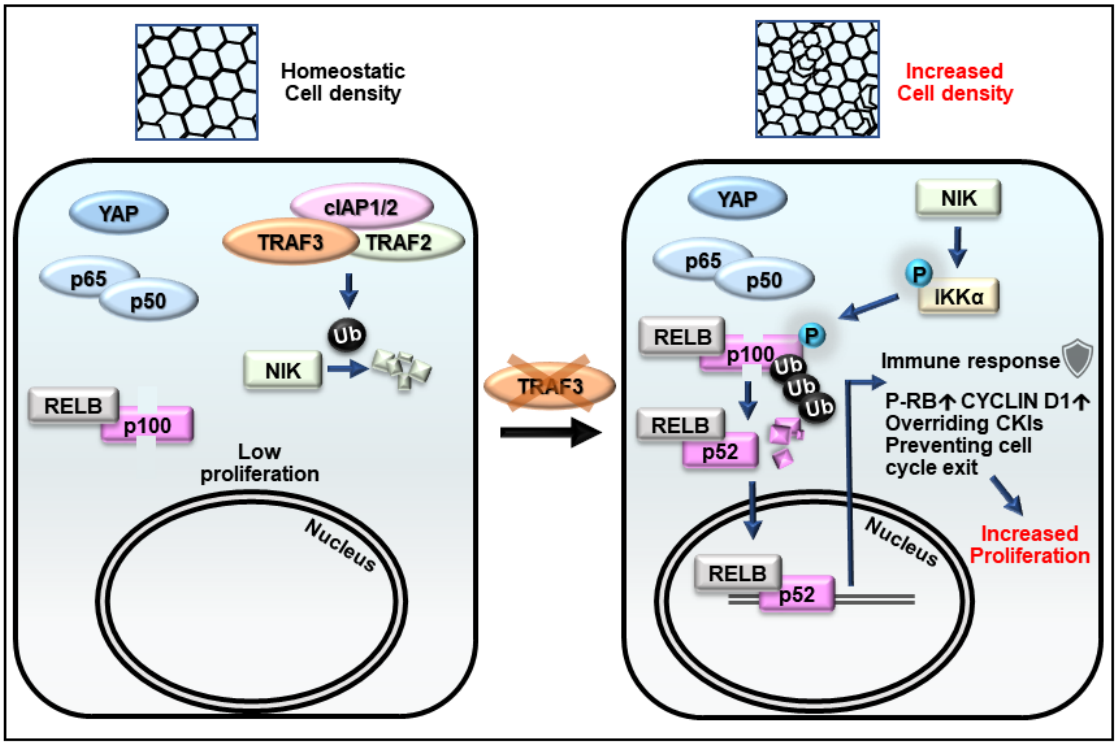

Figure 2-9. Model for the role of TRAF3 in density-dependent proliferation.

Cells at high density rarely proliferate (on the left). They have active Hippo signaling (YAP is cytoplasmic), and inactive canonical NF-κB (p65/p50 is cytoplasmic) and noncanonical NF-κB signaling (NIK is low, p100 is not processed to p52, RELB is cytoplasmic). Upon loss of TRAF3, Hippo and canonical NF-κB signaling remain unaltered, but noncanonical NF-κB signaling is activated (on the right). NIK levels rise in the absence of TRAF3, activates the downstream cascade, resulting in increased p100 processing to p52. The RELB/p52 complex activates innate immune response genes, including antigen presentation and interferon pathway components. It also overrides CKIs, induces CYCLIN D1 expression and prevents entering G0 as shown by increased number of cells with

active CDK2 and phosphorylated RB. Altogether it results in cell over-proliferation at high density.

2.5. Materials and methods

Table 1. Key Resources Table.

Reagent (species) or resource	Designation	Source or reference	Identifiers	Additional information
Recombinant DNA reagent (Mus musculus)	Gecko v2 KO Pooled Library	Sanjana et al, 2014, PMID: 25075903; Addgene	CAT: 1000000052	
Recombinant DNA reagent (Mus musculus)	Scrambled control shRNA	Sigma MISSION shrna library	CAT: SHC016-1EA	
Recombinant DNA reagent (Mus musculus)	The p27 shRNA	Sigma MISSION shrna library	CAT: TRCN0000287390	
Recombinant DNA reagent (Mus musculus)	P27-qPCR-FWD primer	This paper	N/A	TCAAACGTGAGAGTGTCTAACG
Recombinant DNA reagent (Mus musculus)	P27- qPCR-REV primer	This paper	N/A	CCGGGCCGAAGAGATTTCTG
Recombinant DNA reagent (Mus musculus)	Puromycin-qPCR-FWD primer	This paper	N/A	CTGCAAGAACTCTTCCTCACG

Recombinant DNA reagent (Mus musculus)	Puromycin-qPCR-REV primer	This paper	N/A	GGGAACCGCTCAACTCGG
Recombinant DNA reagent (Mus musculus)	Control non-targeting (NT) sgRNA	This paper	N/A	GCGAGGTATTCGGCTCCGCG
Recombinant DNA reagent (Mus musculus)	Nf2 sgRNA KO1	This paper	N/A	CGAGATGGAGTTCAACTGCG
Recombinant DNA reagent (Mus musculus)	Nf2 sgRNA KO2	This paper	N/A	ATACTGCAGTCCAAAGAACC
Recombinant DNA reagent (Mus musculus)	Traf3 sgRNA KO1	This paper	N/A	GTGCTCGTGCCGGAGCAAGG
Recombinant DNA reagent (Mus musculus)	Traf3 sgRNA KO2	This paper	N/A	TGGCCCTTCAGGTCTACTGT
Recombinant DNA reagent (Mus musculus)	Ube2m sgRNA KO1	This paper	N/A	GCGCAGCTCCGGATTCAGAA
Recombinant DNA reagent (Mus musculus)	Ube2m sgRNA KO2	This paper	N/A	GAGTCGGCCGGCGGCACCAA

Recombinant DNA reagent (Mus musculus)	Nfkb2/p100 sgRNA KO1	This paper	N/A	CTGAGCGTGATAAATGACGT
Recombinant DNA reagent (Mus musculus)	Nfkb2/p100 sgRNA KO2	This paper	N/A	CTGTTCCACAATCACCAGAT
Recombinant DNA reagent (Mus musculus)	Map3k14/NIK sgRNA KO1	This paper	N/A	TCAGAGCGCATTTTCATCGC
Recombinant DNA reagent (Mus musculus)	Map3k14/NIK sgRNA KO2	This paper	N/A	GTCGAGGCAGTACCGGTCGC
Recombinant DNA reagent (Homo sapiens)	Traf3 sgRNA KO1	This paper	N/A	AGATTCGCGACTACAAGCGG
Recombinant DNA reagent (Homo sapiens)	Traf3 sgRNA KO2	This paper	N/A	CCTCACATGTTTGCTCTCGC
Recombinant DNA reagent (Homo sapiens)	DHB-mVenus	Spencer et al., 2013, PMID: 24075009; Addgene	CAT: 136461, RRID: Addgene_136461	
Recombinant DNA reagent (synthetic)	ES-FUCCI	Sladitschek and Neveu, 2015, PMID: 25909630; Addgene	CAT: 62451, RRID: Addgene_62451	

Recombinant DNA reagent (Mus musculus)	pWPI-mScarlet NIK-ΔT3	This paper	N/A	Mouse NIK with deleted TRAF3 binding motif (amino acids 78–84) cloned into pWPI-mScarlet vector
Antibody	Anti-NF2/MERLIN (rabbit monoclonal)	CST	CAT: 6995S, RRID: AB_10828709	1:750, WB
Antibody	Anti-TRAF3 (mouse monoclonal)	Santa Cruz	CAT: sc-6933, RRID: AB_628390	1:200, WB
Antibody	Anti-UBE2M (rabbit polyclonal)	Proteintech	CAT: 14520-1-AP	1:500, WB
Antibody	Anti-NF-κB2 p100/p52 (rabbit polyclonal)	CST	CAT: 4882, RRID: AB_10695537	1:750, WB
Antibody	Anti-NIK (rabbit polyclonal)	CST	CAT: 4994S, RRID: AB_2297422	1:500, WB
Antibody	Anti-RELB (rabbit monoclonal)	Abcam	CAT: ab180127	1:1000, WB; 1:300, IF
Antibody	Anti-NF-κB Pathway Sampler Kit Antibody	CST	CAT: 9936, RRID: AB_561197	1:1000, WB

Antibody	Anti-CDKN1B/p27 (rabbit polyclonal)	BD Transduction Laboratories	CAT: 610241, RRID: AB_610241	1:1000, WB
Antibody	Anti-p21 (mouse monoclonal)	Invitrogen	CAT: ma5-14353, RRID: AB_10986834	1:1000, WB
Antibody	Anti-p19 (rabbit polyclonal)	Santa Cruz	CAT: sc-1063, RRID: AB_2078865	1:200, WB
Antibody	Anti-p18 (rabbit polyclonal)	Santa Cruz	CAT: sc-1064, RRID: AB_2078729	1:200, WB
Antibody	Anti-GAPDH (rabbit monoclonal)	CST	CAT: 2118S, RRID: AB_561053	1:2000, WB
Antibody	Anti-α-tubulin (mouse monoclonal)	Sigma-Aldrich	CAT: T-9026, RRID: AB_477593	1:4000, WB
Antibody	Anti-actin (mouse monoclonal)	Sigma-Aldrich	CAT: A4700, RRID: AB_476730	1:4000, WB
Antibody	Anti-BrdU antibodies	Abcam	CAT: ab6326,	1:800, IF, Flow

	(rat monoclonal)		RRID: AB_305426	
Antibody	Anti-YAP (rabbit polyclonal)	Novus Biologicals	CAT: NB110-58358, RRID: AB_922796	1:200, IF
Antibody	Phospho-RB Ser807/811 (rabbit monoclonal)	CST	CAT: 8516S, RRID: AB_11178658	1:1000, IF
Antibody	Anti-CYCLIN D1 (mouse monoclonal)	Invitrogen	CAT: MA5-11387, RRID: AB_10987096	1:50, IF
Antibody	Anti-KI-67 (rabbit polyclonal)	Invitrogen	CAT: 18-0191Z, RRID:AB_86661	1:70, IF
Antibody	Anti-Phospho-HISTONE H3 (Ser10) (mouse monoclonal)	CST	CAT: 9706S, RRID:AB_331748	1:300, IF
Antibody	Anti-E-CADHERIN (rat monoclonal)	Thermo Fisher Scientific	CAT: 14-3249-80, RRID:AB_1210459	1:500, IF
Fluorescent dye	Hoechst 33342	Life Technologies	CAT: 62249	1:1000, IF

Fluorescent dye	DAPI	Sigma-Aldrich	CAT: 422801	1:500, IF
Fluorescent dye	DRAQ5	CST	CAT: 4084	1:1000, IF
Cell line (Mus musculus)	EpH4	Dr. Jurgen Knoblich, Institute of Molecular Biotechnology, Vienna, Austria		Identity verified by rnaseq, DNA sequencing and immunofluorescent staining for epithelial markers
Cell line (Homo sapiens)	HEK293T	ATCC	RRID: CVCL_0063	
Cell line (Homo sapiens)	MCF10a	ATCC	RRID: CVCL_0598	
Cell line (Mus musculus)	NIH 3T3	ATCC	RRID: CVCL_0594	
Strain (Mus musculus)	C3H/HeNCrl	Charles River Laboratories	CAT: CRL:025, RRID: IMSR_CRL: 025	
Chemical compound, drug	BV6	Apexbio	Cat: B4653	
Software	GraphPad Prism	Graphpad	RRID:SCR_ 002798	
Software	CLC Genomics Workbench	Qiagen	RRID:SCR_ 011853	
Software	Ingenuity Pathway	Qiagen	RRID:SCR_ 008653	

	Analysis (Qiagen)			
Software	Fiji is just ImageJ	N/A	RRID:SCR_002285	
Software	MAGeCK software	Li et al., 2014, pmid: 25476604	N/A	

2.5.1. Whole-genome CRISPR KO screen

Mouse CRISPR GeCKO v2 Knockout Pooled Library (Sanjana et al., 2014; Shalem et al., 2014) was purchased from Addgene. The library was amplified according to the developer's protocol (Sanjana et al., 2014; Shalem et al., 2014). Library lentiviruses were produced as described below. EpH4-FUCCI cells transduced with the library were grown for 10 d to allow time for gene-editing and depletion of the target proteins. The cells were then seeded at 100,000 cells/cm^2 and cultured for 4 d, then trypsinized with 0.25% Trypsin (Gibco) and 4x10^7 cells (about 300 cells per sgRNA) were sorted on a FACSAria lll for mCitrine+ (proliferating) cells. This population was replated, expanded, and resorted for mCitrine+ cells. This process was repeated for a total of three sorts. Genomic DNA from 4x10^7 cells before sorting, and after the 1st, 2nd and 3rd rounds of sorting was purified using Blood & Cell Culture DNA Midi Kit (Qiagen). The sgRNA sequences were PCR amplified (26 x100µl reactions) from genomic DNA (~260 µg) using adaptor primers developed by the Zhang laboratory. The products of the first PCR reactions were amplified again with Illumina index primers to add barcodes and Illumina adaptors. The products of this reaction were purified and sequenced on a Novaseq instrument. We

utilized MAGeCK software (W. Li, Xu, et al., 2014) to analyze the fastq files. A read count distribution graph was generated using RStudio.

2.5.2. Plasmid constructs and primers

ES-FUCCI (plasmid # 62451 (Sladitschek & Neveu, 2015)) and DHB-mVenus (plasmid #136461 (Spencer et al., 2013)) were purchased from Addgene. The *p27* shRNA clone TRCN0000287390 in pLKO1 was obtained from the Sigma MISSION shRNA library. *p27* knockdown was tested by qPCR and compared to cells transduced with a scrambled non-targeting control shRNA (Figure 2-1 - source data 2).

The sgRNAs used in this study are listed in the Key Resources Table (Table 1). sgRNAs were cloned into lentiCRISPR v2 vector at the *BsmB*I restriction site using Zhang lab protocol (Sanjana et al., 2014; Shalem et al., 2014). p100 sgRNAs were cloned into a modified pLVTHM GFP vector between *Cla*I and *Mlu*I sites or into lentiCRISPR v2 vector.

Deletion of TRAF3 binding motif (amino acids 78–84) from wildtype NIK cDNA was performed by site-directed mutagenesis. NIK-ΔT3 cDNA was cloned into the pWPI mScarlet vector between *BamH*I and *Asc*I sites.

2.5.3. Cell culture, lentiviral transductions, transfections and chemicals

EpH4 cells were obtained from Dr. Jurgen Knoblich (Institute of Molecular Biotechnology, Vienna, Austria). HEK293T, MCF10a, and NIH 3T3 were obtained from the ATCC. EpH4, NIH 3T3 and HEK293T cells were cultured in DMEM (Gibco)

supplemented with 10% fetal bovine serum (Atlanta Biologicals), and 1x penicillin/streptomycin (Life Technologies). MCF10a cells were cultured in DMEM/F12 media (Gibco) supplemented with 5% Horse Serum (Gibco), EGF 20 ng/ml (Sigma), hydrocortisone 0.5 mg/ml (Sigma), cholera toxin 100 ng/ml (MP Biomedicals), insulin 10 µg/ml (Sigma), and 1x penicillin/streptomycin (Life Technologies). EpH4 cells were seeded at 100,000 cells/cm^2 and cultured for 1 or 4 d. MCF10a cells were seeded at 100,000 cells/cm^2 and cultured for 5 d. Lentiviruses were produced by calcium phosphate transfection of HEK293T cells with lentivectors and lentiviral packaging vectors psPAX2 and pMD2.G. Lentiviruses were collected and concentrated 48 hrs after transduction, utilizing Amicon centrifugal filter units. EpH4 and MCF10a cells were transduced by lentiviruses by shaking cells and viruses in suspension at 400 rpm, 37°C for 1 hr. Transduced cells were selected by puromycin (CRISPR v2 vectors) or FACS (pWPI mScarlet, pLVTHM GFP and DHB-mVenus vectors). EpH4 cells used for mixing experiments were NT pWPI mScarlet, NT pLVTHM GFP, and Traf3 KO1 pWPI mScarlet. SMAC mimetic BV6 was purchased from ApexBio (B4653).

To develop the EpH4 ES-FUCCI stable cell line we linearized the ES-FUCCI vector with *Ase*I and transduced cells using Xfect (Clontech) according to the manufacturer's protocol. Cells were selected with 300 µg/mL Hygromycin followed by FAC sorting of mCitrine+ and/or mCherry+ cells.

2.5.4. Flow cytometry analysis

Cells were treated with 3 µg/ml BrdU (Sigma-Aldrich) for 1 hr, then washed in sterile PBS and trypsinized. Trypsin was blocked with complete medium plus 50 µg/mL

DNase to reduce clumping of cells. Cells were pelleted, incubated in 5 mM EDTA in PBS on ice for 10 min and fixed in 4% paraformaldehyde for 15 min at room temperature. BrdU incorporation was detected after treatment with 2N HCl for 20 min at 37°C, washing with 1.5 M Na2B4O7, blocking in Western Blocking reagent (Roche) and staining with anti-BrdU antibodies (1:800, Abcam, ab6326). Cells were analyzed using a Fortessa flow cytometer and analyzed using FlowJo.

2.5.5. Immunoblotting

Cells were lysed in buffer containing 0.1% Triton-X100, 20mM HEPES (pH 7.4), 50mM NaCl, and 2mM EDTA supplemented with a protease inhibitor cocktail (Roche), Calyculin A, and PhosStop phosphatase inhibitors (Roche). Cell lysates were briefly sonicated and centrifuged at 16,100 g for 10 min. After centrifugation, the soluble fraction was boiled with SDS sample buffer for 5 min. Antibodies used for Western blotting are listed in the Key Resources Table (Table 1).

2.5.6. Immunofluorescence staining, image acquisition and analysis

Cells were grown on LabTek II chamber slides (Thermo Scientific) for the indicated times and fixed with 4% paraformaldehyde at room temperature for 15 min. Cells were permeabilized with 0.2% Triton X-100, blocked in 1xWestern Blocking Reagent (Roche) and labeled for IF imaging. Primary antibodies used for IF are listed in the Key Resources Table (Table 1). Secondary labelling was performed using Alexa Fluor secondary antibodies (1:500-1:1000, Life Technologies). Samples were mounted using Fluoromount G (Electron Microscopy Sciences). Laser scanning confocal images were acquired using

20x/0.75 Plan Apo or 100x/1.40 Plan Apo oil immersion objectives on a Nikon A1R inverted confocal microscope (Nikon Instruments Inc). Epifluorescence images were acquired using an EVOS FL inverted microscope (Life Technologies). Fiji software was used for post-acquisition processing.

Fiji Temporal Color Code function (fire color scale) was used for depth color coding of cells for visualization of multilayering. To measure the percent of multilayering in KO cells, we used Fiji software to process confocal image stacks of cells that had been grown to high density and stained for a nuclear marker. A single slice above the monolayer (about 8 µm above the center of the nuclei in the first layer of cells) was processed using Gaussian blur and Threshold to create a binary mask. It was analyzed using Measure particles function to determine the percent of total area that is above the monolayer. Data were collected for 5 fields of view in 3 biological repeats.

Nuclear/cytoplasmic ratio of YAP was measured using the ImageJ Intensity Ratio Nuclei CytoplasmTool: (https://github.com/MontpellierRessourcesImagerie/imagej_macros_and_scripts/wiki/Intensity-Ratio-Nuclei-Cytoplasm-Tool).

2.5.7. Real-time qPCR

Total RNA was extracted with TRIzol (Life Technologies). cDNA was reverse transcribed using the SuperScript III First-Strand Synthesis System (Invitrogen). qPCR was performed with triplicate replicates on a BioRad CFX96 Thermocycler and analyzed using the ΔΔCt method. Expression levels were calculated relative to *Gapdh*. *p27* levels

were assessed using *p27* primers. The primers are listed in the Key Resources Table (Table 1). The enrichment of cells containing sh-*p27* after FACS was assessed using puromycin resistance gene primers, because the Puro cassette was integrated into the cell genome together with the *p27* shRNA.

2.5.8. RNA sequencing

NT, TRAF3 KO1 and TRAF3/p100 double KO EpH4-FUCCI cells were sorted for non-proliferating cells (mCherry+) by FACS. RNA from NT, TRAF3 KO1 and TRAF3/p100 double KO cells from 2 experimental repeats was isolated using the RNeasy Mini Kit (Qiagen). RNA quality control was performed using a 2100 Bioanalyzer (Agilent Technologies). Samples had RNA integrity numbers in the range 8.1-9.3. Sequencing was performed using the NovaSeq 6000 Sequencing System (Illumina, San Diego, CA). Data were processed and analyzed with CLC Genomics Workbench and Ingenuity Pathway Analysis (Qiagen).

2.5.9. Mouse mammary gland organoids

Mammary glands were isolated from 8-week-old C3H mice as described previously (Pasic et al., 2011). Cells were then briefly treated with 0.25% Trypsin and filtered through a 40 μm strainer. Primary mammary cells were transduced with lentiCRISPR v2 NT control and *Traf3* KO1 and grown for 8 d in 50% Matrigel (Corning) supplemented with Organoid Growth Medium (DMEM/F12 (Gibco), 5 ng/mL EGF (Sigma), 3 ng/mL mFGF2 (R&D Systems), 1xITS (Millipore Sigma)). Then organoids were then fixed with PFA and immunostained. All mouse experimental procedures were approved by Vanderbilt

Institutional Animal Care and Use Committee; IACUC protocol number M1800045, Exp: 04/26/2021.

2.5.10. Statistical analysis

Data were tested for normality by Shapiro-Wilk test and then analyzed by Student's t-test, one-way ANOVA, or mixed model two-way ANOVA statistical test using GraphPad Prism software. When using ANOVA, post hoc analysis was done using Tukey or Dunnett multiple comparison tests. All statistical analysis was considered significant at $p<0.05$. Data presented as SuperPlots (Lord et al., 2020) combine individual measurements (small dots color-coded for each replicate), mean values for each replicate (large dots color-coded for each replicate), and mean ± std.

2.5.11. Data availability

All data that support the findings of this study are available within the article and its Supplementary Information, or from the authors upon reasonable request. RNAseq data have been submitted to the GEO repository (accession number GSE147767).

2.5.12. Acknowledgements

This work was supported by NCI grant R35CA132898 to I.G.M. We would like to thank members of the Macara lab for their valuable feedback, as well as Christian de Caestecker, Christian Meyer and Daria Episheva for the help with processing Illumina data for the CRISPR screen. We also thank Vivian Gama and Edward Levine for sharing

antibodies. Flow Cytometry experiments were performed in the VMC Flow Cytometry Shared Resource; Illumina sequencing and RNA-seq were performed by Vanderbilt Technologies for Advanced Genomics. These resources are supported by the Vanderbilt Ingram Cancer Center (P30 CA68485) and the Vanderbilt Digestive Disease Research Center (DK058404).

2.5. Supplementary figures

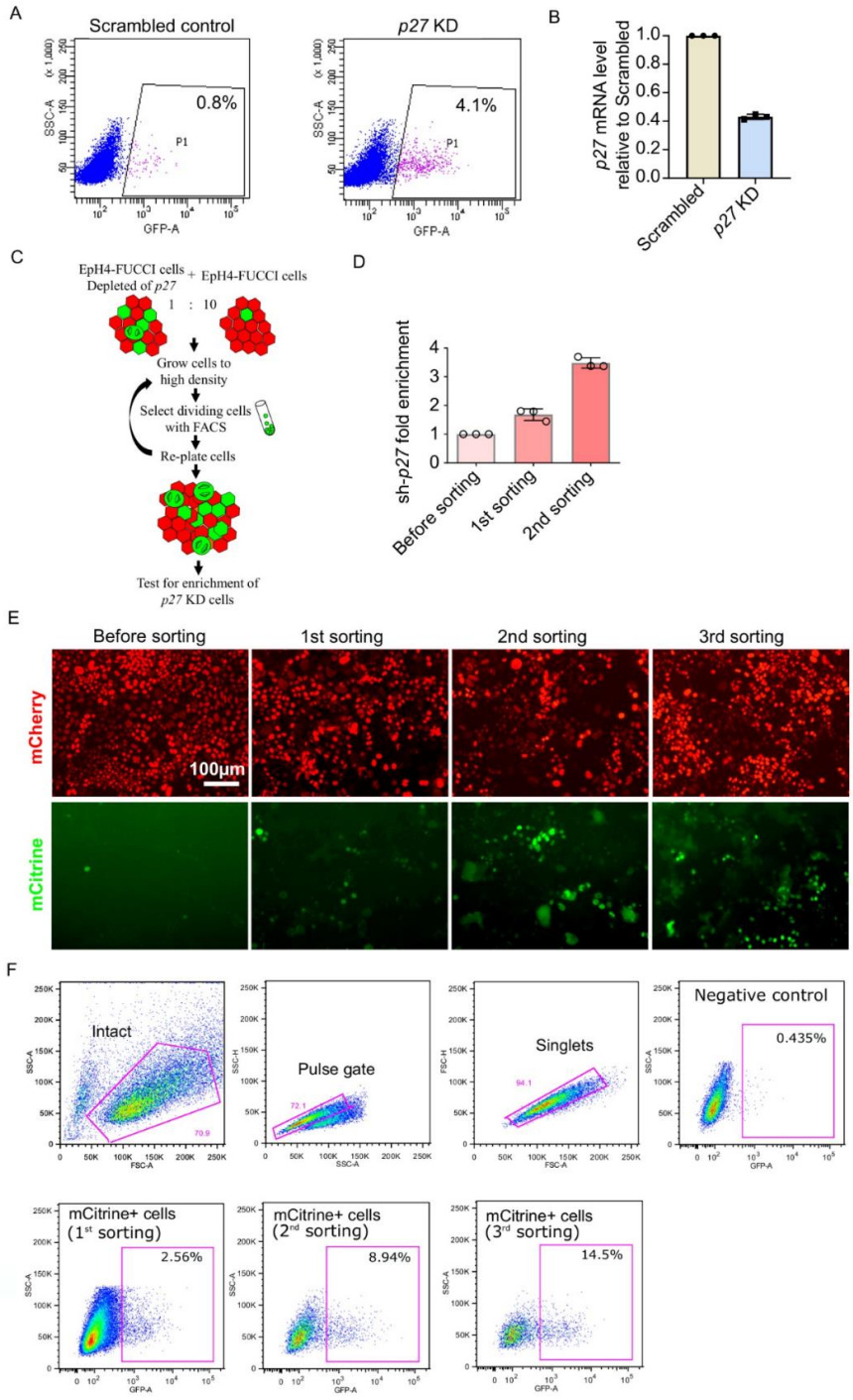

Figure 2-1 - Figure supplement 1. Proof of principle experiments for the whole-genome screen.

(A) Sorting of EpH4-FUCCI cells by FACS. The number of mCitrine+ cells is increased by depletion of *p27*. (B) *p27* mRNA level in *p27* KD cells relative to scrambled control cells measured by qPCR. (C) Strategy for proof-of-principle experiments. (D) Enrichment of sh-*p27* after 1st and 2nd round of sorting, compared to sh-*p27* content before FACS, measured by qPCR. Histogram shows mean ± 1 s.d. (n=3 technical repeats) (E) Imaging of EpH4-FUCCI cells at 4 DPC before sorting and after different rounds of sorting. (F) Gating for sorting EpH4-FUCCI cells by FACS. The number of mCitrine+ cells increases after each round of sorting.

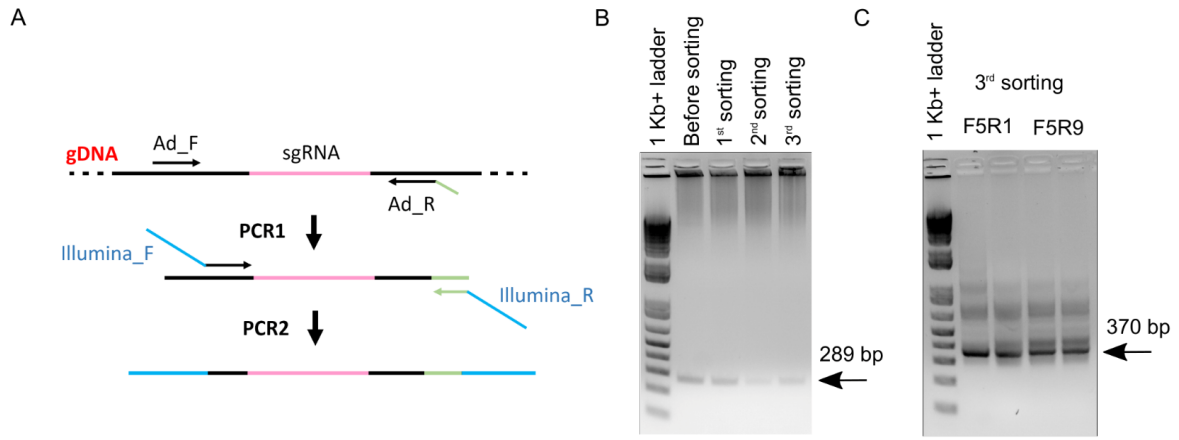

D

Time point	Total sgRNAs	Zero counts	Gini Index
Unsorted control	125,793	2808	0.15
1st sorting	125,793	14779	0.39
2nd sorting	125,793	10365	0.33
3rd sorting	125,793	13612	0.36

D'

Time Point	Reads	Mapped	Percentage
Unsorted control	49,384,395	35,363,444	0.72
1st sorting	21,736,214	13,145,089	0.6
2nd sorting	21,400,849	15,870,963	0.74
3rd sorting	71,162,949	51,610,375	0.73

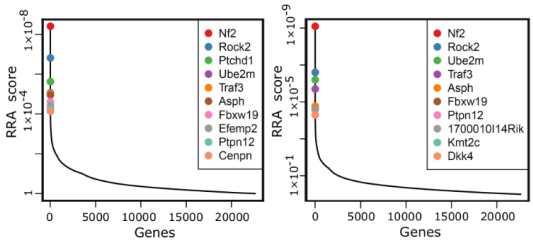

F

Rank	ID	FDR	Enriched/total sgRNAs
1	*Nf2*	0.00495	6/6
2	*Rock2*	0.01733	5/6
3	*Ptchdl*	0.09076	2/6
4	*Ube2m*	0.18069	5/6
5	*Traf3*	0.18069	4/6
6	*Asph*	0.18069	3/6

F'

Rank	ID	FDR	Enriched/total sgRNAs
1	*Nf2*	0.00495	6/6
2	*Rock2*	0.02723	5/6
3	*Ube2m*	0.02805	5/6
4	*Traf3*	0.05817	4/6

Figure 2-1 - Figure supplement 2. sgRNA sequence PCR for NGS and sequence processing.

(A) Schematic of PCR reactions aimed to amplify sgRNA containing fragments from gDNA (PCR1) and attach Illumina primers (PCR2) for NGS. (B) The agarose gel with DNA amplified from gDNA of control samples and samples after different rounds of sorting (PCR1). (C) An agarose gel with PCR2 products for the 3rd sorting sample with different

Illumina primer pairs shown as an example of PCR2 reaction products. (D) The number of lost sgRNA (zero counts) and Gini index in samples before sorting and after different rounds of sorting. (D') Total number of reads, number of mapped reads and the fraction of mapped reads in samples before sorting and after different rounds of sorting. (E), (E') RRA score plots for samples after 1st and 2nd sorts, respectively. (F), (F') The list of genes with FDR below 0.25 and more or equal to three sgRNAs enriched compared to control after 1st and 2nd sort, respectively.

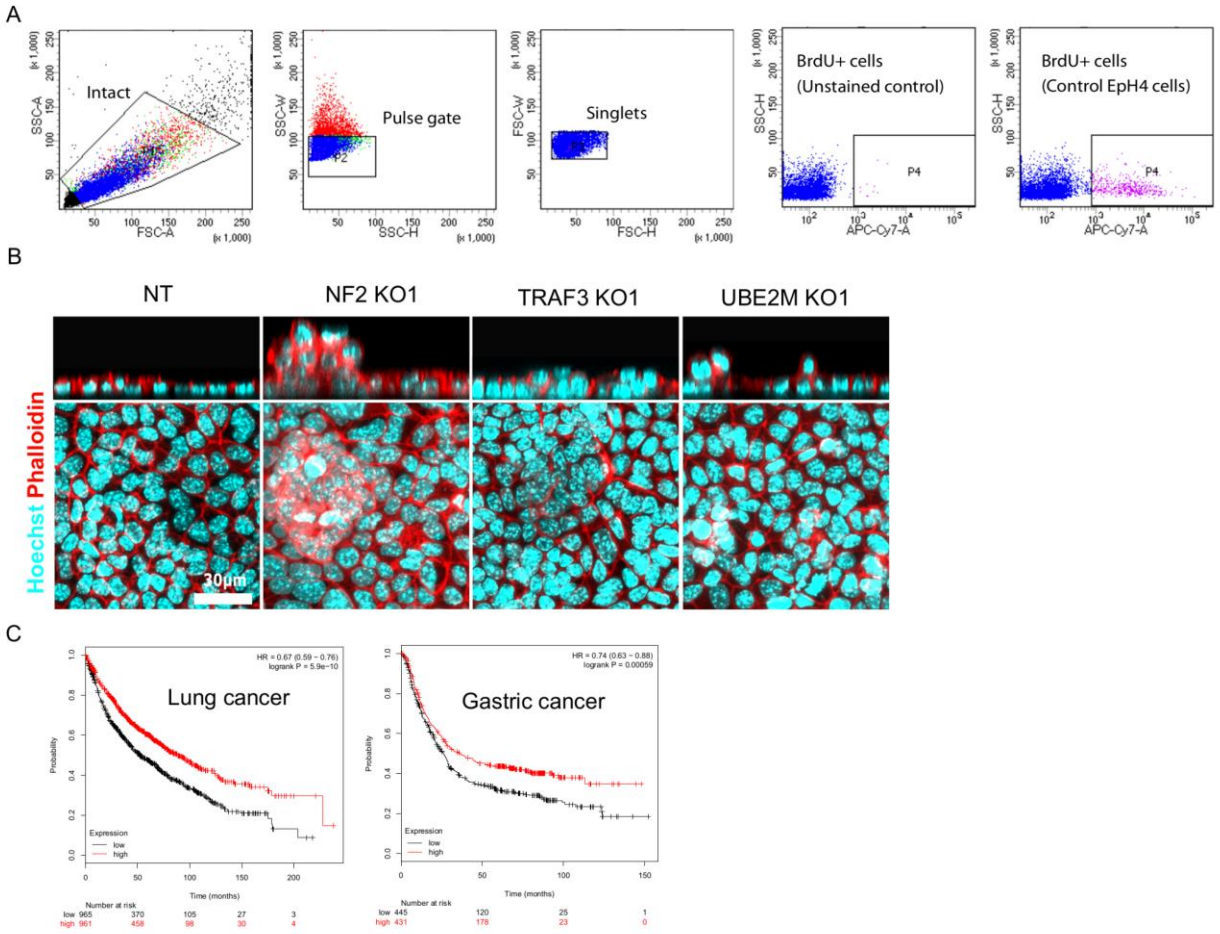

Figure 2-2 - Figure supplement 1. BrdU+ cell cytometry gates and cancer survival based on *Traf3* expression level.

(A) Flow cytometry gating for cells stained for BrdU. (B) Control and KO cells stained by phalloidin and Hoechst. Top panel shows xz view. (C) Kaplan-Meier plots show overall survival in all lung and gastric cancer based on *Traf3* expression level. Red and black curves reflect patients with high and low *Traf3* expression, respectively.

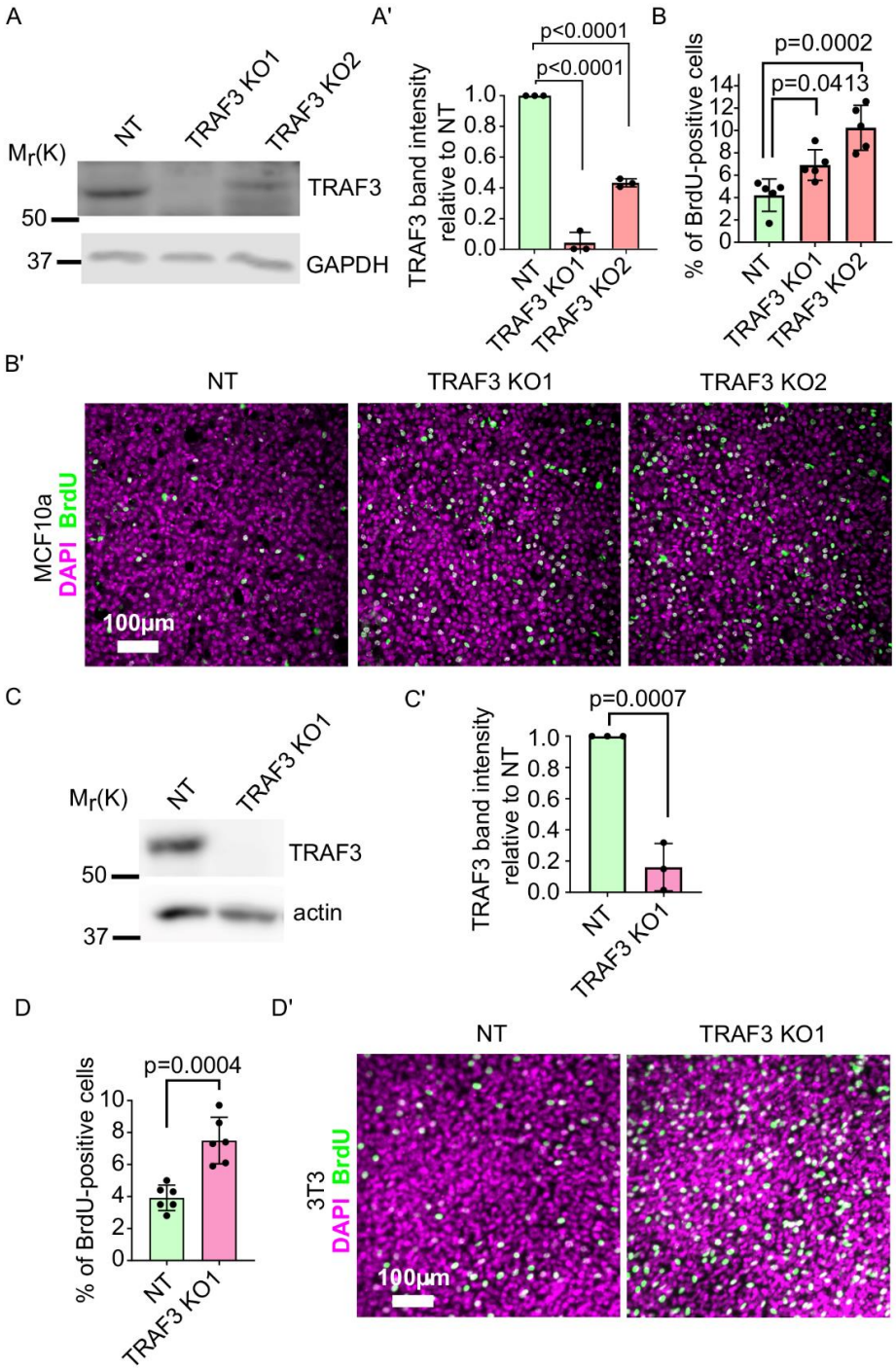

Figure 2-3 - Figure supplement 1. Loss of TRAF3 in MCF10a and NIH 3T3 cells causes over-proliferation.

(A) Immunoblotting of NT and TRAF3 KO MCF10a cells for TRAF3. GAPDH was used as a loading control. (A') Quantifications of TRAF3 levels based on Western blots (A) Histogram shows mean ± 1 s.d. (n=3). P values were calculated by one-way ANOVA followed by Dunnett's multiple comparisons test. (B) Cytometric analysis of NT control and TRAF3 KO MCF10a cells stained for BrdU to assess proliferation at 5 DPC. Histogram shows mean ± 1 s.d. (n=3). P values were calculated by one-way ANOVA followed by Dunnett's multiple comparisons test. (B') NT control and TRAF3 KO MCF10a cells at 5 DPC were treated and stained for BrdU and DAPI as nuclear marker. (C) Immunoblotting of NT and TRAF3 KO NIH 3T3 cells for TRAF3. actin was used as a loading control. (C') Quantifications of TRAF3 levels based on Western blots (C) Histogram shows mean ± 1 s.d. (n=3). P values were calculated by Student t-test. (D) Cytometric analysis of NT control and TRAF3 KO NIH 3T3 cells stained for BrdU to assess proliferation at 4 DPC. Histogram shows mean ± 1 s.d. (n=3). P values were calculated by Student t-test. (D') NT control and TRAF3 KO NIH 3T3 cells at 4 DPC were treated and stained for BrdU and DAPI as nuclear marker.

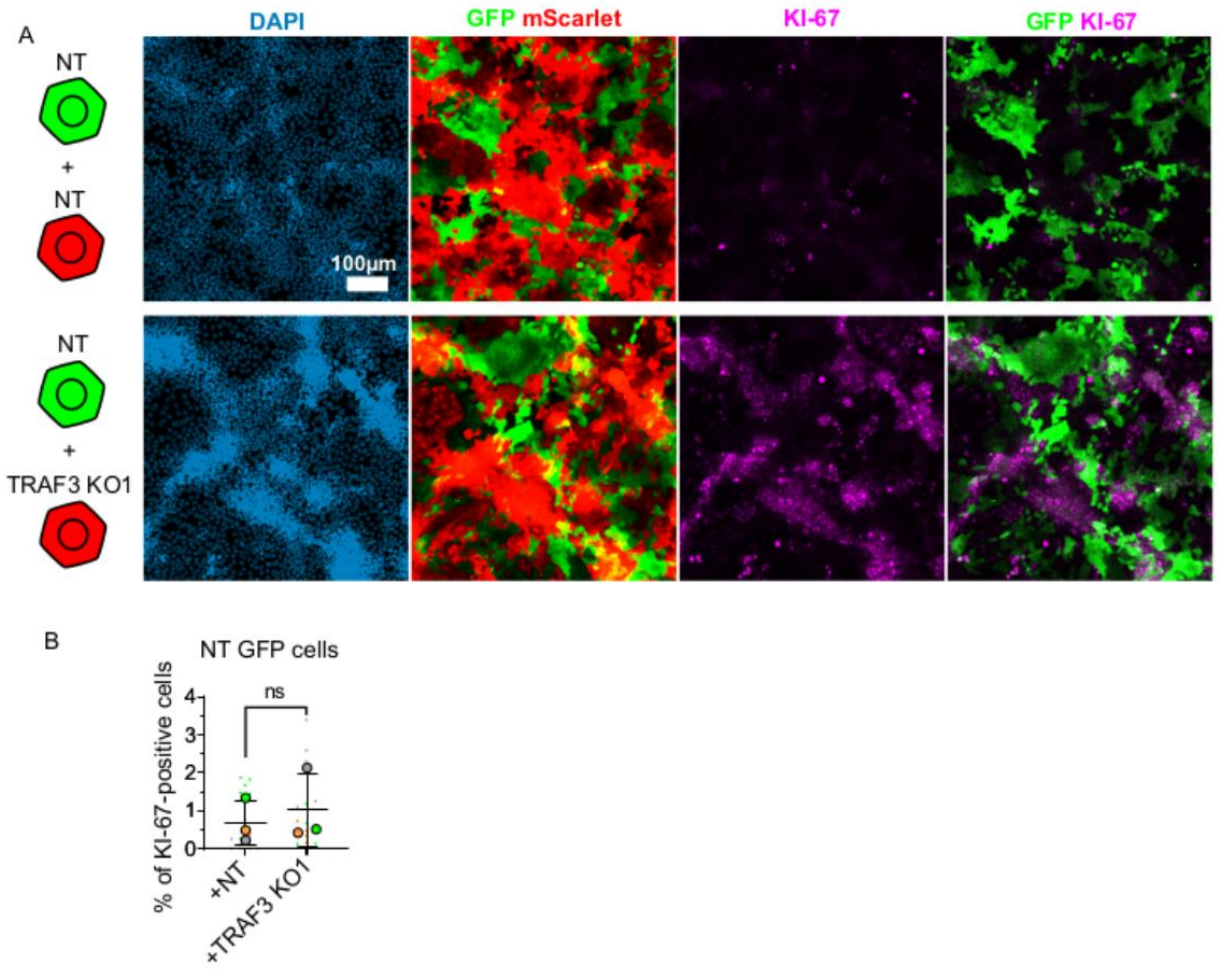

Figure 2-7 - Figure supplement 1. TRAF3 KO cells over-proliferate cell autonomously.

(A) NT and TRAF3 KO1 cells labeled with GFP or mScarlet were mixed at a 1:1 ratio (NT GFP + NT mScarlet, NT GFP + TRAF3 KO1 mScarlet), and grown to 4 DPC. Cells were stained for KI-67 and DAPI. (B) Quantifications of NT GFP cell proliferation in mixture with NT mScarlet or TRAF3 KO1 mScarlet. Proliferation was measured as percent of KI-67-positive cells to the total number of NT GFP cells. Data are presented as a SuperPlot (n=3). P value was calculated by mixed model two-way ANOVA.

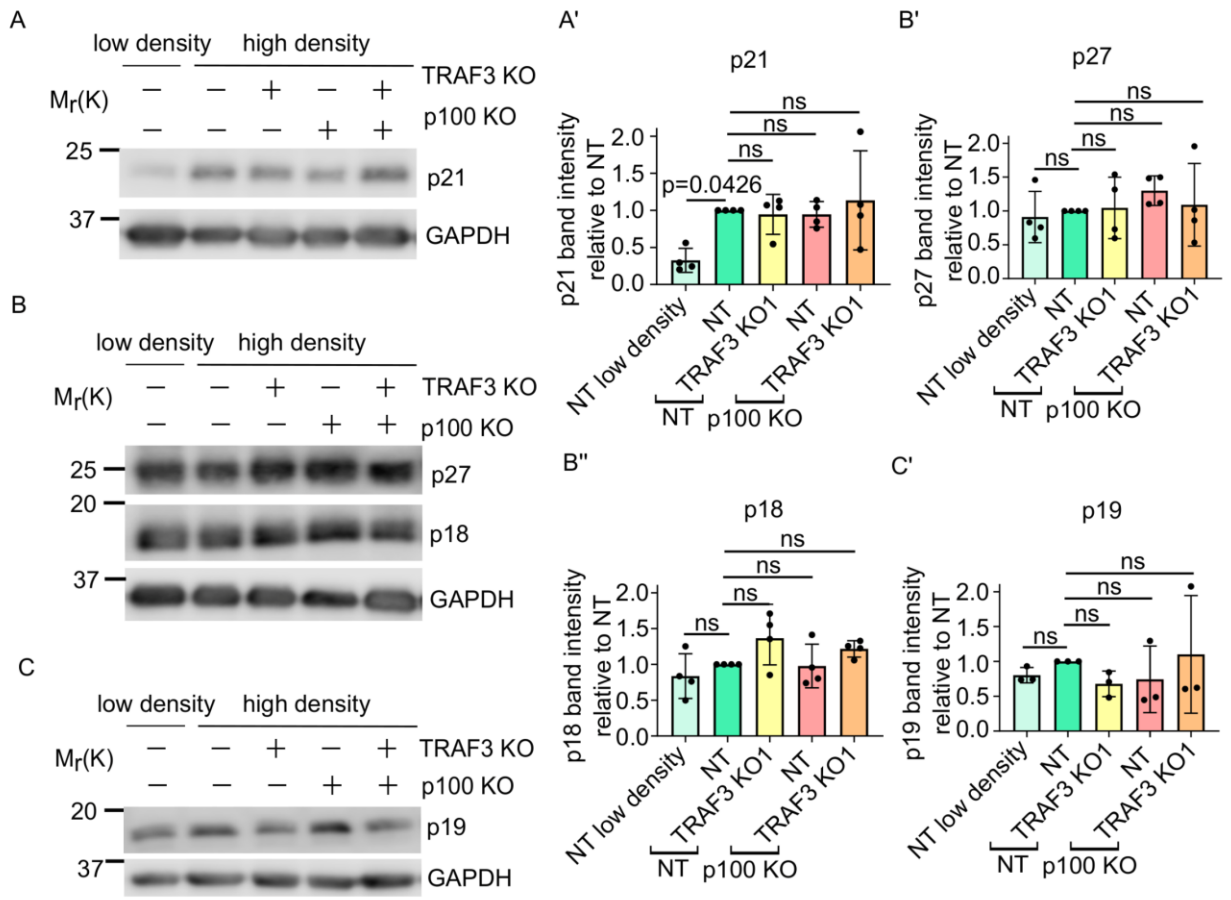

Figure 2-7 - Figure supplement 2. Loss of Traf3 does not affect CKI levels.

(A) Immunoblotting for p21 in sparse NT cells, dense NT, TRAF3 KO1, NT/p100 KO and TRAF3/p100 double KO cells. GAPDH was used as a loading control. (B) Western blotting for p27 and p18 in sparse NT cells, dense NT, TRAF3 KO1, NT/p100 KO and TRAF3/p100 double KO cells. GAPDH was used as a loading control. (C) Western blotting for p19 in sparse NT cells, dense NT, TRAF3 KO1, NT/p100 KO and TRAF3/p100 double KO cells. GAPDH was used as a loading control. (A')-(C') Quantifications of the blots (A)-(C). N=4 for blots (A) and (B). N=3 for blot (C) Histograms show mean ± 1 s.d. P values were calculated by one-way ANOVA followed by Dunnett's multiple comparisons test.

III. CONCLUSIONS

We designed and performed a whole-genome CRISPR KO screen to find novel regulators of density-dependent proliferation in epithelia. We found a known regulator of cell density, NF2, that controls cell proliferation via Hippo signaling. We also found novel regulators of density dependent proliferation – TRAF3 and UBE2M. We confirmed by individual CRISPR KOs that loss of these candidate proteins indeed caused over-proliferation at high density. KO cells proliferated normally at lower densities confirming that hit proteins affect cell proliferation specifically at high density.

We further focused on studying mechanisms of TRAF3 dependent proliferation. First, we knocked out TRAF3 in other cell lines, human mammary gland MCF10a and mouse fibroblast cells NIH 3T3, and confirmed that TRAF3 KO over-proliferation phenotype is not specific to the mouse mammary gland cell line EpH4. These data demonstrated that TRAF3 KO induces over-proliferation not only in epithelial cells, but also in cells of mesenchymal origin. Further, we showed that loss of TRAF3 induces noncanonical NF-κB activation and over-proliferation in primary mammary gland organoids. This is a very important result showing that phenotype observed in TRAF3 loss is not an artifact observed only in immortalized cell lines.

Next, we found that loss of TRAF3 activates the noncanonical NF-κB pathway but not canonical NF-κB signaling. We demonstrated that the noncanonical NF-κB pathway is necessary for the over-proliferation phenotype because loss of a key component, p100 or NIK, restores normal growth control. Importantly, we showed that noncanonical NF-κB

signaling is sufficient for increased cell division at high density since overexpression of a nondegradable version of NIK recapitulates over-proliferation phenotype.

We showed by RNAseq that loss of TRAF3 induces the antigen-presentation and interferon pathways, which can be reversed by p100 KO. Over-proliferation at high density occurs in a cell autonomous manner and independently of Hippo signaling, which is the major known density regulator. TRAF3 KO cells override CKI activity, have increased CYCLIN D1 levels, and do not exit the cell cycle, as shown by increased CDK2 activity and mono-phosphorylation of RB at Ser807/811.

IV. UNPUBLISHED DATA AND FUTURE DIRECTIONS

4.1. Considerations for future screens

We performed a whole-genome screen, in which we utilized the GeCKO whole-genome CRISPR KO library from the Broad Institute (MA). We transduced cells with this library at an MOI (0.3) such that statistically most cells would acquire either no sgRNAs or only a single sgRNA. We used a coverage of 150 cells per single sgRNA to prevent random loss of sgRNAs during the screen. We grew cells to 4 DPC and sorted for cells that proliferated at high density. Then we regrew cells and sorted them again to further enrich for candidate genes. We collected data from three sorts and compared them with control cells (before sort) to find novel regulators of density-dependent proliferation.

If we performed this screen again to find more candidate genes, we would improve a few things in the screen design. We would use a new generation CRISPR KO Brie library that is claimed to have a higher KO efficiency and less off-target activity (Doench et al., 2016). Also, we would not sort the cells three times because the top hits were already enriched after the first sort and, importantly, after the first sort we selected a small population of CRISPR KO cells with a limited number of sgRNAs. For this reason, subsequent sorts did not provide much additional information. Moreover, the repeated sorts might enrich for false positives that were randomly enriched in the first round. A better design would be to perform three independent experimental repeats, each sorting the initial CRISPR KO population. This screen design would allow us to rule out false positives that could arise in one experimental repeat but not in all of them. On the other hand, we would find more true hits that are mildly selected in all three repeats, while in

our single repeat screen we could only rely on hits that were highly enriched compared to control.

Modifications to the screen might also include sensitizing mutations, for instance by altering the expression of redundant Hippo regulators; or reversing the assay to try and identify genes that when deleted result in arrest before the cells reach high density. However, these approaches all have associated technical difficulties.

A CRISPR KO whole-genome screen is a labor-intensive but extremely powerful approach if it is thoroughly designed and executed. The screen must be done at a high scale (150 – 300 cells per sgRNA, total of 20-40 million cells for GeCKO library) with a freshly transduced cell population (about 7 days after transduction to allow the sgRNAs to introduce KO) to avoid the loss of sgRNAs. Another key aspect of the screen is a development of an efficient method to select for candidate genes. Therefore, the selection method must be verified in proof-of-principle experiments before it is applied for the screen.

4.2. What mechanisms underlie UBE2M and ROCK2 proliferation control?

We found multiple hits in our whole-genome CRISPR/Cas9 screen for factors controlling cell density dependent proliferation, including novel factors TRAF3 and UBE2M. In our study, we focused on TRAF3-dependent mechanisms that restrict over-proliferation at high density. However, the mechanisms underlying UBE2M density-dependent proliferation control were not investigated. As mentioned before, UBE2M is a NEDD8 conjugation E2 ligase, which neddylates CULLIN-RING E3 ligases and other

targets to facilitate their activity (Lydeard et al., 2013). Interestingly, the neddylation pathway was shown to be overactivate in some human cancers. Paradoxically, however, under stressed conditions, UBE2M promotes ubiquitylation of UBE2F, the degradation of which can suppress cell proliferation (Zhou et al., 2018). Other recent work suggested that UBE2M KD reduced proliferation in lung cancer cells by triggering G2 phase cell cycle arrest. Loss of UBE2M inhibited CULLIN ligases, which in turn led to accumulation of CULLIN ligase substrates – CKIs p21, p27, and WEE1 (L. Li et al., 2019). Therefore, it is unclear why in our screen the deletion of UBEM2 caused over-proliferation instead of inhibition. It would be of interest to test the impact of UBEM2 loss on UBE2F levels and CK1 levels in mammary epithelial cells.

In addition, we investigated the phenotypes for knock outs of *Rock2* (Rho associated coiled-coil containing protein kinase 2) and/or *Klhl29* (Kelch Like Family Member 29), the hits #2 and #6 from our third round of selection in the screen, respectively. ROCK2 is a kinase that plays an important role in organization of actin cytoskeleton and has multiple substrates. One of the classical substrates is myosin light chain, phosphorylation of which promotes actin contraction (Julian & Olson, 2014). KLHL29 is a protein with unknown functions. Other members of KLHL protein family are transcription factors or are involved in ubiquitination (Dhanoa, Cogliati, Satish, Bruford, & Friedman, 2013).

We observed that ROCK2 KO cells have a trend to over-proliferate at 4 DPC compared to control (Figure 4-1A). Interestingly, we did not observe overcrowding and/or multilayering in ROCK2 KO cells at 4 DPC (Figure 4-1B). ROCK2 cells might even have lower density than control. It is possible that ROCK2 KO cells get extruded and die, such

that the adherent cells do not reach homeostatic cell density and, as a result, they keep proliferating. We observed no differences in proliferation for KLHL29 KO cells, which suggests that it was a false positive hit (Figure 4-1A).

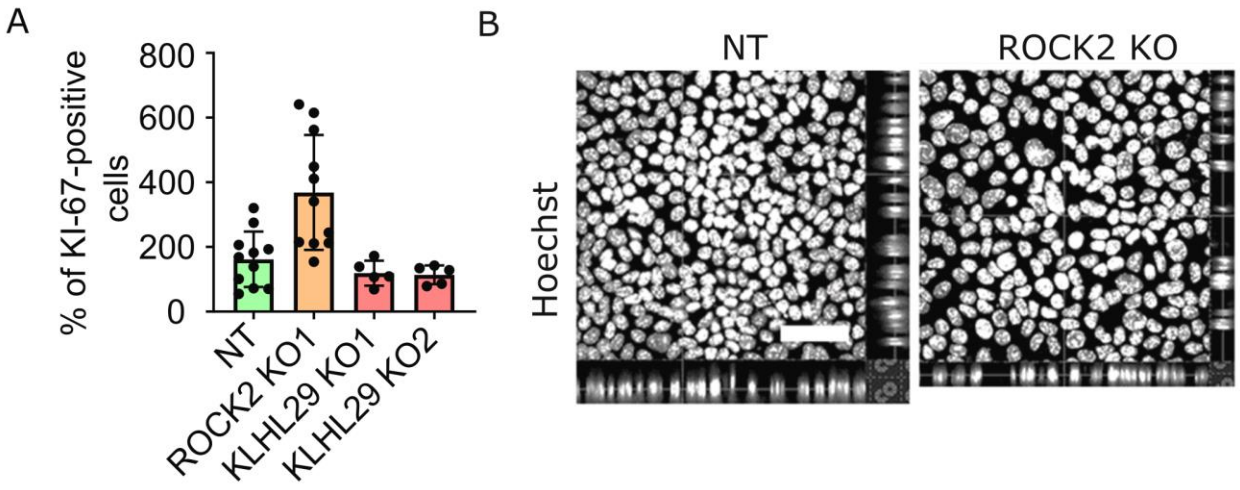

Figure 4-1. Validation of additional hit genes found in whole-genome screen.

A. Quantifications of percent of KI-67 positive cells in ROCK2 and KLHL29 KO cells. B. Hoechst stained NT and ROCK2 KO cells, xy and xz projections.

4.3. What are the mechanisms of multilayering in TRAF3 KO cells?

TRAF3 KO cells over-proliferate and multilayer at high density. We asked what are the mechanisms that allow TRAF3 KO cells escape the monolayer. One well-established mechanism of epithelial cell multilayering is perturbation of cell division orientation. Normally, the epithelial cell mitotic spindle is oriented in the same plane as the epithelial monolayer. Perturbation of mitotic spindle orientation mechanisms leads to a randomized directionality of cell division. As a result, one of the daughter cells that divided in the plane perpendicular to the monolayer will reside above the monolayer and could contribute to the formation of multiple layers (Zheng et al., 2010).

To test whether TRAF3 KO cells have perturbed directionality of cell proliferation, we fixed cells at 2 DPC when cells start getting dense. We stained cells for DAPI, Phalloidin, and PERICENTRIN (centrosomal marker) to clearly see the angle of mitotic spindles in control and KO cells (Figure 4-2). However, we did not observe any differences between control and TRAF3 KO cells: both control and KO cell lines divided in the plane of the monolayer.

Alternatively, TRAF3 KO cells can multilayer because of physical constraints. TRAF3 KO cells do not arrest, and if their numbers exceed the maximal number that can fit in one plane physical forces might cause extrusion of some of the cells from the monolayer to relieve mechanical pressure (Saw et al., 2017).

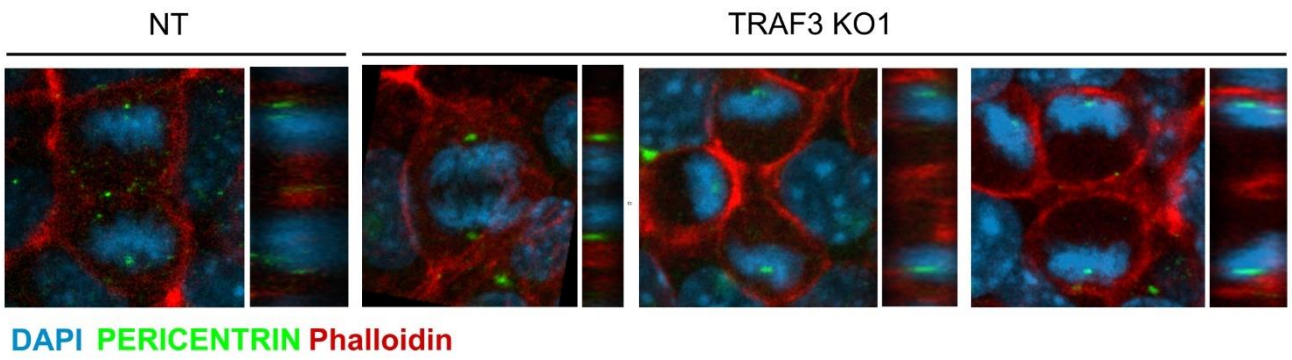

Figure 4-2. Mitotic spindle orientation in NT control and TRAF3 KO cells.

NT and TRAF3 KO cells were stained for DAPI, PERICENTRIN and Phalloidin. xy and xz projections are shown.

4.4. Additional studies are needed to expand our understanding of NF-κB pathway involvement in density control

We performed extensive studies of the role of NF-κB signaling in density-dependent proliferation downstream of TRAF3 (Figure 4-3). However, our examination of the NF-κB literature and experimental work showed the immense complexity of this pathway. There are a lot of questions that remain to be answered about the role of TRAF3 and NF-κB signaling in density dependent growth control.

We showed by using a cIAP inhibitor and TRAF3 CRISPR KO, respectively that cIAP1/2 and TRAF3 are necessary for arresting cell proliferation at high density. However, overexpression of TRAF3 in TRAF3 KO cells did not rescue the over-proliferation phenotype (Figure 4-4). We cloned our top hit genes *Nf2, Traf3* and *Ube2m* in pWPI mScarlet vector and then over-expressed them in NF2 KO, TRAF3 KO and UBE2M KO cells, respectively (Figure 4-4A-C). As a control we used KO cells transduced with empty pWPI mScarlet vector. Overexpression of NF2 rescued over-proliferation in NF2 KO cells. However, overexpression of TRAF3 and UBE2M had no effect on KO cells (Figure 4-4D).

It is likely that the levels of TRAF3 are critical for the correct cellular outputs because previous research demonstrated that over-expression of TRAF3 in mice resulted in the same phenotype as TRAF3 KO in mice (Zapata et al., 2009). To efficiently rescue the WT phenotype in TRAF3 KO cells we would probably need to express TRAF3 at a lower dosage, close to endogenous WT levels.

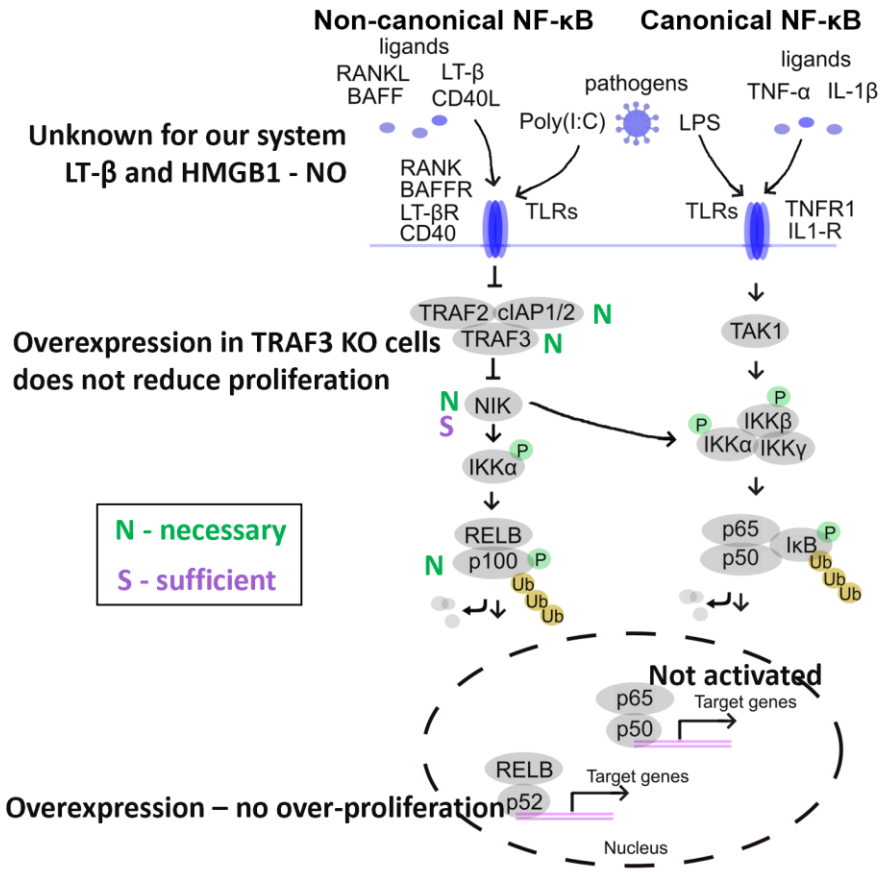

Figure 4-3. Studies of the role of non-canonical NF-κB pathway in over-proliferation at high density.

N – an experiment, showing necessity of the protein for the phenotype; S – an experiment, showing sufficiency of the protein for the phenotype. Experiments that did not work or showed negative results are shown in bold. Details in text.

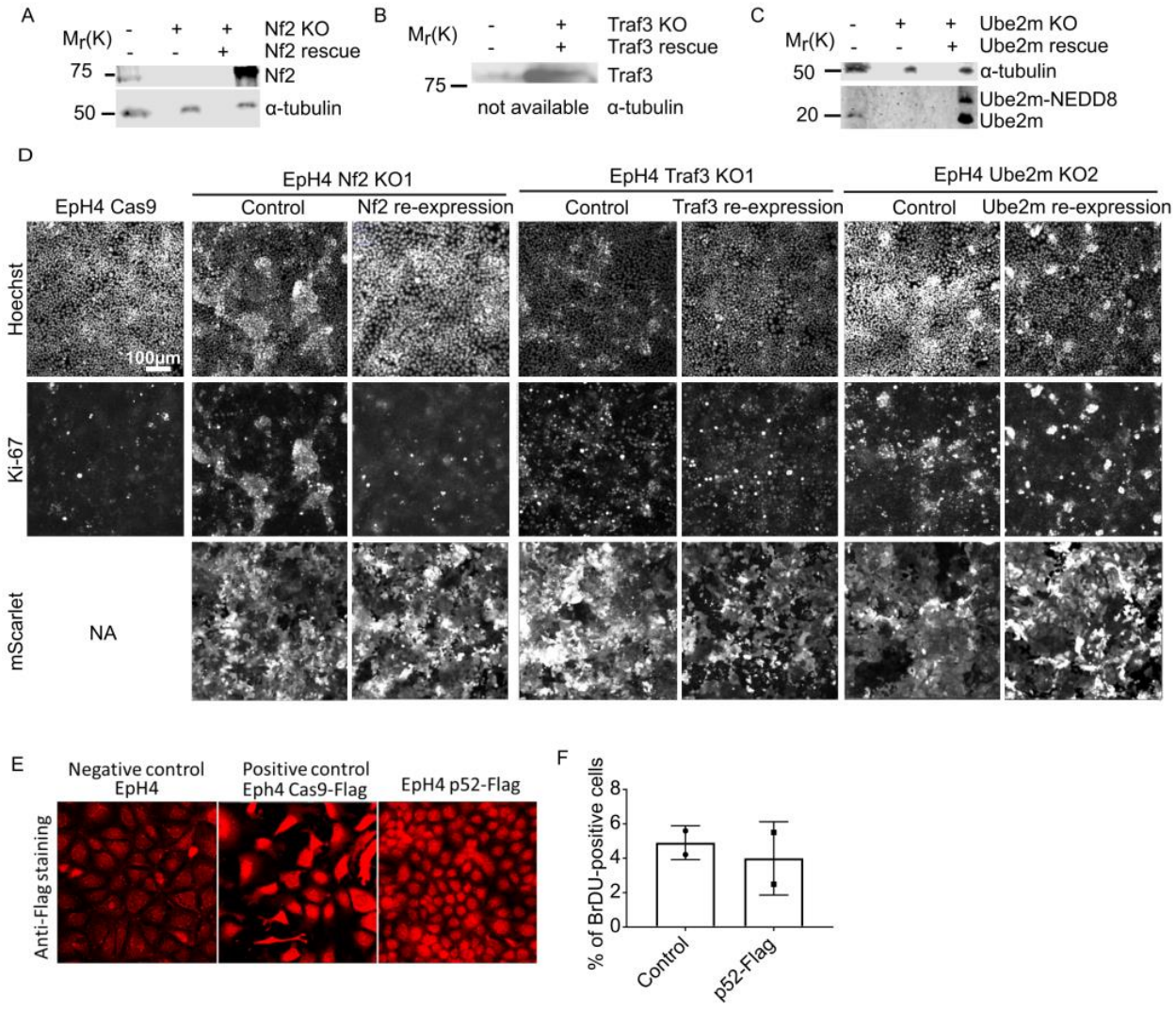

Figure 4-4. Overexpression of hit genes in respective KO cell lines. Overexpression of p52 in EpH4 cells.

(A)-(C) Western blots of lysates from control, NF2, TRAF3, and UBE2M KO cells, as well as KO cells overexpressing NF2, TRAF3, or UBE2M. (D) Control, KO, and KO cell lines overexpressing hit genes were grown to 4 DPC and stained for Hoechst and KI-67. Cells expressing empty or overexpression vector also express mScarlet. (E) EpH4 (negative control), EpH4 Cas9-Flag (positive control), and EpH4 p52-Flag cells stained with anti-

Flag antibody. (F) Cytometric analysis of control and p52-Flag expressing cells grown to 4 DPC and stained for BrdU. n=2.

We also showed the necessity of NIK and p100 for over-expression phenotype in TRAF3 KO cells. Importantly, we demonstrated that over-expression of non-degradable NIK is sufficient to recapitulate over-proliferation phenotype observed in TRAF3 KO cells. However, attempts to over-express p52 (p52 cFlag pcDNA3, Addgene plasmid # 20019) showed no over-proliferation phenotype although p52 was successfully expressed in EpH4 cells as shown by Flag staining of p52-Flag cells (Figure 4-4). REL proteins can form different dimers that can act as transcriptional activators and repressors. p52-p52 dimers were shown to have transcriptional repressor function (T. Li et al., 2010; V. Y. Wang et al., 2012). In addition, p100 is still present in p52-expressing cell line. It is known that p100 suppresses non-canonical NF-κB pathway by sequestering RELB in the cytoplasm (Novack, 2011; Solan, Miyoshi, Carmona, Bren, & Paya, 2002). Therefore, to successfully force constitutive activation of non-canonical NF-κB signaling we would need to KO p100 and express p52 in a dose-controlled way. The simpler solution was to overexpress NIK, which we successfully did by cloning and expressing the mutant NIK lacking its TRAF3 binding domain to allow NIK to escape degradation.

Another standing question is under what physiological conditions TRAF3 is degraded. We performed preliminary testing of two ligands that might induce TRAF3 degradation – HMGB1 and Lymphotoxin-β (LT-β). Unfortunately, we observed no activation of noncanonical NF-κB signaling when we treated cells with either of these ligands (not shown). Other PAMPs, DAMPs, and TNFRs should be tested to shed light on the upstream signals that induce cell over-proliferation at high density.

4.5. Further studies are needed to understand the role of genes upregulated by TRAF3 loss

We studied the downstream effects of TRAF3 loss. We found that TRAF3 deletion prevents cells from entering G0. We also showed that it happens cell autonomously, and independently of the Hippo pathway and CKIs. We also performed RNAseq analysis to identify which genes are changed upon TRAF3 loss, and expression of which of them can be reversed by p100 KO. However, we did not identify any target genes that are clearly associated with cell cycle regulation. Additionally, we found that expression of some genes activated in TRAF3 KO cells was not rescued by p100 KO. Most likely this result is a consequence of activation by TRAF3 of other pathways besides noncanonical NF-κB signaling (discussed in Introduction chapter). If we performed RNAseq on EpH4 cells expressing non-degradable mutant of NIK, we would get a gene signature that is more specific for noncanonical NF-κB pathway activation.

RNAseq data revealed that the interferon pathway is induced in TRAF3 KO cells. This pathway is known to trigger cell death (Apelbaum et al., 2013). Indeed, during culturing of TRAF3 KO cells we observed that they have increased cell death compared to control. We immunostained cells with an apoptotic marker CASPASE 3 and found that TRAF3 KO cells have increased number of CASPASE 3 positive cells compared to control (Figure 4-5). Thus, both cell proliferation and increased cell death are observed in TRAF3 KO cells. Proliferation overbalances cell death since we observe increased cell density (i.e. number of cells) in TRAF3 KO cells compared to control cells. It would be interesting to investigate what is the physiological role of inducing both proliferation and death simultaneously in the same cell.

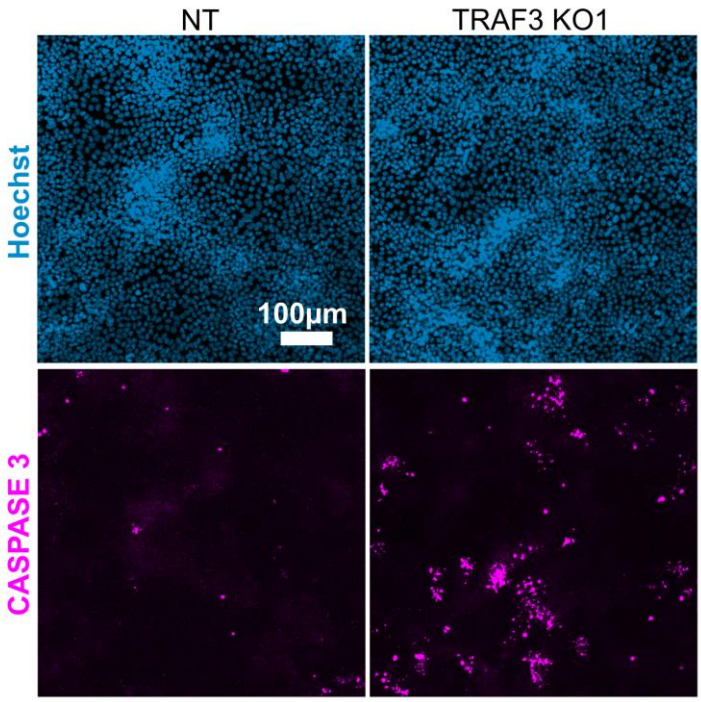

Figure 4-5. Comparing the number of apoptotic cells in NT control and TRAF3 KO cells.

NT and TRAF3 KO cells were grown to 4 DPC, fixed and stained for Hoechst and CASPASE 3.

4.6. The role of TRAF3 in epithelial density control *in vivo*

It would be an important and intriguing project to study whether loss of TRAF3 in epithelial cells *in vivo* also induces over-proliferation. Studies of whole body TRAF3 KO mice did not report epithelial defects. However, these studies focused on blood cell development and functions therefore epithelial cells were not tested. In addition, TRAF3 KO mice died within 10 days after birth (Xu, Cheng, & Baltimore, 1996). It is possible that longer time is needed to observe benign or malignant growth in epithelial TRAF3 KO cells. To prevent mouse early death, researchers used conditional TRAF3 KO in myeloid cells, however, to our knowledge, no epithelial-specific TRAF3 KO mice were developed. It would be interesting to knock out TRAF3 in skin or mammary gland and test whether they would have increased proliferation.

A quicker approach to test TRAF3 KO phenotype *in vivo* is to perform mammary gland transplantation assay (Figure 4-6). For this assay, we would transduce freshly isolated primary mouse mammary gland cells with NT control vector or TRAF3 sgRNA vector. After a few days, we would stain a part of the cells with RELB to confirm TRAF3 KO. Our organoid data showed that, similar to EpH4 cell line, primary mammary gland cells have cytoplasmic RELB, but it translocates to the nucleus upon TRAF3 KO. Then we would transplant cells to cleared fat pads of donor mice. After mammary glands regrow for 6 weeks, we would isolate mammary glands and stain them for Carmine Alum to examine overall mammary gland morphology. TRAF3 KO glands might have thickened or excessive branches or disorganized growth of mammary gland cells.

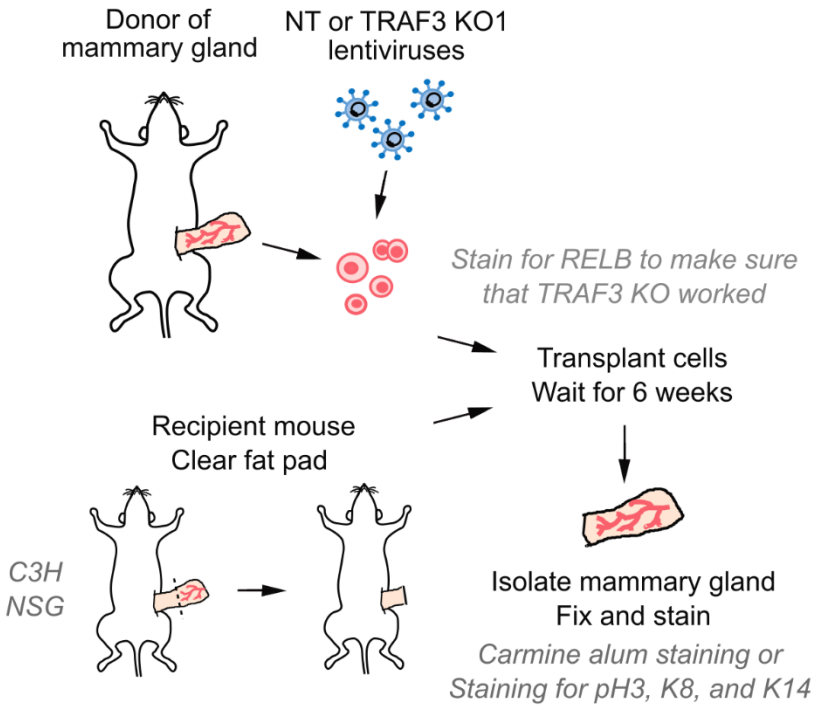

Figure 4-6. The schematic of mammary gland transplantation assay to test the phenotype of TRAF3 KO mammary glands.

Details in text.

We would also stain mammary glands for proliferation marker phospho-HISTONE 3 (pH3), as well as KERATIN 8 and 14 (K8 and K14, luminal and myoepithelial markers, respectively) to test for changes in lineage specification and/or morphology, such as ductal overgrowth or lumen filling.

We performed a preliminary mammary gland transplantation assay using C3H mouse line since it was empirically shown to have an efficient mammary gland outgrowth. However, we observed poor outgrowth in our experiment, especially in mammary fat pads injected with TRAF3 KO cells. It is possible that TRAF3 KO cells survive worse that NT control cells because TRAF3 KO cells have activated immune pathways and get eliminated by the mouse immune system. If we reproducibly observe that control cells regrow a mammary gland, but TRAF3 KO cells fail to do so, we will perform this experiment in NSG (NOD scid gamma) mice that lack both the innate and adaptive immunity response. We expect to see that TRAF3 KO cells will not be eliminated in NSG mice, and we will be able to compare mammary gland morphology and proliferation rate in control and TRAF3 KO glands.

Besides experimental KO of TRAF3, it would be extremely interesting to study what kind of infections and/or damage of epithelial cells would result in TRAF3 loss and whether it would lead to increased cell division. There were a few studies showing activation of noncanonical NF-κB signaling pathway with subsequent overgrowth of epithelial cells in *H. pylori* stomach infection, as well as otitis infection (Cho et al., 2016; Feige et al., 2018). It would be interesting to test if infections of mammary gland would induce TRAF3 loss and subsequent prevention of exiting cell cycle. It is also not clear what is a physiological role of over-proliferation in damaged tissues. Further studies are

needed to better understand the role of TRAF3 and its downstream targets in epithelial cells *in vivo*.

4.7. Concluding remarks

We developed a novel approach to screen for proteins controlling cell density dependent proliferation. We found novel regulators of density control, TRAF3 and UBE2M. We studied the mechanisms of TRAF3 dependent proliferation and found that loss of TRAF3 induces activation of noncanonical NF-κB signaling pathway, which in turn triggers an innate immune response, overrides Hippo signaling and CKIs, and cell autonomously prevents cells at high density from entering quiescence. More studies both *in vitro* and *in vivo* are needed to better understand the molecular pathways activated by the loss of TRAF3 protein.

REFERENCES

Annunziata, C. M., Davis, R. E., Demchenko, Y., Bellamy, W., Gabrea, A., Zhan, F., . . . Staudt, L. M. (2007). Frequent engagement of the classical and alternative NF-kappaB pathways by diverse genetic abnormalities in multiple myeloma. *Cancer Cell, 12*(2), 115-130. doi:10.1016/j.ccr.2007.07.004

Apelbaum, A., Yarden, G., Warszawski, S., Harari, D., & Schreiber, G. (2013). Type I interferons induce apoptosis by balancing cFLIP and caspase-8 independent of death ligands. *Mol Cell Biol, 33*(4), 800-814. doi:10.1128/MCB.01430-12

Aragona, M., Panciera, T., Manfrin, A., Giulitti, S., Michielin, F., Elvassore, N., . . . Piccolo, S. (2013). A mechanical checkpoint controls multicellular growth through YAP/TAZ regulation by actin-processing factors. *Cell, 154*(5), 1047-1059. doi:10.1016/j.cell.2013.07.042

Balda, M. S., Garrett, M. D., & Matter, K. (2003). The ZO-1-associated Y-box factor ZONAB regulates epithelial cell proliferation and cell density. *J Cell Biol, 160*(3), 423-432. doi:10.1083/jcb.200210020

Balda, M. S., & Matter, K. (2000). The tight junction protein ZO-1 and an interacting transcription factor regulate ErbB-2 expression. *EMBO J, 19*(9), 2024-2033. doi:10.1093/emboj/19.9.2024

Besson, A., Dowdy, S. F., & Roberts, J. M. (2008). CDK inhibitors: cell cycle regulators and beyond. *Dev Cell, 14*(2), 159-169. doi:10.1016/j.devcel.2008.01.013

Bishop, G. A., Stunz, L. L., & Hostager, B. S. (2018). TRAF3 as a Multifaceted Regulator of B Lymphocyte Survival and Activation. *Front Immunol, 9*, 2161. doi:10.3389/fimmu.2018.02161

Bonizzi, G., Bebien, M., Otero, D. C., Johnson-Vroom, K. E., Cao, Y., Vu, D., . . . Karin, M. (2004). Activation of IKKalpha target genes depends on recognition of specific kappaB binding sites by RelB:p52 dimers. *EMBO J, 23*(21), 4202-4210. doi:10.1038/sj.emboj.7600391

Cao, Y., Bonizzi, G., Seagroves, T. N., Greten, F. R., Johnson, R., Schmidt, E. V., & Karin, M. (2001). IKKalpha provides an essential link between RANK signaling

and cyclin D1 expression during mammary gland development. *Cell, 107*(6), 763-775. doi:10.1016/s0092-8674(01)00599-2

Cho, C. G., Pak, K., Webster, N., Kurabi, A., & Ryan, A. F. (2016). Both canonical and non-canonical NF-kappaB activation contribute to the proliferative response of the middle ear mucosa during bacterial infection. *Innate Immun, 22*(8), 626-634. doi:10.1177/1753425916668581

Claudio, E., Brown, K., Park, S., Wang, H., & Siebenlist, U. (2002). BAFF-induced NEMO-independent processing of NF-kappa B2 in maturing B cells. *Nat Immunol, 3*(10), 958-965. doi:10.1038/ni842

Codelia, V. A., Sun, G., & Irvine, K. D. (2014). Regulation of YAP by mechanical strain through Jnk and Hippo signaling. *Curr Biol, 24*(17), 2012-2017. doi:10.1016/j.cub.2014.07.034

Combes, A. N., Phipson, B., Lawlor, K. T., Dorison, A., Patrick, R., Zappia, L., . . . Little, M. H. (2019). Single cell analysis of the developing mouse kidney provides deeper insight into marker gene expression and ligand-receptor crosstalk. *Development, 146*(12). doi:10.1242/dev.178673

Coope, H. J., Atkinson, P. G., Huhse, B., Belich, M., Janzen, J., Holman, M. J., . . . Ley, S. C. (2002). CD40 regulates the processing of NF-kappaB2 p100 to p52. *EMBO J, 21*(20), 5375-5385. doi:10.1093/emboj/cdf542

Cordenonsi, M., Zanconato, F., Azzolin, L., Forcato, M., Rosato, A., Frasson, C., . . . Piccolo, S. (2011). The Hippo Transducer TAZ Confers Cancer Stem Cell-Related Traits on Breast Cancer Cells. *Cell, 147*(4), 759-772. doi:10.1016/j.cell.2011.09.048

Danes, C. G., Wyszomierski, S. L., Lu, J., Neal, C. L., Yang, W., & Yu, D. (2008). 14-3-3 zeta down-regulates p53 in mammary epithelial cells and confers luminal filling. *Cancer Res, 68*(6), 1760-1767. doi:10.1158/0008-5472.CAN-07-3177

de Oliveira, K. A., Kaergel, E., Heinig, M., Fontaine, J. F., Patone, G., Muro, E. M., . . . Scheidereit, C. (2016). A roadmap of constitutive NF-kappaB activity in Hodgkin lymphoma: Dominant roles of p50 and p52 revealed by genome-wide analyses. *Genome Med, 8*(1), 28. doi:10.1186/s13073-016-0280-5

Dejardin, E., Droin, N. M., Delhase, M., Haas, E., Cao, Y., Makris, C., . . . Green, D. R. (2002). The lymphotoxin-beta receptor induces different patterns of gene expression via two NF-kappaB pathways. *Immunity, 17*(4), 525-535. doi:10.1016/s1074-7613(02)00423-5

Demicco, E. G., Kavanagh, K. T., Romieu-Mourez, R., Wang, X., Shin, S. R., Landesman-Bollag, E., . . . Sonenshein, G. E. (2005). RelB/p52 NF-kappaB complexes rescue an early delay in mammary gland development in transgenic mice with targeted superrepressor IkappaB-alpha expression and promote carcinogenesis of the mammary gland. *Mol Cell Biol, 25*(22), 10136-10147. doi:10.1128/MCB.25.22.10136-10147.2005

Dhanoa, B. S., Cogliati, T., Satish, A. G., Bruford, E. A., & Friedman, J. S. (2013). Update on the Kelch-like (KLHL) gene family. *Hum Genomics, 7*, 13. doi:10.1186/1479-7364-7-13

Dhillon, B., Aleithan, F., Abdul-Sater, Z., & Abdul-Sater, A. A. (2019). The Evolving Role of TRAFs in Mediating Inflammatory Responses. *Front Immunol, 10*, 104. doi:10.3389/fimmu.2019.00104

Dimitrakopoulos, F. D., Antonacopoulou, A. G., Kottorou, A. E., Panagopoulos, N., Kalofonou, F., Sampsonas, F., . . . Kalofonos, H. P. (2019). Expression Of Intracellular Components of the NF-kappaB Alternative Pathway (NF-kappaB2, RelB, NIK and Bcl3) is Associated With Clinical Outcome of NSCLC Patients. *Sci Rep, 9*(1), 14299. doi:10.1038/s41598-019-50528-y

Doench, J. G., Fusi, N., Sullender, M., Hegde, M., Vaimberg, E. W., Donovan, K. F., . . . Root, D. E. (2016). Optimized sgRNA design to maximize activity and minimize off-target effects of CRISPR-Cas9. *Nat Biotechnol, 34*(2), 184-191. doi:10.1038/nbt.3437

Dolcet, X., Llobet, D., Pallares, J., & Matias-Guiu, X. (2005). NF-kB in development and progression of human cancer. *Virchows Arch, 446*(5), 475-482. doi:10.1007/s00428-005-1264-9

Dupont, S., Morsut, L., Aragona, M., Enzo, E., Giulitti, S., Cordenonsi, M., . . . Piccolo, S. (2011). Role of YAP/TAZ in mechanotransduction. *Nature, 474*(7350), 179-183. doi:10.1038/nature10137

Eisenhoffer, G. T., Loftus, P. D., Yoshigi, M., Otsuna, H., Chien, C. B., Morcos, P. A., & Rosenblatt, J. (2012). Crowding induces live cell extrusion to maintain

homeostatic cell numbers in epithelia. *Nature, 484*(7395), 546-549. doi:10.1038/nature10999

Espin-Palazon, R., & Traver, D. (2016). The NF-kappaB family: Key players during embryonic development and HSC emergence. *Exp Hematol, 44*(7), 519-527. doi:10.1016/j.exphem.2016.03.010

Ewald, A. J., Brenot, A., Duong, M., Chan, B. S., & Werb, Z. (2008). Collective epithelial migration and cell rearrangements drive mammary branching morphogenesis. *Dev Cell, 14*(4), 570-581. doi:10.1016/j.devcel.2008.03.003

Feige, M. H., Vieth, M., Sokolova, O., Tager, C., & Naumann, M. (2018). Helicobacter pylori induces direct activation of the lymphotoxin beta receptor and non-canonical nuclear factor-kappa B signaling. *Biochim Biophys Acta Mol Cell Res, 1865*(4), 545-550. doi:10.1016/j.bbamcr.2018.01.006

Fomicheva, M., & Macara, I. G. (2020). Genome-wide CRISPR screen identifies noncanonical NF-kappaB signaling as a regulator of density-dependent proliferation. *Elife, 9*. doi:10.7554/eLife.63603

Fomicheva, M., Tross, E. M., & Macara, I. G. (2019). Polarity proteins in oncogenesis. *Curr Opin Cell Biol, 62*, 26-30. doi:10.1016/j.ceb.2019.07.016

Frank, S. A. (2007). In *Dynamics of Cancer: Incidence, Inheritance, and Evolution*. Princeton (NJ).

Ge, J., Xu, H., Li, T., Zhou, Y., Zhang, Z., Li, S., . . . Shao, F. (2009). A Legionella type IV effector activates the NF-kappaB pathway by phosphorylating the IkappaB family of inhibitors. *Proc Natl Acad Sci U S A, 106*(33), 13725-13730. doi:10.1073/pnas.0907200106

Gehart, H., & Clevers, H. (2019). Tales from the crypt: new insights into intestinal stem cells. *Nat Rev Gastroenterol Hepatol, 16*(1), 19-34. doi:10.1038/s41575-018-0081-y

Gookin, S., Min, M., Phadke, H., Chung, M., Moser, J., Miller, I., . . . Spencer, S. L. (2017). A map of protein dynamics during cell-cycle progression and cell-cycle exit. *PLoS Biol, 15*(9), e2003268. doi:10.1371/journal.pbio.2003268

Gopinathan, L., Ratnacaram, C. K., & Kaldis, P. (2011). Established and novel Cdk/cyclin complexes regulating the cell cycle and development. *Results Probl Cell Differ, 53*, 365-389. doi:10.1007/978-3-642-19065-0_16

Guan, K., Wei, C., Zheng, Z., Song, T., Wu, F., Zhang, Y., . . . Zhong, H. (2015). MAVS Promotes Inflammasome Activation by Targeting ASC for K63-Linked Ubiquitination via the E3 Ligase TRAF3. *J Immunol, 194*(10), 4880-4890. doi:10.4049/jimmunol.1402851

Hacker, H., Redecke, V., Blagoev, B., Kratchmarova, I., Hsu, L. C., Wang, G. G., . . . Karin, M. (2006). Specificity in Toll-like receptor signalling through distinct effector functions of TRAF3 and TRAF6. *Nature, 439*(7073), 204-207. doi:10.1038/nature04369

Hacker, H., Tseng, P. H., & Karin, M. (2011). Expanding TRAF function: TRAF3 as a tri-faced immune regulator. *Nat Rev Immunol, 11*(7), 457-468. doi:10.1038/nri2998

Halder, G., & Johnson, R. L. (2011). Hippo signaling: growth control and beyond. *Development, 138*(1), 9-22. doi:10.1242/dev.045500

Hauer, J., Puschner, S., Ramakrishnan, P., Simon, U., Bongers, M., Federle, C., & Engelmann, H. (2005). TNF receptor (TNFR)-associated factor (TRAF) 3 serves as an inhibitor of TRAF2/5-mediated activation of the noncanonical NF-kappaB pathway by TRAF-binding TNFRs. *Proc Natl Acad Sci U S A, 102*(8), 2874-2879. doi:10.1073/pnas.0500187102

He, J. Q., Zarnegar, B., Oganesyan, G., Saha, S. K., Yamazaki, S., Doyle, S. E., . . . Cheng, G. (2006). Rescue of TRAF3-null mice by p100 NF-kappa B deficiency. *J Exp Med, 203*(11), 2413-2418. doi:10.1084/jem.20061166

Hoebe, K., & Beutler, B. (2006). TRAF3: a new component of the TLR-signaling apparatus. *Trends Mol Med, 12*(5), 187-189. doi:10.1016/j.molmed.2006.03.008

Hoesel, B., & Schmid, J. A. (2013). The complexity of NF-kappaB signaling in inflammation and cancer. *Mol Cancer, 12*, 86. doi:10.1186/1476-4598-12-86

Jarnicki, A., Putoczki, T., & Ernst, M. (2010). Stat3: linking inflammation to epithelial cancer - more than a "gut" feeling? *Cell Div, 5*, 14. doi:10.1186/1747-1028-5-14

Julian, L., & Olson, M. F. (2014). Rho-associated coiled-coil containing kinases (ROCK): structure, regulation, and functions. *Small GTPases, 5*, e29846. doi:10.4161/sgtp.29846

Khodarev, N. N., Roizman, B., & Weichselbaum, R. R. (2012). Molecular pathways: interferon/stat1 pathway: role in the tumor resistance to genotoxic stress and aggressive growth. *Clin Cancer Res, 18*(11), 3015-3021. doi:10.1158/1078-0432.CCR-11-3225

Lalani, A. I., Moore, C. R., Luo, C., Kreider, B. Z., Liu, Y., Morse, H. C., 3rd, & Xie, P. (2015). Myeloid cell TRAF3 regulates immune responses and inhibits inflammation and tumor development in mice. *J Immunol, 194*(1), 334-348. doi:10.4049/jimmunol.1401548

Li, L., Kang, J., Zhang, W., Cai, L., Wang, S., Liang, Y., . . . Jia, L. (2019). Validation of NEDD8-conjugating enzyme UBC12 as a new therapeutic target in lung cancer. *EBioMedicine, 45*, 81-91. doi:10.1016/j.ebiom.2019.06.005

Li, T., Morgan, M. J., Choksi, S., Zhang, Y., Kim, Y. S., & Liu, Z. G. (2010). MicroRNAs modulate the noncanonical transcription factor NF-kappaB pathway by regulating expression of the kinase IKKalpha during macrophage differentiation. *Nat Immunol, 11*(9), 799-805. doi:10.1038/ni.1918

Li, W., Cooper, J., Zhou, L., Yang, C., Erdjument-Bromage, H., Zagzag, D., . . . Giancotti, F. G. (2014). Merlin/NF2 loss-driven tumorigenesis linked to CRL4(DCAF1)-mediated inhibition of the hippo pathway kinases Lats1 and 2 in the nucleus. *Cancer Cell, 26*(1), 48-60. doi:10.1016/j.ccr.2014.05.001

Li, W., Xu, H., Xiao, T., Cong, L., Love, M. I., Zhang, F., . . . Liu, X. S. (2014). MAGeCK enables robust identification of essential genes from genome-scale CRISPR/Cas9 knockout screens. *Genome Biol, 15*(12), 554. doi:10.1186/s13059-014-0554-4

Liao, G., Zhang, M., Harhaj, E. W., & Sun, S. C. (2004). Regulation of the NF-kappaB-inducing kinase by tumor necrosis factor receptor-associated factor 3-induced degradation. *J Biol Chem, 279*(25), 26243-26250. doi:10.1074/jbc.M403286200

Lin, W. W., Hostager, B. S., & Bishop, G. A. (2015). TRAF3, ubiquitination, and B-lymphocyte regulation. *Immunol Rev, 266*(1), 46-55. doi:10.1111/imr.12299

Lin, W. W., Yi, Z., Stunz, L. L., Maine, C. J., Sherman, L. A., & Bishop, G. A. (2015). The adaptor protein TRAF3 inhibits interleukin-6 receptor signaling in B cells to limit plasma cell development. *Sci Signal, 8*(392), ra88. doi:10.1126/scisignal.aaa5157

Lord, S. J., Velle, K. B., Mullins, R. D., & Fritz-Laylin, L. K. (2020). SuperPlots: Communicating reproducibility and variability in cell biology. *J Cell Biol, 219*(6). doi:10.1083/jcb.202001064

Lowe, J. S., Anderson, P. G., & Anderson, S. I. *Stevens & Lowe's : human histology* (Fifth edition. ed.).

Lydeard, J. R., Schulman, B. A., & Harper, J. W. (2013). Building and remodelling Cullin-RING E3 ubiquitin ligases. *EMBO Rep, 14*(12), 1050-1061. doi:10.1038/embor.2013.173

Ma, S., Meng, Z., Chen, R., & Guan, K. L. (2018). The Hippo Pathway: Biology and Pathophysiology. *Annu Rev Biochem*. doi:10.1146/annurev-biochem-013118-111829

Ma, S., Meng, Z., Chen, R., & Guan, K. L. (2019). The Hippo Pathway: Biology and Pathophysiology. *Annu Rev Biochem, 88*, 577-604. doi:10.1146/annurev-biochem-013118-111829

Mambetsariev, N., Lin, W. W., Stunz, L. L., Hanson, B. M., Hildebrand, J. M., & Bishop, G. A. (2016). Nuclear TRAF3 is a negative regulator of CREB in B cells. *Proc Natl Acad Sci U S A, 113*(4), 1032-1037. doi:10.1073/pnas.1514586113

Manches, O., Fernandez, M. V., Plumas, J., Chaperot, L., & Bhardwaj, N. (2012). Activation of the noncanonical NF-kappaB pathway by HIV controls a dendritic cell immunoregulatory phenotype. *Proc Natl Acad Sci U S A, 109*(35), 14122-14127. doi:10.1073/pnas.1204032109

Marcheque, J., Bussolati, B., Csete, M., & Perin, L. (2019). Concise Reviews: Stem Cells and Kidney Regeneration: An Update. *Stem Cells Transl Med, 8*(1), 82-92. doi:10.1002/sctm.18-0115

Michallet, M. C., Meylan, E., Ermolaeva, M. A., Vazquez, J., Rebsamen, M., Curran, J., . . . Tschopp, J. (2008). TRADD protein is an essential component of the RIG-like

helicase antiviral pathway. *Immunity, 28*(5), 651-661. doi:10.1016/j.immuni.2008.03.013

Mitchell, S., Vargas, J., & Hoffmann, A. (2016). Signaling via the NFkappaB system. *Wiley Interdiscip Rev Syst Biol Med, 8*(3), 227-241. doi:10.1002/wsbm.1331

Moore, C. R., Liu, Y., Shao, C., Covey, L. R., Morse, H. C., 3rd, & Xie, P. (2012). Specific deletion of TRAF3 in B lymphocytes leads to B-lymphoma development in mice. *Leukemia, 26*(5), 1122-1127. doi:10.1038/leu.2011.309

Mulero, M. C., Wang, V. Y., Huxford, T., & Ghosh, G. (2019). Genome reading by the NF-kappaB transcription factors. *Nucleic Acids Res, 47*(19), 9967-9989. doi:10.1093/nar/gkz739

Nagy, A., Lanczky, A., Menyhart, O., & Gyorffy, B. (2018). Validation of miRNA prognostic power in hepatocellular carcinoma using expression data of independent datasets. *Sci Rep, 8*(1), 9227. doi:10.1038/s41598-018-27521-y

Novack, D. V. (2011). Role of NF-kappaB in the skeleton. *Cell Res, 21*(1), 169-182. doi:10.1038/cr.2010.159

Oganesyan, G., Saha, S. K., Guo, B., He, J. Q., Shahangian, A., Zarnegar, B., . . . Cheng, G. (2006). Critical role of TRAF3 in the Toll-like receptor-dependent and -independent antiviral response. *Nature, 439*(7073), 208-211. doi:10.1038/nature04374

Ohmae, T., Hirata, Y., Maeda, S., Shibata, W., Yanai, A., Ogura, K., . . . Omata, M. (2005). Helicobacter pylori activates NF-kappaB via the alternative pathway in B lymphocytes. *J Immunol, 175*(11), 7162-7169. doi:10.4049/jimmunol.175.11.7162

Oudenaarden, C. R. L., van de Ven, R. A. H., & Derksen, P. W. B. (2018). Re-inforcing the cell death army in the fight against breast cancer. *J Cell Sci, 131*(16). doi:10.1242/jcs.212563

Pack, L. R., Daigh, L. H., & Meyer, T. (2019). Putting the brakes on the cell cycle: mechanisms of cellular growth arrest. *Curr Opin Cell Biol, 60*, 106-113. doi:10.1016/j.ceb.2019.05.005

Pandey, S., Singh, S., Anang, V., Bhatt, A. N., Natarajan, K., & Dwarakanath, B. S. (2015). Pattern Recognition Receptors in Cancer Progression and Metastasis. *Cancer Growth Metastasis, 8*, 25-34. doi:10.4137/CGM.S24314

Park, H. H. (2018). Structure of TRAF Family: Current Understanding of Receptor Recognition. *Front Immunol, 9*, 1999. doi:10.3389/fimmu.2018.01999

Park, S. G., Chung, C., Kang, H., Kim, J. Y., & Jung, G. (2006). Up-regulation of cyclin D1 by HBx is mediated by NF-kappaB2/BCL3 complex through kappaB site of cyclin D1 promoter. *J Biol Chem, 281*(42), 31770-31777. doi:10.1074/jbc.M603194200

Parker, B. S., Rautela, J., & Hertzog, P. J. (2016). Antitumour actions of interferons: implications for cancer therapy. *Nat Rev Cancer, 16*(3), 131-144. doi:10.1038/nrc.2016.14

Pasic, L., Eisinger-Mathason, T. S., Velayudhan, B. T., Moskaluk, C. A., Brenin, D. R., Macara, I. G., & Lannigan, D. A. (2011). Sustained activation of the HER1-ERK1/2-RSK signaling pathway controls myoepithelial cell fate in human mammary tissue. *Genes Dev, 25*(15), 1641-1653. doi:10.1101/gad.2025611

Perkins, N. D. (2012). The diverse and complex roles of NF-kappaB subunits in cancer. *Nat Rev Cancer, 12*(2), 121-132. doi:10.1038/nrc3204

Petrilli, A. M., & Fernandez-Valle, C. (2016). Role of Merlin/NF2 inactivation in tumor biology. *Oncogene, 35*(5), 537-548. doi:10.1038/onc.2015.125

Philpott, D. J., Girardin, S. E., & Sansonetti, P. J. (2001). Innate immune responses of epithelial cells following infection with bacterial pathogens. *Curr Opin Immunol, 13*(4), 410-416. doi:10.1016/s0952-7915(00)00235-1

Ramakrishnan, P., Wang, W., & Wallach, D. (2004). Receptor-specific signaling for both the alternative and the canonical NF-kappaB activation pathways by NF-kappaB-inducing kinase. *Immunity, 21*(4), 477-489. doi:10.1016/j.immuni.2004.08.009

Rocha, S., Martin, A. M., Meek, D. W., & Perkins, N. D. (2003). p53 represses cyclin D1 transcription through down regulation of Bcl-3 and inducing increased association of the p52 NF-kappaB subunit with histone deacetylase 1. *Mol Cell Biol, 23*(13), 4713-4727.

Rojo, F., Gonzalez-Perez, A., Furriol, J., Nicolau, M. J., Ferrer, J., Burgues, O., . . . Eroles, P. (2016). Non-canonical NF-kappaB pathway activation predicts outcome in borderline oestrogen receptor positive breast carcinoma. *Br J Cancer, 115*(3), 322-331. doi:10.1038/bjc.2016.204

Ross, K. F., & Herzberg, M. C. (2016). Autonomous immunity in mucosal epithelial cells: fortifying the barrier against infection. *Microbes Infect, 18*(6), 387-398. doi:10.1016/j.micinf.2016.03.008

Rubin, S. M. (2013). Deciphering the retinoblastoma protein phosphorylation code. *Trends Biochem Sci, 38*(1), 12-19. doi:10.1016/j.tibs.2012.10.007

Ruckle, A., Haasbach, E., Julkunen, I., Planz, O., Ehrhardt, C., & Ludwig, S. (2012). The NS1 protein of influenza A virus blocks RIG-I-mediated activation of the noncanonical NF-kappaB pathway and p52/RelB-dependent gene expression in lung epithelial cells. *J Virol, 86*(18), 10211-10217. doi:10.1128/JVI.00323-12

Sanjana, N. E., Shalem, O., & Zhang, F. (2014). Improved vectors and genome-wide libraries for CRISPR screening. *Nat Methods, 11*(8), 783-784. doi:10.1038/nmeth.3047

Sasaki, Y., Calado, D. P., Derudder, E., Zhang, B., Shimizu, Y., Mackay, F., . . . Schmidt-Supprian, M. (2008). NIK overexpression amplifies, whereas ablation of its TRAF3-binding domain replaces BAFF:BAFF-R-mediated survival signals in B cells. *Proc Natl Acad Sci U S A, 105*(31), 10883-10888. doi:10.1073/pnas.0805186105

Saw, T. B., Doostmohammadi, A., Nier, V., Kocgozlu, L., Thampi, S., Toyama, Y., . . . Ladoux, B. (2017). Topological defects in epithelia govern cell death and extrusion. *Nature, 544*(7649), 212-216. doi:10.1038/nature21718

Shalem, O., Sanjana, N. E., Hartenian, E., Shi, X., Scott, D. A., Mikkelson, T., . . . Zhang, F. (2014). Genome-scale CRISPR-Cas9 knockout screening in human cells. *Science, 343*(6166), 84-87. doi:10.1126/science.1247005

Sladitschek, H. L., & Neveu, P. A. (2015). MXS-Chaining: A Highly Efficient Cloning Platform for Imaging and Flow Cytometry Approaches in Mammalian Systems. *PLoS One, 10*(4), e0124958. doi:10.1371/journal.pone.0124958

Solan, N. J., Miyoshi, H., Carmona, E. M., Bren, G. D., & Paya, C. V. (2002). RelB cellular regulation and transcriptional activity are regulated by p100. *J Biol Chem, 277*(2), 1405-1418. doi:10.1074/jbc.M109619200

Sovak, M. A., Bellas, R. E., Kim, D. W., Zanieski, G. J., Rogers, A. E., Traish, A. M., & Sonenshein, G. E. (1997). Aberrant nuclear factor-kappaB/Rel expression and the pathogenesis of breast cancer. *J Clin Invest, 100*(12), 2952-2960. doi:10.1172/JCI119848

Spencer, S. L., Cappell, S. D., Tsai, F. C., Overton, K. W., Wang, C. L., & Meyer, T. (2013). The proliferation-quiescence decision is controlled by a bifurcation in CDK2 activity at mitotic exit. *Cell, 155*(2), 369-383. doi:10.1016/j.cell.2013.08.062

Stanifer, M. L., Pervolaraki, K., & Boulant, S. (2019). Differential Regulation of Type I and Type III Interferon Signaling. *Int J Mol Sci, 20*(6). doi:10.3390/ijms20061445

Strandberg, Y., Gray, C., Vuocolo, T., Donaldson, L., Broadway, M., & Tellam, R. (2005). Lipopolysaccharide and lipoteichoic acid induce different innate immune responses in bovine mammary epithelial cells. *Cytokine, 31*(1), 72-86. doi:10.1016/j.cyto.2005.02.010

Struzik, J., & Szulc-Dabrowska, L. (2019). Manipulation of Non-canonical NF-kappaB Signaling by Non-oncogenic Viruses. *Arch Immunol Ther Exp (Warsz), 67*(1), 41-48. doi:10.1007/s00005-018-0522-x

Sullivan, J. C., Wolenski, F. S., Reitzel, A. M., French, C. E., Traylor-Knowles, N., Gilmore, T. D., & Finnerty, J. R. (2009). Two alleles of NF-kappaB in the sea anemone Nematostella vectensis are widely dispersed in nature and encode proteins with distinct activities. *PLoS One, 4*(10), e7311. doi:10.1371/journal.pone.0007311

Sun, S. C. (2017). The non-canonical NF-kappaB pathway in immunity and inflammation. *Nat Rev Immunol, 17*(9), 545-558. doi:10.1038/nri.2017.52

Tak, P. P., & Firestein, G. S. (2001). NF-kappaB: a key role in inflammatory diseases. *J Clin Invest, 107*(1), 7-11. doi:10.1172/JCI11830

Tao, Z., Fusco, A., Huang, D. B., Gupta, K., Young Kim, D., Ware, C. F., . . . Ghosh, G. (2014). p100/IkappaBdelta sequesters and inhibits NF-kappaB through

kappaBsome formation. *Proc Natl Acad Sci U S A, 111*(45), 15946-15951. doi:10.1073/pnas.1408552111

Terzi, M. Y., Izmirli, M., & Gogebakan, B. (2016). The cell fate: senescence or quiescence. *Mol Biol Rep, 43*(11), 1213-1220. doi:10.1007/s11033-016-4065-0

Wang, J. Q., Jeelall, Y. S., Ferguson, L. L., & Horikawa, K. (2014). Toll-Like Receptors and Cancer: MYD88 Mutation and Inflammation. *Front Immunol, 5*, 367. doi:10.3389/fimmu.2014.00367

Wang, V. Y., Huang, W., Asagiri, M., Spann, N., Hoffmann, A., Glass, C., & Ghosh, G. (2012). The transcriptional specificity of NF-kappaB dimers is coded within the kappaB DNA response elements. *Cell Rep, 2*(4), 824-839. doi:10.1016/j.celrep.2012.08.042

Wharry, C. E., Haines, K. M., Carroll, R. G., & May, M. J. (2009). Constitutive non-canonical NFkappaB signaling in pancreatic cancer cells. *Cancer Biol Ther, 8*(16), 1567-1576. doi:10.4161/cbt.8.16.8961

Williams, L. M., & Gilmore, T. D. (2020). Looking Down on NF-kappaB. *Mol Cell Biol, 40*(15). doi:10.1128/MCB.00104-20

Xie, P. (2013). TRAF molecules in cell signaling and in human diseases. *J Mol Signal, 8*(1), 7. doi:10.1186/1750-2187-8-7

Xie, P., Poovassery, J., Stunz, L. L., Smith, S. M., Schultz, M. L., Carlin, L. E., & Bishop, G. A. (2011). Enhanced Toll-like receptor (TLR) responses of TNFR-associated factor 3 (TRAF3)-deficient B lymphocytes. *J Leukoc Biol, 90*(6), 1149-1157. doi:10.1189/jlb.0111044

Xu, Y., Cheng, G., & Baltimore, D. (1996). Targeted disruption of TRAF3 leads to postnatal lethality and defective T-dependent immune responses. *Immunity, 5*(5), 407-415. doi:10.1016/s1074-7613(00)80497-5

Yamashita, K., Ide, M., Furukawa, K. T., Suzuki, A., Hirano, H., & Ohno, S. (2015). Tumor suppressor protein Lgl mediates G1 cell cycle arrest at high cell density by forming an Lgl-VprBP-DDB1 complex. *Mol Biol Cell, 26*(13), 2426-2438. doi:10.1091/mbc.E14-10-1462

Yi, Z., Lin, W. W., Stunz, L. L., & Bishop, G. A. (2014). The adaptor TRAF3 restrains the lineage determination of thymic regulatory T cells by modulating signaling via the receptor for IL-2. *Nat Immunol, 15*(9), 866-874. doi:10.1038/ni.2944

Yu, F. X., & Guan, K. L. (2013). The Hippo pathway: regulators and regulations. *Genes Dev, 27*(4), 355-371. doi:10.1101/gad.210773.112

Yue, F., Cheng, Y., Breschi, A., Vierstra, J., Wu, W., Ryba, T., . . . Mouse, E. C. (2014). A comparative encyclopedia of DNA elements in the mouse genome. *Nature, 515*(7527), 355-364. doi:10.1038/nature13992

Zapata, J. M., Llobet, D., Krajewska, M., Lefebvre, S., Kress, C. L., & Reed, J. C. (2009). Lymphocyte-specific TRAF3 transgenic mice have enhanced humoral responses and develop plasmacytosis, autoimmunity, inflammation, and cancer. *Blood, 113*(19), 4595-4603. doi:10.1182/blood-2008-07-165456

Zarnegar, B., Yamazaki, S., He, J. Q., & Cheng, G. (2008). Control of canonical NF-kappaB activation through the NIK-IKK complex pathway. *Proc Natl Acad Sci U S A, 105*(9), 3503-3508. doi:10.1073/pnas.0707959105

Zhang, J., Warren, M. A., Shoemaker, S. F., & Ip, M. M. (2007). NFkappaB1/p50 is not required for tumor necrosis factor-stimulated growth of primary mammary epithelial cells: implications for NFkappaB2/p52 and RelB. *Endocrinology, 148*(1), 268-278. doi:10.1210/en.2006-0500

Zheng, Z., Zhu, H., Wan, Q., Liu, J., Xiao, Z., Siderovski, D. P., & Du, Q. (2010). LGN regulates mitotic spindle orientation during epithelial morphogenesis. *J Cell Biol, 189*(2), 275-288. doi:10.1083/jcb.200910021

Zhou, W., Xu, J., Tan, M., Li, H., Li, H., Wei, W., & Sun, Y. (2018). UBE2M Is a Stress-Inducible Dual E2 for Neddylation and Ubiquitylation that Promotes Targeted Degradation of UBE2F. *Mol Cell, 70*(6), 1008-1024 e1006. doi:10.1016/j.molcel.2018.06.002

Zhu, S., Jin, J., Gokhale, S., Lu, A. M., Shan, H., Feng, J., & Xie, P. (2018). Genetic Alterations of TRAF Proteins in Human Cancers. *Front Immunol, 9*, 2111. doi:10.3389/fimmu.2018.02111

http://www.bu.edu/nf-kb/gene-resources/target-genes/

https://github.com/MontpellierRessourcesImagerie/imagej_macros_and_scripts/wiki/Intensity-Ratio-Nuclei-Cytoplasm-Tool/

https://maayanlab.cloud/Harmonizome/